Investigating novel direct Notch targets in *Drosophila* neural stem cells

Shiyun Feng

Hughes Hall

University of Cambridge

January 2018

This dissertation is submitted to the University of Cambridge for the degree of Doctor of Philosophy

Investigating novel direct Notch targets in *Drosophila* neural stem cells

Shiyun Feng

Summary

Notch signalling is an evolutionary highly conserved signalling pathway. It plays various important roles in the regulation of many fundamental cellular processes such as proliferation, stem cell maintenance and differentiation during embryonic and adult development. Notch signalling has a simple transduction pathway. Upon Notch ligand binding to the receptor, the Notch intracellular domain (NICD) is released into the nucleus. The nuclear NICD interacts with the DNA-binding protein Suppressor of Hairless (Su(H)) to activate the expression of target genes, which are silenced by the Su(H)-corepressor complex in the absence of Notch activity. The functions of Notch are very context-dependent, making it important to identify the Notch regulated genes in different processes.

Neural stem cells (NSCs) are cells that can divide and differentiate into all kinds of cells within the brain while they self-renew. Notch signalling is one of the key regulators in maintaining NSCs and performs a similar function in both *Drosophila* and vertebrate NSCs. *Drosophila* NSCs serve as an ideal model for studying the relationship between Notch function and stem cell behaviours. Although many target genes, such as the Hes genes, have been identified, they cannot fully account for the diversity of Notch responses. Therefore, further functional study of more potential target genes is needed to gain understanding about Notch-regulated NSC maintenance. In this thesis, a group of potential direct Notch target genes are examined for their responsiveness to Notch regulation and their functions in *Drosophila* NSCs. Previous genome-wide study in the Bray lab has found a number of potential Notch target genes in the *Drosophila* larval brain, with the characteristics of Notch transcription factor Su(H) binding and mRNA upregulation by Notch over-activation (Zacharioudaki et al. 2016). I first examined the Notch responsive element (NRE) activity of these potential Notch targets and their regulation by Notch both *in vivo* and in cell lines. The presented findings validated *path*, *cables* and *Asph* as direct Notch target genes in *Drosophila* NSCs, while *syp*, *lola* and *Fer2* do not exhibit characteristics of Notch responsive targets in NSCs.

The functional roles of two of the responsive genes, *path* and *cables*, were subsequently explored in *Drosophila* larval brains. Firstly, I found that Path, a potential amino acid transporter, is not only important for protecting NSC proliferation under normal and abnormal conditions through integrating growth pathways, but is also required for protecting brain growth under nutrition deprivation. Secondly, the *cables* gene was connected to a distal NRE through knocking out the suspected NRE region and the gene itself using the CRISPR/Cas9 technique. Subsequent experiments revealed that *cables* is also required for NSC proliferation.

In summary, a group of direct Notch target genes were validated and as a consequence two genes that are important for protecting NSC proliferation were identified.

Declaration

I hereby declare that this dissertation is the result of my own work and includes nothing which is the outcome of work done in collaboration except as declared in the Preface and specified in the text.

It is not substantially the same as any that I have submitted, or, is being concurrently submitted for a degree or diploma or other qualification at the University of Cambridge or any other University or similar institution except as declared in the Preface and specified in the text. I further state that no substantial part of my dissertation has already been submitted, or, is being concurrently submitted for any such degree, diploma or other qualification at the University of Cambridge or any other University of similar institution except as declared in the Preface and specified in the text.

I also declare that this thesis does not exceed the word limit specified by the Degree Committee for the Faculty of Biology, i.e. 60,000 words excluding bibliography, figures, appendices etc.

Acknowledgements

I would like to express my gratefulness to people who helped me along this unforgettable adventure in my life.

First and most, I would like to thank my supervisor, Dr Sarah Bray, for accepting me to Cambridge, giving me constructive suggestions, shielding me while I was in difficult, and supporting me to complete my study no matter what. I wish I could learn more from a creative and rigorous mentor like you. In the future, I will keep your words in mind and keep going forward.

Dr Bill Harris and Dr Matthias Landgraf were the examiners for my first-year viva, and I am grateful for advice they gave me at that time.

Special thanks to Aileen Jordan, our department administrator, for talking with me when I was downhill and helping me out with all kinds of applications when I could not do things.

The Bray Lab is where I spent most of my time for these years. I am very lucky to study in a cooperative and sharing lab where I received a lot of kindness and support:

Eva Zacharioudaki, you are like my day-to-day supervisor, and I want to thank you for sharing your experiences with me, enlightening me with your brightness and warming me up with your passion (and your lovely family too) in life and in science.

Kat Millen, our dearest lab manager, thanks to your excellent technical support and organization, I could carry out experiments efficiently. Also, Kat and Eva helped me proofread my thesis very carefully and gave me a lot of suggestions.

Jinghua Li, you are like a sister to me even before I came to the lab. I would like to thank you for being helpful and supportive when I felt bad and giving me a lot of advice.

Stephan, Stella and Matt, you guys made the lab a place of joy. It is my honour to study, grow and have fun with you.

Agnes Asselin, thank you for taking care of my stocks while I was away and your gift is one of Leo's favourite.

I would like also thank Maria, Hadi, Sara, Zoe, Lenka, Gus and Silvie for being nice and supportive to me all the time.

I learned my experiment techniques from different people and with these techniques I build this thesis. From Jinghua and Burcu, I learned essential skills in cloning and imaging to initiate my work, from Eva I learned how to improve my genetics design and analyse my results, from Maria I learned how to use the SP8, and from Matt and Kat I gained a lot of experiences in CRISPR. I appreciate your help from deep down my heart.

I also would like to thank my funding body, China Scholarship Council and Cambridge Overseas Trust, without the support I could not start and survive this adventure. Also, the support from my college Hughes Hall is very important to me and I am very grateful.

Last but not least, I shall express my appreciation and affection to my family: my parents, my husband and my son. Thank you, my dearest mother and father, for bringing me up

and giving me the best you ever have. My beloved husband, Chaoqun, thanks for being the shining star in my life, standing by my side through all these, and giving me your hand whenever I need. And my little man, Leo, thanks for coming to my life and lighting it up. You are the reason I could sail over all the hurdles and finally approaching the finish line.

I have tried my best to mention the names, but as I no longer have the as good memory as I had before, I am very sorry if I neglect any.

Index

Summary 1
Declaration 2
Acknowledgements 3
Abbreviations 9
Chapter I: Introduction 11
1.1 Notch signalling pathway 11
1.1.1 The core Notch pathway 12
1.1.2 Consequences of Notch activation 17
1.1.3 Known Notch targets 18
1.2 Genome-wide approaches to identify diverse Notch targets 20
1.3 Role of Notch signalling in neural stem cells 21
1.3.1 Neural stem cells 21
1.3.2 Notch signalling in neural stem cells 24
1.3.3. Role of Hes genes and other Notch target genes in NSCs 27
1.4 Model: *Drosophila* Neural stem cell 29
1.5 Aim of the study 33
Chapter II: Materials and Methods 35
2.1 Materials 35
2.2 Molecular Cloning 35
2.2.1 PCR reaction 35
2.2.2 Ligated product transformation 37
2.2.3 Motif point mutagenesis 38
2.3 Cell Culture and Luciferase Assay 39
2.4 Fly Husbandry and Genetics 41
2.4.1 Generation of Transgenic NRE-GFP flies 41
2.4.2 Gal4/UAS system 42
2.4.3 MARCM system 42
2.4.4 Nutrition restriction treatment 44
2.4.5 CRISPR/Cas9-mediated Homology-directed Repair (HDR) 45

2.5 Dissection and Immunohistochemistry 46
2.6 EdU labelling of NBs and lineages 47
2.7 Imaging and Analysis 47
Chapter III: Candidate Notch target genes in neural stem cells 59
3.1 Introduction 59
3.2 Results 64
3.2.1 General strategy 64
3.2.2 *pathetic* contains a Notch-regulated enhancer that directs expression in neural stem cells 65
3.2.3 An enhancer associated with CABLES directs GFP expression in neuroblasts and responds to Notch activity 77
3.2.4. Su(H) bound region from *Asph* confers expression in NBs and responds to Notch 80
3.2.5 Two *lola-NRE* reporters exhibit different expression patterns in the brain 84
3.2.6 *Fer2NRE* directs expression in a subset of neurons 87
3.3 Discussion 91
3.4 Summary 95
Chapter IV: The SLC36 transporter Pathetic as a novel direct Notch target is required for protecting neural stem cell proliferation under abnormal conditions 96
4.1 Introduction 96
4.2 Results 101
4.2.1 Path is expressed in neural stem cells and glia 101
4.2.2 Depletion of Path causes an increase in neural stem cell size and a reduction in the number of NB progeny 103
4.2.3 *path* switches from promoting to restricting proliferation when Notch is over-activated 108
4.2.4 Loss of Path promotes 4EBP phosphorylation under conditions where Notch is over-activated 110
4.2.5 *path* is not upstream of Alk/Jeb signalling in NBs 113
4.2.6 *path* does not alter expression of the temporal factor Broad 113
4.2.7 *pathNRE* is a nutrition-dependent enhancer 117

4.2.8 Glia-expressed Path is required for protecting brain growth under nutrition restriction 121
4.3 Discussion 128
4.3.1 Function of *path* in neuroblasts 128
4.3.2 Function of *path* in glia 131
4.4 Summary 134
Chapter V: A remote NRE is required for *cables* expression in neural stem cells 135
5.1 Introduction 135
5.2 Results 142
5.2.1 Generation of CRISPR deletions of the remote NRE and *cables* 142
5.2.2 Identification of *CG6191Big*-regulated genes 147
5.2.3 *CG6191Big* and *cables* are both required for normal NB proliferation 149
5.2.4 Neither E2F nor Dap expression are affected by ΔCG6191Big 154
5.4 Discussion 157
Chapter VI: General Conclusion and Discussion 161
6.1 Notch target genes in NSCs 162
6.2 Notch target genes and stem cell identity 164
6.3 Concluding remarks 167
Reference 168

Abbreviations

Abbreviation	Full Name
ACI	after clone induction
Alk	Anaplastic lymphoma kinase
ANK	ankyrin
Ase	Asense
Asph	Aspartyl-asparaginyl-beta-hydroxylase
BCM	brain culturing medium
bHLH	basic-helix-loop-helix
Br	Broad
CABLES1/2	CDK5 and ABL1 enzyme substrate 1/2
Cas9	CRISPR associated protein 9
CB	central brain
CBP	CREB-binding protein
ChIP	chromatin immunoprecipitation
CRISPR	Clustered Regularly Interspaced Short Palindromic Repeats
CSL	CBF1-Suppressor of Hairless-LAG1
Dap	Dacapo
dgRNA	double-guided RNA
DLL	Delta-like molecules
Dpn	Deadpan
DSL	Delta, Serrate/Jagged and Lag2
E(spl)	Enhancer of split
ECD	extracellular domain
EdU	5-ethynyl-2’-deoxyuridine
EGF	epidermal growth factor
ESC	embryonic stem cell
ER	endoplasmic reticulum
FACS	fluorescence-activated cell sorting
FBW7	F-box and WD repeat domain-containing 7
Fer2	48-related 2
FLP	Flippase
GMC	ganglion mother cell
Grh	Grainyhead
HDR	homology-directed repair
Hes	hairy/Enhancer of split
HnRNP R	heterogeneous nuclear ribonucleoprotein R
iINP	immature intermediate progenitor cell
Insc	Inscutable
IPC	intermediate progenitor cell
Klu	Klumpfuss
LNRs	Lin-12/Notch repeats

Lola	Longitudinals lacking
MAM	Mastermind
MARCM	mosaic analysis with a repressible cell marker
Mbt	Mushroom bodies tiny
mINP	mature intermediate progenitor cell
Mira	Miranda
NΔECD	Notch receptor with deleted extracellular domain
NB	neuroblast
NE	neuroepithelial cell
NICD	Notch intracellular domain
NR	nutrient restriction
NRE	Notch responsive element
NRNAi	Notch-RNAi
NRR	negative regulatory region
NSC	neural stem cell
OFUT1	O-fucosyltransferase 1
OL	optic lobe
oRG	outer radial glial cell
p4EBP	phosphorylated 4E-BP
PAM	Protospacer Adjacent Motif
PAT	Proton-assisted trasnporter
Path	Pathetic
PEST	peptide sequence enriched in proline(P), glutamic acid(E), serine(S) and theronine(T)
PFA	paraformaldehyde
pGR	pGreenRabbit
Pros	Prospero
RAM	RBPJ-associated module
Su(H)	Suppressor of Hairless
SVZ	subventricular zone
Syp	Syncrip, synaptotagmin-binding cytoplasmid RNA-interacting protein
VNC	ventral nerve cord

Chapter I Introduction

1.1 Notch signalling pathway

The description of typical Notch phenotypes (Notches on the wing margin) was documented in *Drosophila* as early as a century ago (Mohr 1919). Yet not until the 1980s was *Notch* found to encode a transmembrane receptor. In the 1990s the key components of the pathway including the ligands Delta and Serrate (Fehon et al. 1990; Gu et al. 1995), transcription factor Suppressor of Hairless (Su(H)) (Schweisguth & Posakony 1992), and primary targets the *Enhancer of split (E(spl))* genes (Bailey & Posakony 1995; Lecourtois & Schweisguth 1995) were subsequently identified. From studies of these key elements emerged a model of the Notch signalling pathway, a cell-cell contact mediated pathway that is highly conserved. It has since become evident that Notch is an essential signalling pathway involved in many cellular and developmental aspects, including stem cell regulation (Gaiano & Fishell 2002; Yoon & Gaiano 2005; Louvi & Artavanis-Tsakonas 2006).

The canonical Notch pathway activates signalling following the interaction of two transmembrane proteins on adjacent cell membranes: ligand on the signal sending cell and the Notch receptor on the signal receiving cell. Through a series of proteolytic cleavages, the intracellular domain of the Notch receptor (NICD) is released into the nucleus, interacts with the transcription factor CSL (CBF1–Suppressor of Hairless–LAG1; also known as RBPJ; Su(H) in *Drosophila*), recruits the coactivator complex including

Mastermind (MAM), and initiates transcription of target genes (Fig 1.1) (Bray 2006; Bray 2016). In this way the major outcome of Notch activation is a change in transcription. This means that identification of the regulated genes ("target genes") is important for understanding Notch function. In addition, as it is now known that defective Notch signalling contributes to many diseases and cancers such as T-cell leukaemia and glioma (reviewed by Siebel & Lendahl 2017), knowledge of target genes is informative for understanding why dysregulated Notch activity is causal in disease and cancer.

1.1.1 The core Notch pathway

The core players in the Notch-transduction pathway are the same in most Notch-dependent processes. Both Notch ligands and receptors are type I single-pass transmembrane proteins with their N-terminal domains exposed to the endoplasmic reticulum (ER) lumen during synthesis and anchored to the membrane with a stop-transfer sequence (Fig 1.2). There are two *Drosophila* Notch ligands, Delta and Serrate, while the first identified Notch ligand of the nematode is Lag2, therefore the canonical Notch ligands are also known as DSL (Delta, Serrate/Jagged and Lag2) proteins. A number of Notch ligands have also been found in vertebrates, these are either highly homologous to Delta, known as Delta-like molecules (DLL), or are highly homologous to Serrate, known as Jagged, giving a repertoire of 3 Delta-like ligands DLL1, DLL3 and DLL4 and two Jagged ligands (JAG1&JAG2). The ligand extracellular domain is highly conserved in evolution and is required for the interaction of ligand and receptor (Bray 2006; Fortini 2009; D'Souza et al. 2010).

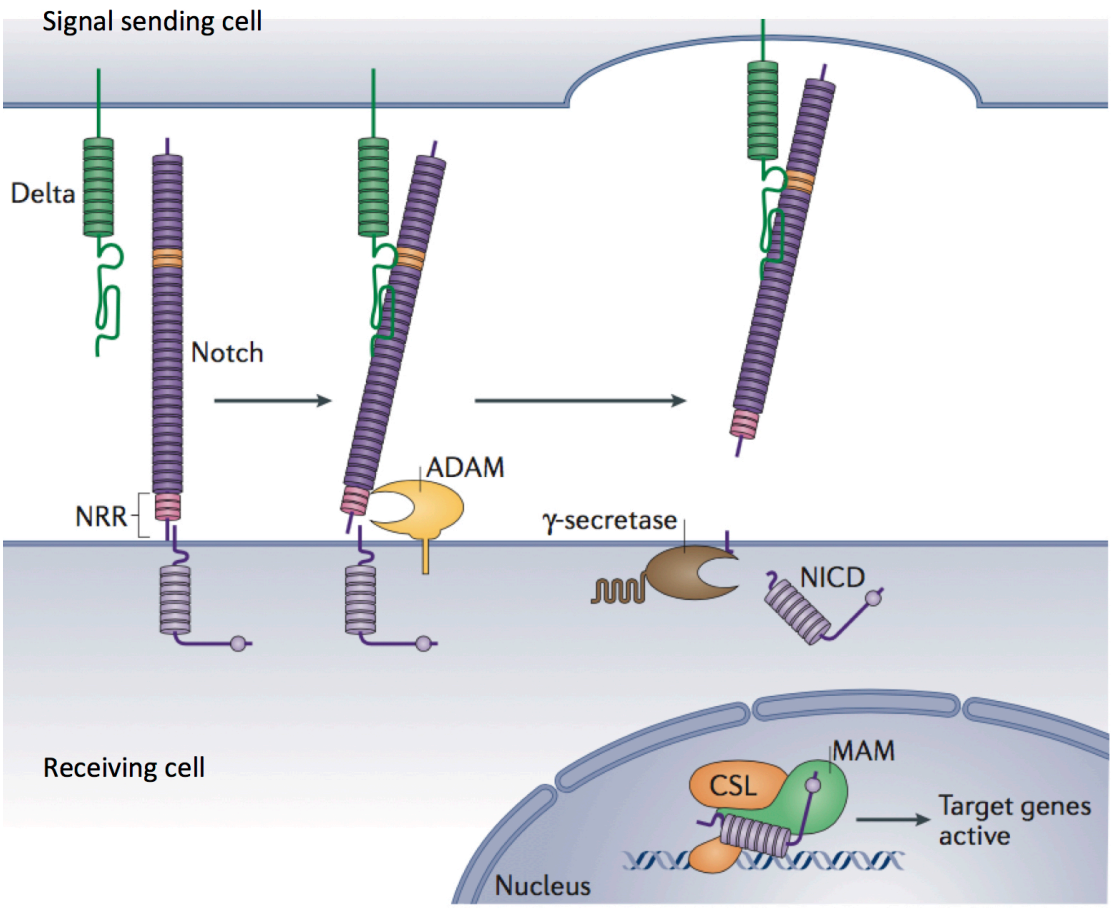

Figure 1.1. Model depicting the core Notch pathway (Bray, 2016). Notch activation includes two proteolytic cleavage steps, which are mediated by ADAM and γ-secretase complex, respectively. Upon Notch ligand binding, the negative regulatory region (NRR) is exposed to ADAM and Notch undergoes first cleavage. Then γ-secretase complex catalyses the second cleavage and releases Notch intracellular domain (NICD) from cell membrane. After nuclear translocation, NICD interacts with CSL and co-activator MAM (Mastermind) to promote the expression of target genes.

Notch is synthesised in the endoplasmic reticulum in a single stranded precursor mode where it can be cleaved by a Furin-like convertase (S1 cleavage) into a large extracellular fragment with a molecular mass of 180,000, and a 120,000 Da small fragment containing the transmembrane and intracellular regions. These associate through Ca^{2+}-dependent noncovalent interactions and it is thought that this heterodimer forms the functional receptor which is then transported to the cell membrane (Weinmaster 2000). Although mammals have four Notch receptors (Notch1, 2, 3 and 4), there is only one in *Drosophila*.

Notch receptors, including *Drosophila* Notch, have a large extracellular domain (ECD) that contains a set of serially linked Epidermal growth factor (EGF)-like repeats and three family-specific LNRs (Lin-12/Notch repeats) (Fig 1.2). EGF repeats play a key role in the binding of Notch receptors to their ligands (Luca et al. 2015). Glycosylation at EGF sites is important for the formation of a functional receptor (N Haines & Irvine 2003; Bray 2006; Stanley 2007). The enzyme O-fucosyltransferase 1 (OFUT1) adds the first fucose and depletion of OFUT1 in *Drosophila* leads to the phenotypes similar to that of loss-of Notch signalling. OFUT1 not only glycosylates the EGF domains of Notch, but also serves as a Notch chaperone required for the trafficking of Notch out of the ER (Okajima 2005). After adding the first fucose, other glycosyltransferases, such as Fringe, further modify the protein by adding more glycosyl residues in the EGF repeats (Moloney et al. 2000). Glycosyl modifications can largely influence the ligand-binding activation of Notch-receptors. In the wing, Fringe potentiates the ability of Delta to activate Notch, but inhibits the Notch-activation ability of Serrate, suggesting that Fringe glycosylation affects binding affinities between ligands and specific EGF domains (Fleming et al. 1997; Panin et al. 1997; Nicola Haines & Irvine 2003; Bray 2006). Indeed, glycosylation has

been shown to contribute to the interaction between ligands and specific EGF domains of Notch by the crystal structure of the interacting regions of the Notch1-DLL4 complex (Luca et al. 2015).

Compared with other signalling pathways, Notch has a simple transduction pathway

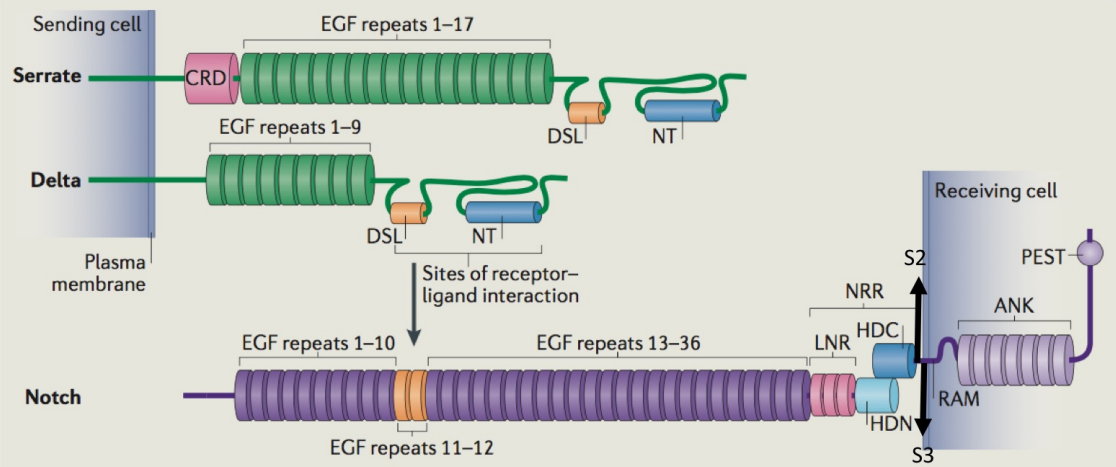

Figure 1.2. Model showing the Notch pathway players in *Drosophila* (Bray, 2016). Both of the two types of Notch ligands Serrate and Delta contain the extracellular Dealta-Serrate-LAG2(DSL) domain and amino-terminal (NT) domain, which interact with EGF repeat in the extracellular domain of Notch receptor. Notch receptor contains a large EGF repeats in the extracellular domain and the NRR on the cell surface, which includes HDN, HDC and cysteine-rich Lin12/Notch repeats (LNR). Upon ligand binding, Notch receptor is cleavaged at S2 and S3 sites and release NICD. NICD consists of RBPJ-associated module (RAM) domain and ankyrin (ANK) repeats, both of which are required to interact with the CSL. The NICD also contains a PEST domain at the carboxyl terminus, which modulates NICD degradation.

without the involvement of second messengers. The negative regulatory region (NRR) of the Notch receptor, which is formed of two heterodimeric parts (HDN and HDC) and cysteine-rich LNRs (Gordon et al. 2007), prevents Notch activation by occluding the cleavage site of the Notch receptor. Notch activation involves two steps of proteolytic cleavage (Fig 1.1). Notch ligand binding leads to the exposure of the cleavage site previously occluded by the NRR to ADAM-family metalloproteases and the Notch receptor undergoes its first cleavage at site 2 (S2, Fig 1.2; the S1 site cleavage by furin-like convertase happens in the Golgi system prior to Notch receptor maturation) upon ligand binding. Upon completion of the first cleavage, the truncated receptor is cleaved

at site 3 (S3 cleavage, Fig 1.2) in the plasma membrane by the γ-secretase complex, which is composed of the enzyme component presenilin, nicastrin, Aph-1 and Pen-2 (Bray 2016; Siebel & Lendahl 2017). Regulation of the activity and localisation of the γ-secretase complex can consequently affect Notch signalling (Bray 2016). After cleavage by the γ-secretase complex, NICD is released from the cell membrane and enters the nucleus to induce the expression of Notch target genes. The endosomal trafficking plays an important role in Notch activation. Upon ligands binding, the dynamic membrane invagination pulls the Notch extracellular domain away and reveals the S2 cleavage site; after the cleavage, Notch receptors are internalized into endosomal routes. Ligand-activated Notch is sorted into multi-vesicular bodies and then to lysosomes for degradation; nonligand-activated Notch can undergo trafficking to the cell surface via recycling endosomes. (Vaccari et al. 2008; Fortini & Bilder 2009).

The NICD consists of an RBPJ-associated module (RAM) domain, ankyrin (ANK) repeats and a PEST domain at the carboxyl terminus. Both RAM and ANK repeats are required for interactions with the DNA-binding complex CSL. The PEST domain regulates the degradation of NICD. Between ANK repeats and PEST, there are nuclear localisation signals and a region with transactivation activity (Bray 2016).

In summary, the core Notch signalling pathway takes a direct route from the cell membrane to the nucleus, and ligand-receptor binding brings about Notch cleavage to release NICD which enters the nucleus to bring about changes in transcription.

1.1.2 Consequences of Notch activation

In the cell nucleus, NICD interacts with CSL to regulate transcription of downstream genes (Fig 1.1). Initially, it was proposed that before Notch activation the enhancers of Notch target genes were silenced by a CSL-corepressors complex, which could recruit histone deacetylases or other modifying enzymes (Kao et al. 1998). The nuclear translocation of NICD was believed to remove corepressors from CSL and activate the enhancers. However, this model has been challenged in many aspects. For example, there is no difference in binding affinity to CSL between NICD and corepressors (KyoT2 and MINT), suggesting that NICD is not able to simply displace the corepressors (Vanderwielen et al. 2011; Collins et al. 2014). Furthermore, increased CSL binding after Notch activation was observed at the enhancers of target genes (Krejčí & Bray 2007; Castel et al. 2013; Wang et al. 2014). Accumulating evidence suggests that the binding of CSL occurs dynamically, so that there is an exchange of different CSL complexes on the DNA (Krejčí & Bray 2007; Housden et al. 2013; Wang et al. 2014).

To confer specificity on the response, it is proposed that in the absence of cooperating transcription factors, CSL binding motifs in chromosomes are hidden by nucleosomes. This may also involve the activity of specific inhibitory transcription factors, such as Hamlet and Ikaros, coordinating with chromatin-modifying enzymes, chromatin-remodelling enzymes and histone chaperones (Endo et al. 2012; Witkowski et al. 2015). In contrast, cooperating transcription factors, such as RUNT-related transcription factor (RUNX) and GATA, are proposed to promote chromatin remodelling to expose CSL-binding motifs (Barbarulo et al. 2011; Skalska et al. 2015). It is suggested that, when complexed with corepressors the interactions of CSL with the exposed DNA motifs in

chromatin are relatively unstable and transient. Once NICD enters the nucleus, it forms a complex with CSL and MAM that has a more stable existence at the CSL-binding motifs (Gomez-Lamarca et al., manuscript under revision). This complex further recruits coactivators including the CREB-binding protein (CBP), which modify chromatin at the target enhancers and stimulate the transcription of target genes. Notch-dependent histone modifications include a widespread increase in histone H3 Lys27 acetylation (H3K27ac) and a decrease in H3K27 trimethylation (Wang et al. 2014; Skalska et al. 2015; Bray 2016).

The levels and stability of NICD are thought to directly determine the levels and duration of transcription. It was reported that the nuclear NICD interacts with F-box and WD repeat domain-containing 7 (FBW7), the substrate-recognition component in a ubiquitin ligase complex, and as a consequence becomes polyubiquitylated and targeted for proteasomal degradation. This degradation is essential to quench Notch activity, and mutations that prevent the interaction with FBW7 result in increased NICD activity in some T-ALL patients, (O'Neil et al. 2007; Kim et al. 2011).

1.1.3 Known Notch targets

The classic Notch target genes, *hairy/Enhancer of split* (Hes) genes are highly conserved, and, just like Notch, they were first described as neurogenic genes in *Drosophila* (like Notch, Delta and Mastermind) because they are required for restricting embryo neural stem cell number (Artavanis-Tsakonas et al. 1999; Anon 1998). Multiple lines of evidence suggest that Hes genes are indeed direct Notch targets in various cell types (Iso et al. 2003; Fischer & Gessler 2007; Zacharioudaki et al. 2012). In mammals, the best characterised Notch target genes are the transcription factors Hes1, Hes5 and Hey1

(Fischer & Gessler 2007; Kageyama & Ohtsuka 1999). Hes1 and Hes5 are important in the early central nervous system (CNS) and act as inhibitors of neuronal differentiation (Shimojo et al. 2008; Siebel & Lendahl 2017). Hey1 is an important Notch downstream gene with a role in endocardial differentiation (Siebel & Lendahl 2017). In *Drosophila*, *E(spl)-C bHLH* genes are important downstream genes of the Notch pathway. Accumulation of E(spl)bHLH proteins is dependent on the activation of the Notch signalling pathway (Jennings et al. 1994), and these proteins in turn carry out many functions of the Notch pathway during neurogenesis, regulating the activity and expression of the proneural proteins (Nakao & Campos-Ortega 1996; Bray 1997).

In *Drosophila*, *E(spl)-C* is a complex locus that contains 12 genes, seven of which (m8, m7, m5, m3, mβ, mγ and mδ) encode bHLH (basic-helix-loop-helix) proteins. These bHLH proteins are themselves transcription factors that bind to DNA via their basic domain and can thus regulate genes e.g. to suppress neural development (Bray 1997; Zacharioudaki et al. 2012). Early evidence that *E(spl)-bHLH* gene expression is directly dependent on Notch came from the observation that their regulation depends on Su(H) (Bailey & Posakony 1995). The upstream regions of all 7 *E(spl)-bHLH* genes contain multiple Su(H) binding motifs, and alteration of these sites hindered the binding of Su(H) (Torella et al. 2014). The proteins encoded by the *E(spl)-bHLH* genes are thus nuclear effectors of the Notch signal which in turn regulate the transcription of other downstream genes to regulate cell fates.

Although the *Hes* genes are important Notch targets in many processes they cannot fully account for the diversity of Notch responses. Therefore, further functional study of potential target genes is needed to gain an understanding of Notch-related physiological

and pathological processes, for which the identification of Notch targets is a prerequisite.

1.2 Genome-wide approaches to identify diverse Notch targets

In order to identify Notch target genes, CSL/Su(H)-binding sites in the *Drosophila* genome have been predicted with a computational approach using whole-genome sequence data (Rebeiz et al. 2002). Furthermore, genome-wide chromatin immunoprecipitation (ChIP) analysis technology allows us to explore the binding of CSL/Su(H) to enhancers in the whole genome. Using genome-wide ChIP analysis, not only binding sites close to the transcription start site could be identified (for example in Hes1 and Hey1), but also the distal binding sites (Siebel & Lendahl 2017). Indeed, it was reported that around 90% of CSL binding sites in T-lymphoblastic leukaemia cells located distally (>2kb) (H. Wang et al. 2015). In addition, two different configurations of CSL binding sites have been observed through genome-wide ChIP: solitary recognition sites and sequence-paired sites (frequently head-to-head CSL binding sites) (Arnett et al. 2010). The sequence-paired sites contribute about 30% of Notch target gene binding sites in T-lymphoblastic leukaemia cells (Severson et al. 2017).

Utilising a combination of the genome-wide CSL ChIP and expression arrays, putative Notch target genes have been identified in different cells/organs from distinct organisms, including *Drosophila*, human and mouse (Wang et al. 2011; Alexandre Djiane et al. 2013; Zacharioudaki et al. 2016; Severson et al. 2017). By comparing the ChIP data, considering the simple signalling pathway the high diversity in the signalling outputs is surprising, even in different tissues from the same organism. For example, there are only

nine overlapping genes between 246 putative Notch target genes identified in NSCs hyperplasia and 278 putative target genes found in epithelial hyperplasia (Kannan et al. 2013; Zacharioudaki et al. 2016), suggesting that Notch signalling is highly dependent on the context. This explains why such a simple signalling pathway could exert distinct functions in different contexts. For example, it could promote tumorigenesis in breast cancer and T-cell acute lymphoblastic leukaemia or act as a tumour suppressor in lung adenocarcinoma and B-cell malignancies (Zweidler-McKay et al. 2005; Robinson et al. 2011; Hassan et al. 2013; Witkowski et al. 2015).

Many different regulatory mechanisms have been shown to contribute to the context-dependency of Notch activity, including the receptor-ligand landscape, tissue topology, the nuclear environment and cross-talk with other signalling pathways (Bray 2016).

1.3 Role of Notch signalling in neural stem cells

1.3.1 Neural stem cells

In 1992, Reynolds isolated a population of cells from the mouse striatum that could proliferate *in vitro* and had multiple differentiation potentials *in vivo*, and formally proposed the concept of neural stem cells (NSCs) (Reynolds 1992). NSCs are cells that can divide and differentiate into all kinds of cells within the brain while they self-renew. In mammals, neural stem cells are called neuroepithelial cells (NEs), they initiate from the neuroepithelium and persist throughout the whole life, from embryonic development to adult brain. Before neurogenesis, NEs maintain the stem cell pool through symmetric division. During neurogenesis, NEs acquire glial markers and become

radial glia cells (RGs) which hereafter divide asymmetrically. In rodents, one RG could divide and directly become a daughter RG and a postmitotic neuron (direct neurogenesis). In other cases, one RG might divide into a daughter RG and an intermediate progenitor cell (IPC) with less differentiating potential. An IPC usually forms a pair of neurons through one final division (indirect neurogenesis). In many mammals including primates, a further step is introduced to generate many more neurons: asymmetric division of RGs to outer radial glial cells (oRGs), which undergo multiple asymmetric divisions to form a pool of IPCs and in this way generate a large number of neurons (Homem et al. 2015) (Fig 1.3C). Neural stem cells are responsible for generating multiple types of neurons and remain potent through rounds of asymmetric divisions. Different mechanisms are adopted for maintaining NSC pools during early CNS development and in adults (Homem et al. 2015).

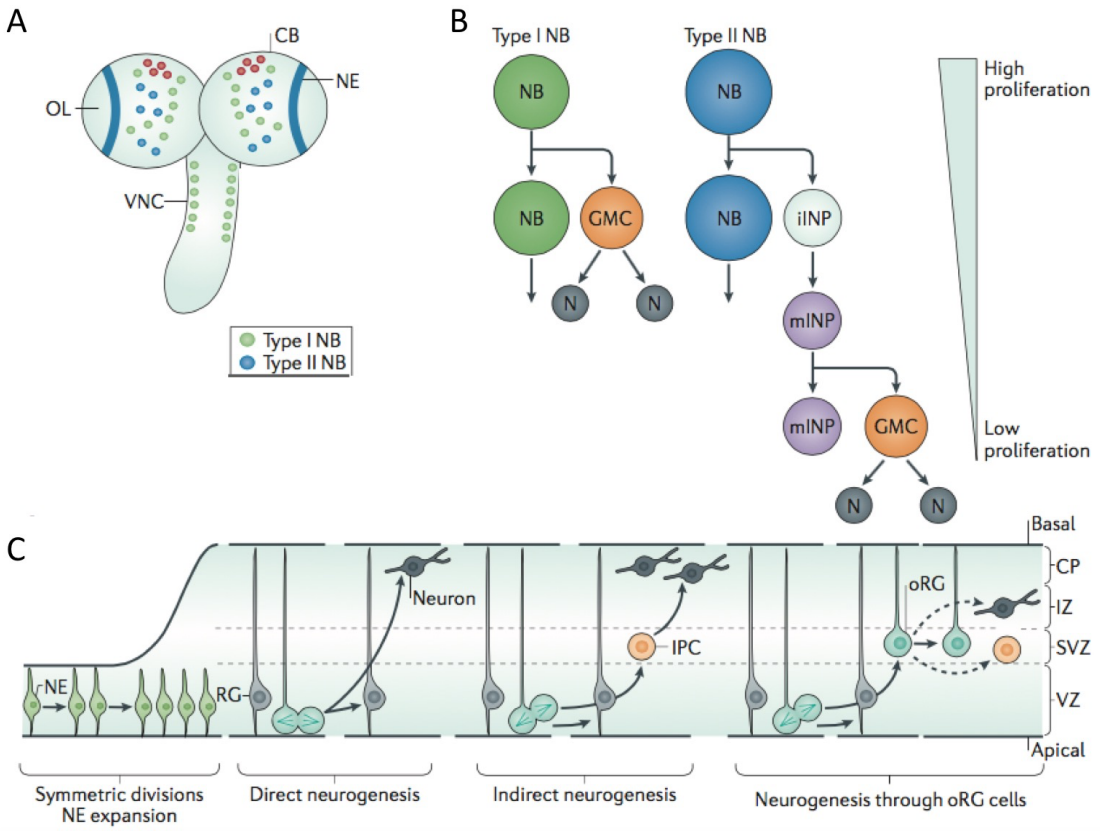

Figure 1.3. Neural stem cell types in *Drosophila* and mammal (Adapted from Homem et al. 2015). (A) *D.melanogaster* 3rd instar larval brain that consists of central brain (CB), optic lobe (OL) and ventral nerve cord (VNC). (B) *Drosophila* neural stem cell types and their lineages. Type I NBs (green), divide once to self-renew and generate a Ganglion Mother cell (GMCs).Type II NBs (blue) generate Intermediate Progenitors(INPs) that transform from inmature INPs to mature INPs and then divide into GMCs. (C) Mammalian neurogenesis types. Neuroepithelial cells (NEs) undergo symmetric divisions to maintain the stem cell pool. Radial glial cells (RGs) are transformed from NEs and undergo direct neurogenesis to become neurons, indirect neurogenesis to generate intermediate progenitor cell (IPC), or divisions to generate outer radial glia cells (oRGs) which further divide into IPCs or neurons. CP, corticalplate; IZ, intermediate zone; SVZ, subventricular zone; VZ, ventricular zone.

1.3.2 Notch signalling in neural stem cells

Notch signalling is one of the key regulators in regulating early CNS development. In vertebrates, the CNS develops from the neuroepithelium in the neural tube, where NSCs first give rise to neurons and in a subsequent step to astrocytes and oligodendrocytes (Siebel & Lendahl 2017). Notch signalling plays an essential role in maintaining an NSC pool during the development of the vertebrate CNS (Chitnis et al. 1995; Dunwoodie et al. 1997; Jen et al. 1997). Conditional knockout of CSL in the mouse embryonic brain causes premature differentiation in almost all NSCs (Imayoshi et al. 2010) and similar results were also observed in loss of Notch activation mutants (Yoon et al. 2008; Chi et al. 2012). Hes1 and Hes5 are two important Notch target genes in the early CNS, which inhibit neuronal differentiation (Kageyama et al. 2015). In addition, the stemness maintenance role of Notch in the early CNS is also supported by the *in vitro* human embryonic stem cell (ESC) differentiation assay. Before differentiating into neurons, ESCs have an intermediate state, the neural rosette stage, and loss of Notch activation ablates this neural rosette stage, resulting in accelerated neuronal differentiation (Elkabetz & Studer 2008).

Notch is not only important for maintaining the NSC pool during embryonic CNS development, but also for regulating NSCs behaviour in postnatal and adult brains. NSCs in the postnatal mammalian brain self-renew and are a source of neurons and glia. In postnatal mouse brains, Notch and its components are expressed in the NSC populations, including those in the subventricular zones (SVZs) (Stump et al. 2002; Nyfeler et al. 2005). *In vitro*, endogenous Jagged1 promotes NSC maintenance and multipotency by activating Notch signalling. On the other hand, suppressing Jagged1/Notch1 signalling

reduces cell proliferation in postnatal mouse SVZs *in vivo* (Nyfeler et al. 2005). These results suggest that Notch activation is required for NSC self-renewal in the postnatal brain (Nyfeler et al. 2005). Similarly, in postnatal mouse telencephalon, in the absence of endogenous and exogenous growth factors (including EGF), only the Notch signalling pathway was sufficient to alternatively support NSC self-renewal. This suggests that for NSCs, the Notch pathway has a similar effect to certain growth factors, or it can promote the production of relevant growth factors by itself (Stump et al. 2002). In the mammalian adult brain, NSCs are found in the SVZs near the ventricles and in the dentate gyrus of the hippocampus (Gonçalves et al. 2016). Consistently, Notch signalling is also active in these adult NSCs and plays an important role in their self-renewal and maintenance (Ehm et al. 2010; Imayoshi et al. 2010; Siebel & Lendahl 2017). Loss of Notch1 or CSL causes the depletion of NSC pools in the SVZs (Basak et al. 2012). Similarly, NSCs depletion is also observed in the CSL-ablated dentate gyrus (Lugert et al. 2010). In addition, when the inhibitors of the Notch pathway were applied to NSCs *in vitro*, the number of NSCs was significantly reduced, resulting in the formation of smaller neurospheres. In these cases, when Notch is compromised, the number of mitotic NSCs are greatly reduced (Pierfelice et al. 2011), indicating that loss of Notch signalling increases the number of NSCs exiting the cell cycle and reduces the number of precursor cells. In contrast, over-expression of Notch and its target genes (Hes1&5) promotes NSC proliferation, resulting in more NSCs and larger neurospheres, suggesting that high levels of Notch activation can promote the proliferation and self-renewal of NSCs and inhibit their differentiation (Jeon 2011).

Besides its role for maintaining self-renewal of NSCs, Notch also strikes a critical balance on NSC fate decisions. NSCs, in vertebrates, can differentiate into oligodendrocytes, astrocytes and neurons while maintaining self-renewal in a timely manner. The process of regulating NSC differentiation involves two steps. The first step is to commit to a differentiation fate rather than remaining as stem cells, and the second step is selective differentiation into specific cell types, neurons or glial cells. This differentiation is regulated temporally and spatially. In the stem cell-promoting state, Notch signalling inhibits neurogenesis through its downstream target Hes1, which blocks the expression of the neurogenesis driver Neurogenin1. When astrocytes need to be produced by CNS differentiation, Notch can switch NSCs to promote gliogenesis (Furukawa et al. 2000; Gaiano et al. 2000; Siebel & Lendahl 2017). The mechanism underlying the function shift is still unclear. Some studies further suggest that normally neurogenesis precedes gliogenesis in the lineages analysed (Sun et al. 2001). Consistent with this finding, the differentiation of glial cells was significantly inhibited during the differentiation of NSCs into neurons. The role of Notch in these fate decisions is controversial, in some cases it was found to promote the differentiation of NSCs into certain cell types, such as astrocytes (Ge 2002) or glia (Pierfelice et al. 2011) , while in others no effect on NSC differentiation was found (Nyfeler et al. 2005).

One possible explanation is the temporal control of differentiation. Altering Notch at different stages of development of the early postnatal brain might generate different or seemingly contrary results. In addition, it is also worthwhile to note the different ways of manipulating the Notch pathway in these studies, for example the earlier *in vitro* experiments (Nyfeler et al. 2005) are often not consistent with more recent studies

using *in vivo* manipulations. Differentiation regulation involves more readable outputs (different end cell types) than proliferation regulation (which only involves a binary choice of more growth or less). So it is also likely that proliferation regulation is also more complex than what can be easily read using the limited markers. One result of Notch promoting proliferation can be a synergy of different events: more mitotic cycles, higher mitotic rates, less cell death, etc.

A similar model may apply in *Drosophila* and mammalian NSCs. Over-activation of Notch signalling in *Drosophila* and in mammalian NSCs induces brain tumours, while reducing Notch signalling causes a reduction in NSC number (Wang et al. 2006; Wang et al. 2007). Therefore, a well-controlled activity of Notch is a necessity for NSC self-renewal and for preventing NSC over-proliferation. However, it is not fully clear what mechanisms are implemented by Notch activity to carry out these functions and maintain a stable balance between proliferation and differentiation in NSCs. Notch signalling regulates NSC behaviours through inducing the expression of its various downstream targets depending on the cellular context. Therefore, looking into Notch function more deeply and widely by revealing more potential Notch targets, would be helpful in uncovering the regulatory network through which Notch helps to maintain NSCs.

1.3.3. Role of Hes genes and other Notch target genes in NSCs

The regulatory effects of the Notch signalling pathway are likely to be carried out through precise activation of target genes dependent on cellular context. As discussed above, the Hes gene family was among the first identified Notch targets (Roese-Koerner,

Stappert et al. 2017) and this group of target genes helps to implement the effects of Notch activity on proliferation and differentiation of neural precursor cells. For example, Hes1 and Hes5 inhibit neuronal differentiation, and their loss results in premature neurogenesis in mice (Ohtsuka et al. 2001). However, contrary to most contexts, when the effects of polyunsaturated fatty acids on the differentiation of NSCs was investigated, Hes6 appeared to promote neurogenesis and differentiation (Katakura 2013). These results suggest that different Hes genes have different roles in regulating NSC behaviours, which might also be affected by metabolic conditions. In *Drosophila*, *E(spl)mγ-HLH*, a Hes family gene, is one significant target of Notch signalling in NSCs (Almeida & Bray 2005). However, mutations removing the entire *E(spl)* locus of Notch target genes only have minor effects on NSC maintenance, suggesting there are further downstream targets (Zacharioudaki et al. 2012). In *Drosophila*, Klumpfuss (Klu), a zinc-finger protein is also regulated directly by Notch in NSCs, and over-expression of *klu* causes similar hyperplasia (Berger et al. 2012; Xiao et al. 2012). Deadpan (Dpn), another bHLH protein in *Drosophila*, has been shown to work in Notch dependent and independent mechanisms to regulate NSC self-renewal (San-Juán & Baonza 2011; Babaoğlan et al. 2013). Thus it seems likely that an array of targets will act in combination to mediate the effects of Notch in these cells.

To identify other NSC Notch targets, a strategy was taken to analyse the genes that were upregulated during Notch hyperactivation in the *Drosophila* brain. This successfully revealed more putative direct Notch targets including transcription factors and various genes associated with NSC maintenance (Zacharioudaki et al. 2016). These included a group of temporal genes, providing an explanation for how Notch could regulate stem

cell and neuron identity, in a strict timely manner. Other genes from this analysis have yet to be characterised and might similarly contribute to NSC behaviours.

1.4 Model: *Drosophila* Neural stem cell

Drosophila melanogaster is an ideal model for studying complicated biological events, including Notch signalling, in the nervous system, because it is a relatively simple organism and shares many similar features and pathways with vertebrates, including humans (Chintapalli et al. 2007; Bellen & Yamamoto 2015). It has been shown that approximately 60% of identified protein-coding genes in *Drosophila* have a counterpart in human (Bellen & Yamamoto 2015). Furthermore, it is easy to keep and work with *Drosophila*, because of its short life cycle, ease of maintenance, low number of chromosomes and small genome size (Homem & Knoblich 2012; Osterfield et al. 2017). Many of the gene functions in vertebrates were first identified in *Drosophila* (Chintapalli et al. 2007). *Drosophila* also serves as an ideal model for studying stem cell biology, including NSCs. Indeed, the hypothesis that Notch activation in vertebrates would inhibit neuronal differentiation was first derived from classic fly genetic studies (Artavanis-Tsakonas et al. 1995; Siebel & Lendahl 2017). The realisation that Notch signalling performed a similar function during both fly and vertebrate neural development led to the identification of many vertebrate orthologues of fly pathway components that, for the most part, exhibited functions predicted by their roles in flies (Pierfelice et al. 2011). Therefore, for a number of years the NSC field was dominated by studies drawing parallels between Notch function in flies and vertebrates.

Stem cells continue to proliferate and generate differentiated progeny during an adult lifetime and throughout the time of tissue growth. How they can maintain this "stemness" has been a long pursued topic. *Drosophila* post-embryonic NSCs, also called neuroblasts (NBs), persist throughout larval life. Their similarity to mammalian NSCs, their comparative simplicity and the versatile tools available for probing gene function (Lin & Schagat 1997; Wodarz & Huttner 2003; Chia et al. 2008), make them a powerful model for investigating how stem cells are maintained. Therefore, *Drosophila* NBs serve as an ideal model for stem cell research.

Drosophila NBs arise from neuroectoderm during embryonic development and enter quiescence at the end of the embryonic stage, until early larval stage where the NBs are reactivated by feeding and enter mitosis (Chell & Brand 2010; Sousa-Nunes et al. 2011). From then on, around 200 NBs reside on the dorsal and ventral surface of the brain and constitute the stem cell pool. They undergo multiple rounds of asymmetric cell division, generating one larger daughter cell that retains stem cell identity (neuroblast) and one smaller daughter cell that divides to generate daughter cells that differentiate into different types of neurons (Boone & Doe 2008). There are two types of NSCs in *Drosophila*: Type I NBs can be identified by the expression of Deadpan and Asense (Bowman et al. 2008) and they constitute the majority of the NSC pool in the brain. These type I NBs undergo asymmetric division to form a renewed NB and a Ganglion Mother Cell (GMC), the latter going on to divide once and differentiate into a certain type of neuron or glia, mimicking the indirect neurogenesis of mammals. Type II NBs express Dpn but not Asense (Ase) and are relatively few in number, with eight on each of the dorsal brain lobes. A Type II NB initially divides asymmetrically into an immature

intermediate neural progenitor (iINP) as they self-renew, and the iINP then undergoes maturation before it becomes a mature INP (mINP) which divides a limited number of times to regenerate and form a GMC. This GMC, like GMCs from type I NBs, enters the final division to generate a neuron or a glia (Bello et al. 2008; Boone & Doe 2008; Bowman et al. 2008). The division route of Type II NBs is remarkably similar to neurogenesis in primates (Homem et al. 2015) (Fig 1.3). Thus, tight regulation of asymmetrical division is important for both types of NBs in *Drosophila*.

Two major mechanisms contribute to the asymmetric cell division of NBs. First, there is asymmetric expression of transcription Factors (TF) in the NB and GMCs. Worniu (Cai, Chia et al. 2001, Lai, Miller et al. 2012), Dpn (San-Juan and Baonza 2011, Zacharioudaki, Magadi et al. 2012), Ase (Wallace, Liu et al. 2000, Southall and Brand 2009) and Klu (Berger et al. 2012) are only expressed in NBs and are depleted in GMCs. In contrast, Prospero is concentrated in the nucleus of the GMC to promote neuronal differentiation (Spana & Doe 1995; Li et al. 1997). Second, a group of proteins becomes asymmetrically distributed in dividing NBs to define the “bigger” and “smaller” daughter cells by positioning the spindle. An asymmetric segregation of protein complexes occurs in the NB before it divides: these include an apical complex which defines the cell that will become the NB (comprising Bazooka, Cdc42, aPKC and Inscutable (Insc)); and a basal complex which defines the differentiating daughter cell (comprising Miranda, Numb, Lethal giant larva , Prospero and Brat), reviewed by (Doe 2008). Among other important functions of this basal complex, Numb inhibits Notch activity in the GMC.

In order to generate sufficient progeny, the NB needs to repeatedly enter the cell cycle, as early exit of the cell cycle will cause NB loss. dMyc and eIF4E were found to be crucial

for the control of neuroblast growth (Song & Lu 2011). dMyc prevents NB loss caused by Notch inhibition, and it has been shown to be a downstream target of Notch. Furthermore, NBs need a continual programming of macromolecular synthesis to keep their size, otherwise after rounds and rounds of division they will become smaller and smaller. For example, the p21-activated kinase Mushroom bodies tiny (Mbt) was reported to be important for maintaining NB cell size, and loss of which resulted in reduced cell size and impaired NB proliferation (Neumuller et al. 2008; Melzer et al. 2013), suggesting that a critical and minimal cell size is required for cell division.

castor (*cas*) and *seven-up* (*svp*), two members of the temporal control genes, were shown to schedule a switch in the cell size and identity of neurons involving the targets Chinmo and Broad Complex (Zhu et al. 2006; Maurange et al. 2008). The growth and size control of NBs is also regulated by nutrition and metabolism state. Under nutrient restriction (NR) condition, anaplastic lymphoma kinase (Alk) was shown to efficiently protect larval NB growth against reductions in amino acids and insulin-like peptides (Cheng et al. 2011). This function of Alk is achieved by suppressing the growth requirement for amino acid sensing via Slimfast/Rheb/TOR pathway as well as activating PI3-kinase signalling (Cheng et al. 2011). Further studies showed that cell size control in NBs could be modified by steroid hormone ecdysone signalling, which could induce changes in energy metabolism, and losing such control of cell size would result in the final loss of NBs (Homem et al. 2014). More recently, from genomic profiling of Notch target genes, a group of genes was identified that could contribute to hyperplasia in conditions of Notch hyperactivity (*grh, wor, mira, numb, svp, cas, hth, Klu, dm*) (Zacharioudaki, et al. 2016), showing that Notch can induce NB hyperplasia through

directly regulating targets that are responsible for NB identity and temporal control of NB maturation. However, the regulatory network for controlling NB size and determining NB identity is still not completely understood.

Many NB effectors have different impacts on type I and type II NBs. For example, Notch, Dpn and Klu are essential for type II NB maintenance, as loss of one of them results in complete loss of type II NBs. However, they only have a mild effect or no effect on type I NB survival. On the other hand, over-expressing these factors in type II NBs generates tumour-like hyperplasia, while type I NBs need longer expression of these genes to over-proliferate, or exhibit less severe phenotypes (Berger et al. 2012; San-Juán & Baonza 2011; Lee et al. 2013). Comparing to type II NBs, the mechanisms maintaining type I NBs are less well known.

Although a number of signalling pathways and molecules that contribute to NB maintenance have been identified, the full extent of the network that regulates NB division and survival remains far from fully understood. Furthermore, it would be interesting to investigate whether there are additional Notch target genes accounting for NB maintenance.

1.5 Aim of the study

The major question in this study is whether existing Notch target genes perform all the effects of Notch or whether more, as yet unknown genes are needed to form the regulatory network that supports the function of NBs. The aim of my project has been to investigate putative targets of Notch and to determine whether they help to interpret

the regulatory mechanisms of NB self-renewal and proliferation. To achieve this I have been using data from genome-wide Su(H) chromatin immunoprecipitation combined with the mRNA expression changes that occur in Notch over-expressing brain tumours (Zacharioudaki et al. 2016). Genes that are directly bound by Su(H) and that have a significant up-regulation in mRNA level after Notch activation are candidates to mediate the function of Notch in brain cells. By investigating these novel Notch targets, I aimed to further understand how Notch helps NBs maintain themselves, and how the hyperplasia observed when over-expressing Notch is induced. Due to conservation of the pathway, these targets may offer a better insight into mammalian NSC regulation and have implications for tumour growth.

Chapter II Materials and Methods

2.1 Materials

Reagents used in the study are listed in Table 2.1.

Antibodies are listed in Table 2.8.

Fly stocks are listed in Table 2.3.

Primers are listed in Table 2.2, 2.5, 2.6 & 2.7.

2.2 Molecular Cloning

Su(H) bound regions of candidate genes (*path, CG6191, syp, Asph, lola, Fer2*) were cloned from *Drosophila* genomic DNA using primers with restriction site ends (Table 2.2) into pGL3 or pGreenRabbit (pGR) vectors (Housden et al. 2012), for luciferase assays or *in vivo* examination respectively.

2.2.1 PCR reaction

PCR mix:

DNA (100ng/µl)	1 µl
10 X Buffer	5 µl
25 mM $MgCl_2$	1.5 µl
10 mM dNTPs	1 µl
Forward primer (10pM)	1 µl
Reverser primer (10pM)	1 µl
Taq DNA Polymerase	0.5 µl
Double distilled H_2O (ddH_2O)	39 µl (up to 50 µl)

PCR program:

96°C	2 minutes (mins)	
95°C	30 seconds (secs)	30 cycles (35 cycles for PCR screening)
56°C	30 secs	
72°C	1 min per kb	
72°C	10 mins	
4°C	Forever	

PCR product purification:

The size of PCR products was examined by agarose gel electrophoresis. After that, ddH_2O was added to the PCR products to make 200 µl final volume and equal volume of phenol:chloroform:isoamylalcohol (25:24:1) was added. Then, the mixture was vortexed and centrifuged at 12,000 rpm for 3 mins. 180 µl of the top layer was transferred to a new tube and 180 µl chloroform:isoamylalcohol (24:1) was added. The mixture was vortexed and centrifuged at 12,000 rpm for 3 mins. 150 µl of the top layer was transferred to a new tube and 375 µl 100% ethanol (2.5 X Vol) and 15 µl NaAc 3 M pH 5.2 (1/10 X Vol) were added. The mixture was vortexed and kept at -80°C for 1 hour, then centrifuged at 12,000 rpm for 15-30 mins at 4°C. The resulting pellet was washed with 1 ml 70% ethanol and centrifuged at 12,000 rpm for 5 mins at 4°C. Then ethanol was removed and the pellet air dried before resuspension in 30 µl ddH_2O.

PCR product and vector digestion and ligation:

Vector/ PCR product	1 µl (500ng)/10 µl
10 X buffer	5 µl
BSA	0.5 µl
Restriction endonuclease 1	1 µl
Restriction endonuclease 2	1 µl
ddH_2O	Make up to 50 µl final volume

The digestion mixtures were incubated at 37°C overnight. The digested vector was dephosphorylated with 2 µl alkaline phosphatase plus 5 µl ddH_2O and 3 µl alkaline phosphatase buffer, and incubated at 37°C for 1 hour. Then the enzymes in the PCR product and vector digestion mixtures were denatured at 65°C for 20 mins. The digested vector and digested PCR products were purified by phenol chloroform extraction as described above and mixed before ethanol precipitation of the DNA. The pellet was resuspended in 10 µl ddH_2O, and its concentration was measured by NanoDrop. Then the vector and PCR product (8 µl) were ligated by 1 µl ligase plus 1µl ligase buffer overnight at 16°.

2.2.2 Ligated product transformation

1-4 µl of ligated product was mixed with 50 µl *E.Coli* competent cells and kept on ice for 30 mins. The cells were then heat shocked at 42 °C for 45 secs and left on ice for 2 mins. Then 1 ml SOC, 5µl 25 mM $MgCl_2$ and 20 µl 1 M glucose were added to the cells, incubating at 37°C with shaking. After 1 hour, the cells were spun down at 12,000 rpm

for 15 secs, and resuspended in 100 µl remaining medium. The cells were then spread onto a selective agar plate and grown at 37°C overnight.

Colony selection and screening: Eight colonies were streaked onto a new plate and grown overnight. The colonies were screened by PCR with 1 µl 10 X buffer, 0.3 µl 25mM $MgCl_2$, 0.2 µl 10mM dNTPs, 0.2 µl forward primer (10pM), 0.2 µl reverse primer (10pM), 0.1 µl Taq DNA Polymerase and 8 µl ddH_2O, using the PCR program described above. Agarose gel electrophoresis was used to examine the size of the PCR products and positive colonies were picked and grown overnight in LB liquid medium at 37 °C. The selected ones were further confirmed by restriction enzyme double digest and sequencing.

2.2.3 Motif point mutagenesis

Mutagenesis was carried out using Pfu Turbo DNA polymerase Kit to mutate high-affinity Su(H) binding sites. The high-affinity Su(H) binding sites are usually in the form of CGTGGGAA or TTCCCACG, and the underlined nucleotides were altered to CGAAGTTA or TAACTTCG to decrease the affinity of Su(H) binding. Primers for mutagenesis are listed in Table 2.2. These primers were designed as complementary to opposite strands of the vector with mutations at the Su(H) binding sites, generating a mutated plasmid with staggered nicks. The PCR reaction listed below was used. 1µl DpnI was added to the PCR product and incubated overnight at 37^{o}C to remove the template plasmids. Then 2 µl of the digested product were transformed into *E. coli* and the mutated plasmids were confirmed by sequencing.

Mutagenesis PCR mix:

DNA (100 ng/µl)	1 µl
10 X Pfu Buffer	5 µl
Pfu	1 µl
10 mM dNTPs	1.5 µl
Forward primer (10 pM)	1 µl
Reverser primer (10 pM)	1 µl
ddH_2O	39.5 µl

Mutagenesis PCR program:

96°C	2 mins	
96°C	30 secs	}
50°C	40 secs	} 18 cycles
68°C	16 mins (2 mins per kb)	
72°C	10 mins	
4°C	Forever	

2.3 Cell Culture and Luciferase Assay

Luciferase assays were performed in *Drosophila* S2 cell line. S2 cells were cultured in Schneider's medium in a 90 mm dish at 25°C until they reached 70-80% confluency. The cells were resuspended in 20 ml medium and 500 µl cells were added into each well of a 24-well plate and left at 25°C for 40 mins while preparing the reagent mix. Opti-MEM and Renilla were mixed well. Renilla plasmid was used as internal control in each well, along with NICD as a Notch-activated positive control and PMTA as a negative control (Fig 2.1). The mixture was left at room temperature (RT) for 5 mins. Fugene was added to the DNA mix (80 µl DNA + 56 µl Fugene) and left at RT for 30 mins. 250 µl medium from each well was removed without disturbing the cells. 65 µl transfection mix was

added into each well (each DNA mix was transfected into 2 wells for technical replicates). The cells were incubated at 25°C for 6 hours (hrs) and then the cell medium was replaced with 0.5 ml fresh medium with 1.5 µl CuSO4 (0.5 mM) per well. After 18 hrs incubation at 25°C, the cells were harvested for measurement using the dual-luciferase reporter assay system: 50 µl of 1 X lysis buffer was added to each well and mixed on the rocker for 10-15 mins. 50 µl/well Luciferase and 50 µl/well of Renilla reagent (Stop and Glow solution added to 1x concentration) were transferred into two glass bottles and mixed well. 45 µl of luciferase reagent and 5 µl of sample were mixed in a cuvette and the Renilla measurements were recorded. Then 45 µl of Renilla reagent was added to the same cuvette, mixed and then the luciferase measurements were recorded. The ratio between luciferase and Renilla measurements were automatically calculated. Two technical replicates were measured each time, and in total three biological replicates were performed to generate an average result.

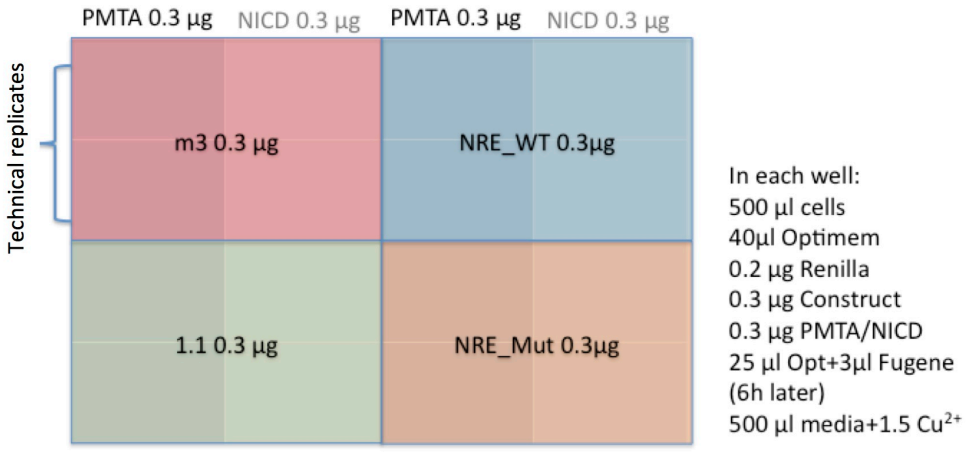

Fig 2.1. Cell transfection system for luciferase assay.

2.4 Fly Husbandry and Genetics

Unless otherwise stated, flies were reared on standard cornmeal media at 25°C. Table 2.3 provides detailed information of all fly strains used in this work.

2.4.1 Generation of Transgenic NRE-GFP flies

To transfect enhancers into flies, the fragments were cloned into pGR vector including the AttB sites, following stated procedures in the reference (Housden et al. 2012). Then the constructs were sequenced and midiprepped for injection. The plasmids were injected into fly embryos containing AttP platform on the 3rd Chromosome (Φ86fb). The injections were performed by Kat Millen. Transgenic fly larvae were collected in the following 48h, transferred to fresh fly food and cultured at 25^{o}C. After 10-12 days, adult male flies were collected and crossed to virgin female *yw* flies. Transgenic F1 flies were selected based on eye colour (red or orange from *w+*) and were subsequently crossed with *w; TM3/TM6B*. *NRE-GFP/TM6B* F1 flies were selected and mated to siblings to produce homogeneous *NRE-GFP/TM6B* flies.

Removal of the RFP platform: Virgin female *yw, cre* flies were crossed to male *NRE-GFP/TM6B* flies. Male F1 expressing CRE were crossed to virgin female *w; TM3/TM6B* and male *NRE-GFP/TM6B* selected to remove CRE. These were crossed again to *w; TM3/TM6B* and homogeneous CRE-cleaned transgenic flies selected. Transgenic fly stocks generated in this study and information about the insertions are listed in Table 2.4.

2.4.2 Gal4/UAS system

Gal4/UAS system is a powerful modulator of gene expression derived from yeast and widely used in model organisms (Fischer et al. 1988; Brand & Perrimon 1993). The system contains two elements: The Gal4 lines with specific expression patterns; and the UAS (Upstream Activation Sequence) that can bind to the Gal4 and activate gene transcription (Fig 2.2A). With this system, one can easily induce expression or RNAi knock down in specific cells with desired UAS lines.

2.4.3 MARCM system

To better analyse gene effects in a cell-autonomous manner, MARCM (Mosaic analysis with a repressible cell marker) system was used in experiments. The MARCM system was first developed for studying the *Drosophila* nervous system, as it allows positive marking of the homozygous mutant cells in a heterozygous background (Wu & Luo 2007). This technique combines both the UAS-Gal4 system and FLP/FRT recombination system. The TubGal80 suppresses expression of tubGal4, which inhibits the expression of UAS-nlsGFP. Upon expression of Flippase (FLP), recombination takes place in mitotic cells and by chance the TubGal80 and TubGal4 are allocated into different daughter cells. As a result, the cells without Gal80 express GFP while having both copies of the desired mutation. In this way one can observe phenotypes generated by homozygous mutation without causing lethality (Fig 2.2B).

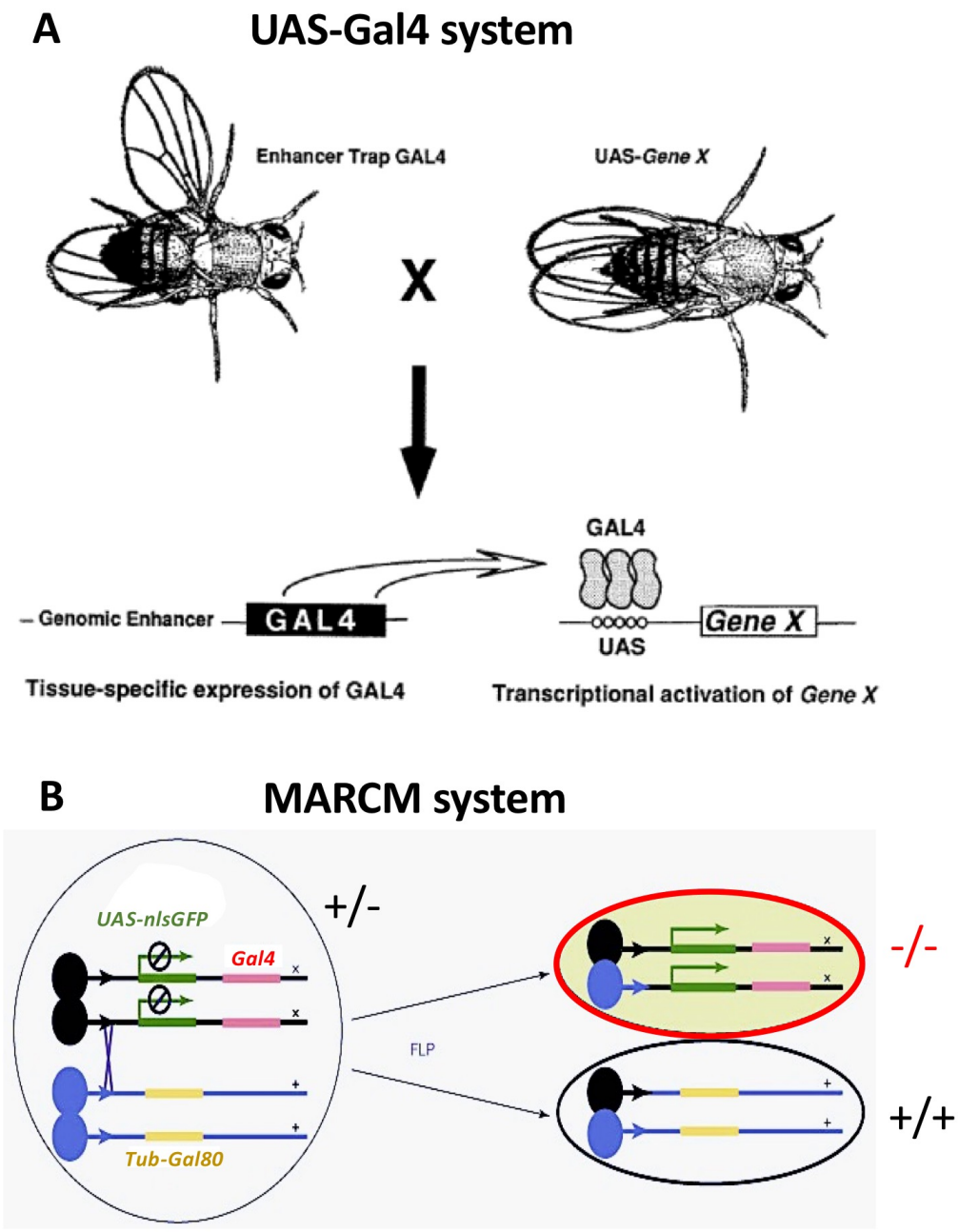

Fig 2.2. Fly genetic manipulations. (A) UAS-Gal4 system (Brand & Perrimon 1993) . (B) MARCM system (Adapted from Wu & Luo 2007).

2.4.4 Nutrition restriction treatment

In order to test the response of larval brain growth to nutrition restriction, flies were given a sucrose-only diet regime, conducted as follows: on day 1, set up cages with crosses (>50 flies); on day 2, flip the cages and save the embryos; on day 3, 24h after larval hatching (ALH), select and transfer hatched larvae to control or NR condition plates with 100-150 larvae in each plate. On day 4-6, add enough yeast to control condition every day, keep the plates in a humidified box and add adequate water to the plates once a day or upon need. On day 6, 96h-120h after larvae hatching, dissect larvae from the two conditions.

Control condition :

100ml Apple juice plates (for 8-9 plates):

Agar 2.66 g

Apple juice 33 ml

Sucrose 1.6 g

ddH_2O up to 100 ml

Yeast paste 10 g per plate

NR condition:

100ml 4% sucrose plates

Agar 2.66g

Sucrose 4g

1xPBS up to 100ml

Add sucrose after mixing and boiling the agar PBS solution. Pour the plates and wait until cooled before storing at 4^{o}C.

2.4.5 CRISPR/Cas9-mediated Homology-directed Repair (HDR)

CRISPR/Cas9 system is a novel technique developed for precise editing of the genome. This system originated in bacteria as an antiviral mechanism through targeted cleavage of foreign DNA. CRISPR is an abbreviation of Clustered Regularly Interspaced Short Palindromic Repeats, a specific DNA sequence for recognition; and Cas9 is short for CRISPR associated protein 9, which can be guided by specific RNA sequences (guide RNA) to the matching site with PAM (Protospacer Adjacent Motif, NGG) and conduct cleavage leaving indels. In *Drosophila* it has been developed into an easily screened technique with visible and removable markers and it can be used in combination with HDR using double-stranded DNA donor templates (homology arms) (Port et al. 2014). In this way one can remove desired fragments from the genome using two guide RNAs at both ends, and replace the fragment with visible screening markers. The *CG6191Big* region deletion and *CG6191gene* deletion were both generated as described above.

For both deletions two target sites were selected, one at each end of the region using CRISPR Optimal Target Finder (http://tools.flycrispr.molbio.wisc.edu/targetFinder/). Two specific DNA fragments (Double-guided RNAs, dgRNA) were designed and constructed to generate a deletion from both ends of the Su(H) bound region (~7kb). dgRNA were cloned into the BbsI site of pCFD4_U6 vector using Gibson Assembly (pCFD4-U6:1_U6:3tandemgRNAs was a gift from Simon Bullock (Addgene plasmid # 49411)). The primers used for cloning are shown in Table 2.5 (for *CG6191Big*) and Table 2.6 (for *cables*). Final colonies were verified by sequencing. Homology arms (~1kb) at both ends of the deletion site were cloned into EcoRI and NotI sites of pHD-DsRed-attP vector by restriction digest (pHD-DsRed-attP-w+ was a gift from Kate O'Connor-Giles

(Addgene plasmid # 80898) (Port et al. 2014)). dgRNA and HDR-pHD-DsRed plasmids were co-injected into embryos expressing Cas9. The injections were performed by Kat Millen. Each male fly (F0) from the embryos was crossed to three to five yw virgin females (up to 50 crosses). Successfully edited flies in F1 would have the NRE/gene region replaced with a DsRed expressing module through HDR. Up to five DsRed-expressing crosses were kept. F1 males from each cross were crossed to balancer virgin female flies to establish a stable F2 stock. Five F1 flies from each cross were used for genotyping to confirm the deletion. Primers used for genotyping are listed in Table 2.7. Fly stocks used for CRISPR are listed in Table 2.3.

2.5 Dissection and Immunohistochemistry

Flies with NRE reporter were raised at 25^{o}C and dissected when they reached the 3rd larval instar. Dissection was performed in pre-chilled PBS and carcasses where then immediately fixed in 4% paraformaldehyde (PFA) for 20 mins, washed 3 times with PBT (PBS plus 0.1% Triton X-100), and blocked with PBT plus 0.1% BSA for 1 hr. Then the samples were incubated in primary antibody overnight at 4^{o}C. After primary antibody incubation, the samples were washed 3 times with PBT and incubated in secondary antibody at RT for 1.5 hrs. Then the samples were washed 3-4 times with PBT and equilibrated in PBS with 70% glycerol overnight before mounting. Brains were mounted in mounting media (Citiflour AF1) for imaging. Primary and secondary antibodies used in this study are listed in Table 2.8 along with their final concentrations.

2.6 EdU labelling of NBs and lineages

Brain culturing medium (BCM) was prepared as follows: 1. BCM base solution: 80% Schneider's medium, 20% FBS, 10 µl of 10 mg/ml insulin; 2. 10 3rd instar larvae were homogenized in 200 µl Schneider's medium and briefly centrifuged to collect the larval carcasses; 3. The larval lysate is subsequently added to 10 ml of the BCM base solution. Fly brains were dissected in Schneider's medium and incubated in BCM containing 50 µM of EdU for 4 hrs at RT. Following EdU incubation, brains were rinsed twice in Schneider's medium and fixed in 4% PFA for 25 mins at RT. Following fixation, brains were rinsed twice in 0.3% PBST, followed by 2 X 20 mins washes in 0.3% PBST. Blocking was carried out by incubating the brains in blocking buffer (0.3% BSA in PBST) for 1 hr at RT. After the blocking, the Click-iT reaction was carried out following the instructions in the manual. Brains were rinsed twice in 0.3% PBST. Nuclear stain DAPI was included in the penultimate wash. Samples were subsequently mounted in VECTASHIELD anti-fade mounting medium and imaged using point scanning confocal microscopy. For antibody co-staining, this was carried out after the Click-iT reaction and the wash steps, according to the manual.

2.7 Imaging and Analysis

Images were taken by Zeiss SP2 and SP8 confocal microscopes. Images were processed and labelled in Fiji (ImageJ). Cell counting in this study was done using the Cell Counter plugin in ImageJ. A cell counting program Counting3D developed by Leila Muresan was used for counting cells in multiple-layer Z-stacks in clonal analysis.

Statistics were conducted with Prism6. For pair-wise samples, a t-test was used if the samples fited a Gaussian distribution, or Kolmogorov-Smirnov test if the samples did not fit Gaussian distribution. For multiple comparison, an one-way ANOVA analysis was used.

Genomic overviews are presented in IGV or IGB genomic browser.

Table 2.1. Reagents used in the study.

REAGENT or RESOURCE	SOURCE	IDENTIFIER
Molecular Biology		
dNTPs	Roche	11969064001
High Fidelity PCR System	Roche	11732641001
DMSO	Sigma	154938
Ampicillin	Sigma	A1066
LB Culture Media	In house	
S.O.C Culture Media	In house	
QIAprep Spin Miniprep	QIAGEN	27104
QIAGEN Plasmid Midi Kit	QIAGEN	12143
QIAquick PCR Purification Kit	QIAGEN	28106
QIAquick Gel Extraction Kit	QIAGEN	28706
DNeasy Blood & Tissue Kit	QIAGEN	69506
Phenol:Chloroform:Isoamyl Alcohol 25:24:1, Saturated with 10mM Tris, pH 8.0, 1mM EDTA	Sigma	P3803
Chloroform:Isoamyl Alcohol (24:1)	Sigma	25666
Isopropanol	Sigma	59304
Ethanol	Sigma	32221
Agarose	Sigma	A9539
Ethidium Bromide	Sigma	E1510
Gel Loading Dye, Blue (6X)	New England Biolabs	B7021S
1Kb DNA ladder	New England Biolabs	N3232S
Alkaline Phosphatase	Roche	10713023001
T4 DNA Ligase/ Ligase Buffer	New England Biolabs	mo202L/b0202s
Cell culture		
Schneider's *Drosophila* Medium	Invitrogen	
10%Fetal Bovine Serum	Sigma	S3652
1% Penicillin-streptomycin	Sigma	P4333
Fugene	Promega	E2691
Opti-MEM	Invitrogen	
Dual-luciferase reporter assay system	Promega	
Immunohistochemistry		
16% Formaldehyde	Agar Scientific	R1026
PBS(Phosphate Buffered Saline)	Oxioid	BR0014
Triton-X-100	Sigma	T9284
BSA(Bovine Serum Albumin)	Sigma	A906
Glycerol	Sigma	
CitiFluor Glycerol PBS solution	Agar Scientific	R1320
VECTASHIELD Mounting Medium with DAPI	Vector Laboratories Ltd.	H1200

Table 2.2. Primers for enhancer cloning and mutation.

Oligo name	Oligo sequence (5' to 3')
path_pGL3_5	TAGGGTACCTAAATGCACAGCAACGAAGG
path_pGL3_3	TAGCTCGAGCGATCAAAAGTTCGTTGACC
cg6191_B_5	ATTGAGCTCGACCGACTTGGCTAGTGACC
cg6191_big_3	CATGGTACCACTACGGCAGCGGAATCATA
Asph_eh1_5	CGCGGTACCGCACTTTACATTTTAAATCAAATAAATC
Asph_eh1_3	AAACTCGAGGATCTGGATCGACGAACAGC
syp_Peak_5	GATGGTACCGGTGTCCTGGCTCTATC
syp_Peak_3	CTACTCGAGATGCGGCAGGATATGG
lola_IN_5	CCCAGATCTAAGGAGAACTGCAGCGGTAA
lola_IN_3	AAAGGTACCGAATGCAGTTGCCAGATGA
lola_beh_5	GATCTCGAGCAACTGCGCACATTTTCACT
lola_beh_3	CGTGGTACCTGGCACATGCATTTGTTTTT
Fer2_new_5	GATCTCGAGGCTTGCCAAGTACAGGGTGT
Fer2_new_3	CTAGGTACCCGCCACAGAGATTCACAGAA
Path-suH-mut-5	GAATCCTGTTTGCGGCATTCAAGCGATGTTATTTTTTTTTTTTTTTGAAAAACG
Path-suH-mut-3	CGTTTTTCAAAAAAAAAAAAAAAATAACATCGCTTGAATGCCGCAAACAGGATTC
Syp_M1_5	GAGATGGCCGAAAGGAGCTTTAACTTTGGCTACTCATCGCTTATCCGC
Syp_M1_3	GCGGATAAGCGATGAGTAGCCAAAGTTAAAGCTCCTTTCGGCCATCTC
Syp_M2_5	TTGTCCTGCGGACCGGTCATTGCAAACTTCCAGGCATCGTATTGACCG
Syp_M2_3	CGGTCAATACGATGCCTGGAAGTTTGCAATGACCGGTCCGCAGGACAA
Syp_M3_5	AGTTTGACCTCAGCGTTCTGCGAATTTAATAGAAGTCGTTCATCTGCC
Syp_M3_3	GGCAGATGAACGACTTCTATTAAATTCGCAGAACGCTGAGGTCAAACT
Aspheh1_M1_5	TGCCCAGCTGTCATCTCTAGCTTTCATCATAACTTCCGGATCTGGCAACGCCACTGTCTCTTTAT
Aspheh1_M1_3	ATAAAGAGACAGTGGCGTTGCCAGATCCGGAAGTTATGATGAAAGCTAGAGATGACAGCTGGGCA
Aspheh1_M2_5	GCAACGCCACTGTCTCTTTATAAATAATTTAACTTCGGTGCGAGCGGTATTTGCATTTAGTAACG
Aspheh1_M2_3	CGTTACTAAATGCAAATACCGCTCGCACCGAAGTTAAATTATTTATAAAGAGACAGTGGCGTTGC
Asph_M3_5	CATATTTAGGCATAAACAATAACTTCCAACCGGCGCCGTCTTATC
Asph_M3_3	GATAAGACGGCGCCGGTTGGAAGTTATTGTTTATGCCTAAATATG
Fer2_M1_5	CCTGCAAATGGAGCGGATGCTGAAGTTAATTCGTTGGACTTATTCGCC

(Table 2.2)	
Fer2_M1_3	GGCGAATAAGTCCAACGAATTAACTTCAGCATCCGCTCCATTTGCAGG
Fer2_M3_5	AGGAAGTGTAAATCACGAACTGAAGTTAAACCAAAAATAAATAGATTG
Fer2_M3_3	CAATCTATTTATTTTTGGTTTAACTTCAGTTCGTGATTTACACTTCCT
Fer2_M5_5	GGCATAATTGAATCAAATGGTAATTTCACACTGGCCAAATAAAGAAAA
Fer2_M5_3	TTTTCTTTATTTGGCCAGTGTGAAATTACCATTTGATTCAATTATGCC

Table 2.3. Fly stocks used in the study.

Stock Name	Chromosome	Source
pathNREGFP	3	This study
pathNRE[Mut]	3	This study
sypEnh/TM6B	3	This study
sypEnh[Mut]/TM6B	3	This study
CG6191BigGFP/TM6B	3	This study
AsphNREGFP	3	This study
lola-inGFP	3	This study
lola-behGFP	3	This study
Fer2NREGFP	3	This study
Fer2NRE[Mut]	3	This study
path80B/TM6B	3	DGRC111613
FRT80B	3	BL1254
NΔECD/CyO,GFP;path FRT80B/TM6B	2;3	This study
NΔECD/CyO,GFP;FRT80B/(TM6B)	2;3	This paper
path-RNAi(X)	1	v44536
path-RNAi(II)	2	v100519
FIG/FM6;;tubGal80FRT80B/TM6B	1;3	This study
FIG/FM6;;tubGal80FRT2A/TM6B	1;3	Eva
yw;;tubGal80,FRT80B	3	Fred3-F4
insc-Gal4,tubGal80ts/CyO,yFP;UAS-mCD8RFP/TM6B	2;3	Eva
insc-Gal4;tubGal80ts	2;3	Burcu
path-RNAi/(CyO,GFP);NICD/TM6B	2;3	This study
path[KG06640]/TM3,sb,Ser	3	BL14607
path[dg50]/(TM6B)	3	Parrish lab
pathΔ/TM6B	3	Parrish lab
path[GFP]/(TM6B)	3	Parrish lab
syp-RNAi(II)	2	GD33011
syp-RNAi(III)	3	GD33012
CG6191BigΔ	3	This study
CG6191geneΔ	3	This study
FRT40A;CG6191BigΔ	2;3	This study
Sco/CyO,GFP;Dicer/TM6B	2;3	Lab stock
cre,y;;D/TM3	1;3	Lab stock
NΔECD/CyO,GFP; MKRS/TM6B	2;3	Lab stock
w; Sco/CyO,GFP; Dr/TM6c	2;3	Lab stock
UAS-stingerGFP/CyO;pros-GAl4,tubGal80ts/TM6B	2;3	Eva
Notch-RNAi;;Sb/TM6B	1;3	Eva

(Table 2.3)		
w-;;repo-Gal4/TM3,sb,krGFP	3	Landgraf lab
FM6/wl;;TM6B/sb	1;3	Eva
GFP-RNAi	2	Lab stock
If/CyO; Dr/TM6B	2;3	Lab stock
CFD2: y1 P(nos-cas9, w+) M(3xP3-RFP.attP)ZH-2A w*	1	BL54591

Table 2.4. Transgenic flies generated in the study.

Construct Name	Insert description	Sequence location
pathMut_pGR	*path* enhancer with Su(H) binding site mutation	chr3L: 9494112-9494798
syp_pGR	*syp* enhancer of Su(H) peak	chr3R: 16592768-16594287
Fer2_pGR	*Fer2* enhancer of Su(H) peak	chr3R: 11977201-11979321
lola_IN_pGR	*lola* enhancer of Su(H) peak in lola intron	chr2R: 6422824-6424105
lola_beh_pGR	*lola* enhancer of Su(H) peak 5' to lola	chr2R: 6433654-6436011
CG6191Big_pGR	*CG6191* enhancer of Su(H) peak in front	chr2R: 9452778-9455564
Fer2_M_pGR	*Fer2* enhancer with 5 Su(H) binding sites mutation	chr3R: 11977201-11979321
syp_M_pGR	*Syp* enhancer with 3 Su(H) binding sites mutation	chr3R: 16592768-16594287

Table 2.5. Primers for *CG6191Big* CRISPR/Cas9 genome editing

Oligo name	**Oligo sequence (5' to 3')**
1_CG6191 big gRNA FWD	TATATAGGAAAGATATCCGGGTGAACTTCTTCCCACAGC CGAGGGCTCTGTTTTAGAGCTAGAAATAGCAAG
2_CG6191 big gRNA REV	ATTTTAACTTGCTATTTCTAGCTCTAAAACACTATAGTCTG ATCGTGTGAGACGTTAAATTGAAAATAGGTC
EcoRI CG6191 big LH F	ATATGAATTCGAAAGCAGCCGATGAGCTCC
NheI CG6191 big LH R	ATATGCTAGCGCCCTCGGCTGTGGGAAA
NotI CG6191 big LH R	ATATGCGGCCGCGCCCTCGGCTGTGGGAAA
SapI CG6191 big RH F	ATATGCTCTTCGTATAGTAGGTTTACAATCTGCATAGG
SapI CG6191 big RH R	ATATGCTCTTCTGACCTCTTCTACCAGGGCATCAG
CG6191 big cPCR 1 R	CCTAAAACCTGTTGCATGGG
CG6191 big cPCR 2 F	CACATCCATTGCATCCAGTG
	Primers for sequencing
CG6191 peak_4_F	GGGCAGGACGATCAAGAGAA
CG6191 peak_4_R	ACCAACCACTTGATTCGCTT
CG6191 peak_5_F	CACTGATTAGCCCGCACATG
CG6191 peak_5_R	GCTTAGCGACGTGTTCACTT
CG6191 peak_6_F	GGCCGCGACTCTAGATCATA
CG6191 peak_6_R	GTGACCTTACATGGCTCAGG
CG6191 peak_7_F	GTGCTCCTTTGTACCGTGC
CG6191 peak_7_R	CCACAGCAATTTCGGTAGCA

Table 2.6. Primers for *cables* CRISPR/Cas9 genome editing

Oligo name	**Oligo sequence (5' to 3')**
EcoRI CG6191 gene sLH F	ATATGAATTCTGCAAATAGTCCCTCGCCAT
NotI CG6191 gene sLH R	ATATGCGGCCGCCATGGGCATCGATGGCGG
SapI CG6191 gene RH F	ATATGCTCTTCGTATTGGACATCGGCGCTGCA
SapI CG6191 gene RH R	ATATGCTCTTCTGACCGGCTAAAACCACTGCAGCT
3_CG6191gene sgRNA FWD	GTCGTGCAGCGCCGATGTCCACAT
4_CG6191gene sgRNA REV	AAACATGTGGACATCGGCGCTGCA
5_CG6191gene dgRNA FWD	TATATAGGAAAGATATCCGGGTGAACTTCGTGTGCCTC CCTCCTGAAACGTTTTAGAGCTAGAAATAGCAAG
6_CG6191gene dgRNA REV	ATTTTAACTTGCTATTTCTAGCTCTAAAACTGCAGCGCCG ATGTCCACATGACGTTAAATTGAAAATAGGTC
EcoRI CG6191 gene dLH F	ATATGAATTCGCGCACAACCAGACAAACAC
NotI CG6191 gene dLH R	ATATGCGGCCGCTCAGGAGGGAGGCACACAAC
CG6191gene_RH_cPCR_R	AGCAACAACAGCAACACAC
CG6191gene_dLH_cPCR_R	AAGTCCTCGTGATGGCAAGA
CG6191gene_sLH_cPCR_R	CTTGAGCGGTATCTTGACGC
Primers for sequencing	
CG6191gene_1_F	CATTTCGGCTGGGATGGAAG
CG6191gene_1_R	GAGTGCCGATAAGTGCCAAG
CG6191gene_2_F	TCCACTATATGCGGACCCAC
CG6191gene_2_R	GCTTAGCGACGTGTTCACTT
CG6191gene_3_F	GCGTGATGAACTTCGAGGAC
CG6191gene_3_R	CCAAATTCGGCGCAACATTC
CG6191gene_4_F	CTTTCTCCGAGCGTTTCTGG
CG6191gene_4_R	GTGAGTGGGTGGGTGTCATA
CG6191gene_5_F	ACAACGAGGACTACACCATC
CG6191gene_5_R	GGCCTCCCGTATTGAATGTA
CG6191gene_6_F	GCTACTACTACGTGGACTCC
CG6191gene_6_R	CTTAGATTTTCCTTGCCGGC

Table 2.7. Primers for real-time PCR.

Oligo name	Oligo sequence (5' to 3')
mgRT-F	AAGTGCCTGGACGAGCTAAA
mgRT-R	CATTGACGGCATGGATGTAG
dpnRT-F	CAGCGTTGTCCAGAAGTTCA
dpnRT-R	AAACAAGCCACCACGGTATC
CG13334RT-3L	ATGAGGCCCATGAAGGAGTTC
CG13334RT-3R	CGAGGATGACCAGGTTCTTGG
CG6191RT-2L	AGCTGAGTTTCGCAAGGAGGAT
CG6191RT-2R	ATCGAATGGCGCATCGTTGATC
CG6191RT-3L	GGCTTAGGGCGTAGCTAAATAAG
CG6191RT-3R	GTCTAGGAATCAGGGACGAAGG
CG6191RT-BL	CCATAACCAAACGTCAAGGC
CG6191RT-BR	GGATCGTCCAAAATGCTAGC
CG13334RT-1L	GCTTGGCTGCAATGCAAAAGAC
CG13334RT-1R	ATGAAGGTGGCATTGGGACTGA
CG13334RT-2L	GTAGCCAAGTGTAACACGCCAC
CG13334RT-2R	GGGCGTGTCTACTAGCAACAATAG
CG42808RT-1L	GTGTCCAAGATACGTCGCCAG
CG42808RT-1R	GGACAATGGGTTCCGTGTTG
CG42807RT-1L	ATACGACGACTTTTGCAGGGGA
CG42807RT-1R	TTGACTGTGTGCCGAACGATTG
CG42807RT-2L	CCGCTCACCTGGATCCCATTAT
CG42807RT-2R	GGTGTTGTAGGTGCTCTCAGGT
fand_Exon1F	GCAACGCCATTTCGATCAGC
fand_Exon1R	TCCTCCACTTCGAAATTGATCTCT
fand_29305_F	ACGTATCTGGATGGACTACGG
fand_29305_R	CGTACAAACTGCAAATACAGTGG
link_1F	AGAGAAGGCTGAAGACGACGAC
link_1R	TTAAACTCAGCTCAGGACGGGG
link_28738_F	CAGAATGCCCTGTACTACAACC
link_28738_R	ATCAGCAGGATAGCCAGAGGT
Roe1_Exon1F	CGAACACACATCGATTGTTGAGA
Roe1_Exon1R	ACAAACGCAGGGCACTCATA
Roe1_Exon2F	TATGAGTGCCCTGCGTTTGTAC
Roe1_Exon2R	GTCCATTAGCTCGGCATTCTGC
slap5_1F	TGCGCGAAACTGGAATCAAG
slap5_1R	AACGCGGGCATTCTCCATAC
slap5_2F	TCCGGAAAGCAAGTAGTCTCCG
slap5_2R	GCTGCTCACGGAACACTAAACC

Table 2.8. Antibodies in the study.

ANTIBODY	SPECIES	SOURCE	CONCENTRATION
Primary antibodies			
GFP	Rabbit	Sigma	1:10000
Grh	Rabbit	Christos Samakovlis	1:2000
Dpn	Guinea pig	J. Skeath	1:5000
Pros (MR1A)	Mouse	DSHB	1:100
Ase	Rabbit	Y.N.Jan	1:100
Mira	Mouse	Ohshiro lab	1:100
Elav (7E8A10)	Rat	DSHB	1:200
Repo (8D12)	Mouse	DSHB	1:500
Path	Guinea pig	Parrish lab	1:50
p4EBP	Rabbit	Cell signalling	1:75
Jeb	Guinea pig	Ruth Palmer	1:15000
Alk	Guinea pig	Ruth Palmer	1:500
Broad (25E9)	Mouse	DSHB	1:200
Dap	Mouse	Stefan Thor	1:200
E2F	Mouse	Stefan Thor	1:200
Secondary antibodies			
FITC	Rabbit	Jackson Immuno Research	1:250
Cy3	Rabbit	Jackson Immuno Research	1:250
Cy5	Rabbit	Jackson Immuno Research	1:250
FITC	Guinea pig	Jackson Immuno Research	1:250
Cy3	Guinea pig	Jackson Immuno Research	1:250
Cy5	Guinea pig	Jackson Immuno Research	1:250
FITC	Mouse	Jackson Immuno Research	1:250
Cy3	Mouse	Jackson Immuno Research	1:250
Cy5	Mouse	Jackson Immuno Research	1:250
Cy3	Rat	Jackson Immuno Research	1:250

Chapter III

Candidate Notch target genes in neural stem cells

3.1 Introduction

Notch signalling is active in neuroblasts, where it is essential for the maintenance of Type II neuroblasts (NBs) and influences the survival of Type I NBs. In addition, over-activation of Notch is sufficient to induce excess stem cell-like cells, leading to hyperplasia and tumours. To discover which genes may execute Notch function in NBs, putative targets were identified through genome-wide approaches (Zacharioudaki, et al. 2016). Specifically, the mRNAs from brains expressing constitutively activated Notch (NΔECD) were profiled, using expression microarrays, to determine which RNAs were upregulated. Under these conditions (*grh-Gal4; UAS-NΔECD*), excessive NB-like cells are generated in the brain and approximately 1576 mRNAs were significantly more highly expressed than in controls. Similarly, 595 DNA regions bound by Su(H), the core transcription factor of the Notch signalling pathway, were identified by chromatin immunoprecipitation from NΔECD expressing brains. The intersection of these data identified 185 putative direct targets of Notch and included many transcription factors

whose function was examined. Several were found to be involved in regulating NB identity and developmental age (Zacharioudaki, et al. 2016).

Only a small number (11; *E(spl)s, dpn, grh, wor, mira, numb, svp, cas, hth, Klu, dm*) (Zacharioudaki, et al. 2016) of the putative target genes identified by these genome-wide approaches have yet been investigated in any depth. Others amongst this dataset are likely to have important roles in regulating the NBs, including genes more directly involved in conferring their specific properties. To prioritise candidates for further study the following criteria were used: (1) binding with Su(H) was detected in intronic or nearby intergenic regions likely indicating enhancer binding, (2) mRNA levels were elevated in *grh-Gal4; NΔECD* brains, (3) expression was specifically enriched in NBs or neurons (Berger et al. 2012), (4) existence of additional evidence linking the gene to Notch or to neural stem cells. Based on these criteria, six genes were selected as summarised below (Table3.1). Like other transcription factors, Su(H) has a preferred binding motif ("YGTGRGAA") (Rebeiz et al. 2002). Using a position weight matrix (PWM), the putative binding motifs were identified in the genome (Rebeiz et al. 2002). All of the identified enhancer regions contained one or more motifs (Table 3. 1).

Gene name	Su(H) bound region number and locations	Number of Su(H) binding motifs	mRNA level fold change	NB/Neuron relative enrichment ratio	NB expression
pathetic (CG3424)	1; intronic	1	0.91*	8.80	NA
syncrip (CG17838)	1; intronic	5	4.54	10.46	Yes (McDermott et al. 2012)
cables (CG6191)	2; Intronic & 13kb downstream	0; 16	1.89	NA	NA
Asph (CG8421)	Promoter	3	2.97	NA	NA
lola (CG18378)	2; Intronic & 3kb upstream	3; 11	1.72	NA	NA
Fer2 (CG5952)	1; 0.4kb upstream	3	2.26	0.01	NA

Table 3.1. Selected candidates and their known characteristics. (Neumüller et al. 2011; Zacharioudaki, et al. 2016; McDermott et al. 2012)
* not statistically significant

The functional characteristics of the six genes of specific interest are summarised below:

pathetic (path) is a member of the SLC36 transporter family, a potential amino acid transporter that has been linked to growth and TOR pathway regulation (Muralidharan Pillai & Meredith 2011; Heublein et al. 2010; Shang et al. 2017). NBs have the unusual ability to maintain their growth and proliferation under conditions of starvation (Cheng et al. 2011). Their exit from quiescence is also dependent on nutrition (Chell & Brand 2010). Notch-regulated expression of a specific transporter, *path*, might explain some of their unique characteristics.

syncrip/CG17838 (syp) is the fly homologue of mammalian synaptotagmin-binding cytoplasmid RNA-interacting protein (Syncrip), also named hnRNPR (heterogeneous nuclear ribonucleoprotein R). It is implicated in the regulation of RNA localisation and processing and its expression is related to the temporal progression of NBs (Liu et al. 2015). If Notch regulates its expression, this would also make a connection between Notch signalling and the developmental age of NBs.

CG6191 is the homologue of *CABLES1/2 (CDK5 and ABL1 enzyme substrate 1/2),* which appears to have tumour suppression role in various types of cancers (Huang et al. 2017). Evidence suggests it functions as a linker between Cdks (2 and 5) and Abl (Zukerberg, Patrick, Nikolic, Humbert, C. Wu, et al. 2000), but its function is currently not well understood. If it has a conserved role in regulating the cell cycle, it could contribute to cell-cycle regulation and NB maintenance.

Aspartyl β-hydroxylase (Asph) is the orthologue of a mammalian enzyme aspartate beta-hydroxylase (ASPH) that catalyses the hydroxylation of EGF repeats including those

in Notch and Jagged extracellular domain (Dinchuk et al. 2002; Dinchuk et al. 2000). ASPH over-expression in humans has been linked to changes in Notch signalling and it may be involved in regulating Notch activity by modulating ligand or receptor function/recycling (Cantarini et al. 2006; Borgas et al. 2015). If Asph is a direct target of Notch, it could contribute to feed forward regulation of the pathway activity.

longitudinals lacking (lola) encodes a zinc finger protein with a BTB domain and has 27 transcripts. Phenotypes of *lola* mutants resemble the *Notch* loss of function phenotype in several contexts (Neumüller et al. 2011) and Lola antagonises Notch function during cell fate determination in *Drosophila* eyes (Zheng & Carthew 2008), making it plausible that it functions with Notch in the NB lineages.

48-related 2 (Fer2) encodes a transcription factor related to PTF1 (Pancreatic Transcription Factor 1), which forms a non-classical bHLH-RBPJ complex with functions independent of Notch (Beres et al. 2006). The possibility that Fer2 interacts similarly with Su(H) to operate in an independent complex downstream of Notch made Fer2 of interest to pursue further.

The initial goal was to determine whether these six genes contain Notch-regulated enhancer in support of the hypothesis that they are downstream Notch targets *in vivo*. Objectives: (1) To select and clone potential Notch-responsive enhancers of the candidate genes; (2) to examine whether the enhancers respond to Notch activation in S2 cell lines; (3) to explore whether the enhancers direct expression in NBs *in vivo*; (4) to examine whether the enhancers respond to Notch regulation *in vivo*; (5) to investigate whether these enhancers are dependent on Su(H) binding in S2 cells/*in vivo*.

3.2 Results

3.2.1 General strategy

To explore the expression pattern and *in vivo* response to Notch of the six genes of interest, the regions bound by Su(H) in the chromatin immunoprecipitation experiments were incorporated into a GFP reporter containing the minimal heat-shock promoter, pGR vector (Krejcí et al. 2009) and the resulting plasmids were stably inserted into the genome of flies. Putative enhancers from each of the candidate genes were then tested for their response to Notch *in vivo*, by manipulating Notch activity in NBs.

In some cases, parallel experiments were carried out in cell culture. For these experiments, DNA fragments encompassing the Su(H) bound regions were subcloned into the luciferase reporter plasmid pGL3-Min. This vector is designed to detect enhancer activity as the fragments are inserted upstream of a minimal promoter (Krejcí et al. 2009). Expression from the resulting plasmids, in the presence and absence of Notch was then analysed following transfection into S2 cells.

Finally, to further investigate whether the enhancers could confer a response to Notch signalling through Su(H), the identified binding-motif(s) were mutated and then the modified enhancer incorporated into the luciferase/GFP reporters for testing. If there are multiple motifs, the ones with higher PWM score for Su(H) were chosen to be mutated (Rebeiz et al. 2002). The hypothesis was that if a candidate region requires the Su(H) motif for a response to Notch activation, any stimulation by Notch should be compromised when the Su(H) motif is mutated. Six of the enhancers were tested in this way.

3.2.2 *pathetic* contains a Notch-regulated enhancer that directs expression in neural stem cells

In Notch-induced hyperplastic brains, the first intron of *path* exhibited robust Su(H) binding (Fig 3.1A). This region of *path*, referred to as *pathNRE*, contains a single conserved match to a Su(H) high-affinity motif (Fig 3.1B). To test whether this region can respond to Notch activation, the response of the wild-type (*pathNRE*) and mutated (*pathNRE[Mut])* enhancers to Notch was first measured in luciferase assays. Expression from the wild-type *pathNRE* was significantly stimulated in response to Notch (Fig 3.1C). In contrast, this response was clearly diminished when the Su(H) high-affinity site was mutated (Fig 3.1C). These results support the hypothesis that the fragment encompasses a Notch-responsive enhancer.

Similarly, the fragment has characteristics of a Notch-regulated enhancer *in vivo*. In transgenic flies, *pathNRE* directed robust GFP expression in NBs as well as part of the optic lobe (Fig 3.1D), as indicated by the co-staining with the NB marker Grh. Mutating the Su(H) motif (*pathNRE[Mut])* strongly compromised the enhancer, resulting in a much lower level of GFP expression in NBs and in the optic lobe (Fig 3.1E). However, the GFP expression from *pathNRE[Mut]* in NBs was not completely eliminated, suggesting that the enhancer is also regulated by other factors. It was also notable that the *pathNRE* enhancer exhibited variable expression between NBs (Fig 3.1D insets), suggesting that the expression might be regulated by cell cycle or other temporal factors.

To assess whether *pathNRE* responds to Notch signalling as predicted, Notch activity in NBs was depleted by expression of Notch-RNAi (NRNAi), or enhanced by expression of NΔECD. Compared with *pathNRE* control (Fig 3.2A), down-regulating Notch by RNAi

(with *insc-Gal4*, which directs expression in NBs and optic lobe) caused substantial loss of pathNRE-GFP expression from most NBs, including those in the central brain (Fig 3.2C), Conversely, higher levels of expression were detected when excessive Notch was generated by expressing UAS-NΔECD in a similar manner (Fig 3.2D). In contrast, there was no increase in *pathNRE[Mut]* expression when it was exposed to similar conditions (Fig 3.2E), in agreement with it having lost the ability to respond to Notch.

Altogether the above results support the hypothesis that *path* has direct input from Notch signalling, *via pathNRE*. Given these data, *path* was selected for further functional studies as summarised in *Chapter 4*.

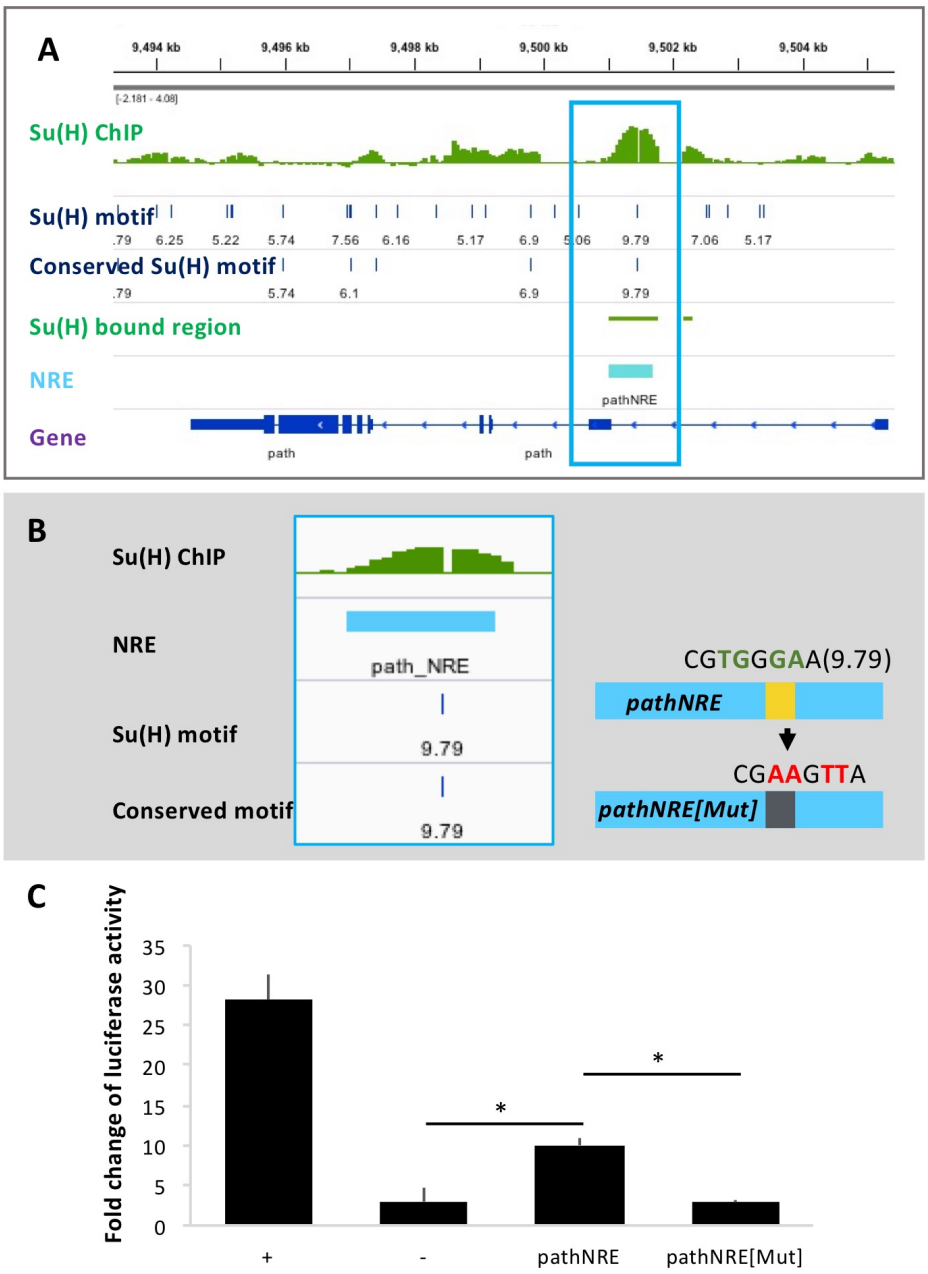

Fig 3.1. A direct Notch responsive element (NRE) in *path* intronic region that directs expression in neural stem cells. (A) A genomic overview of the *path* gene region with the Su(H) binding profile from *NΔECD*-expressing brains (green graph, enrichment in ChIP, log2 (scale)), Su(H)motifs/conserved motifs (dark blue), significant Su(H)-bound regions (green), and cloned *pathNRE* region (cyan). (B) Zoomed in snapshot of the *pathNRE* region (left) and illustration of how the high-affinity Su(H) binding motif was mutated (right), the number refers to the PWM score. (C) Response of *pathNRE* to a transient activation of Notch in S2 cells . (+): positive control showing response of E(spl)*m3NRE*, a known Notch target; (-): negative control showing response of a NME (Notch mutated enhancer) with mutated Su(H) motifs. Error bars represent the SD of three biological replicas; *p<0.05. (D&E) Expression from *pathNRE* (D) and *pathNRE[mut]* (E) GFP reporter in L3 larval brains. Reporter expression from the indicated enhancers is detected with anti-GFP (green and grey panel). Neuroblasts and GMCs are detected with anti-Grainyhead (Grh, magenta). Dorsal and ventral sides of the brains are shown (compartments of brain and neural stem cell types refer to Fig 1.3). Insets show individual NBs with varied expression level. Scale bar, 100 µm; insets scale bar, 10 µm.

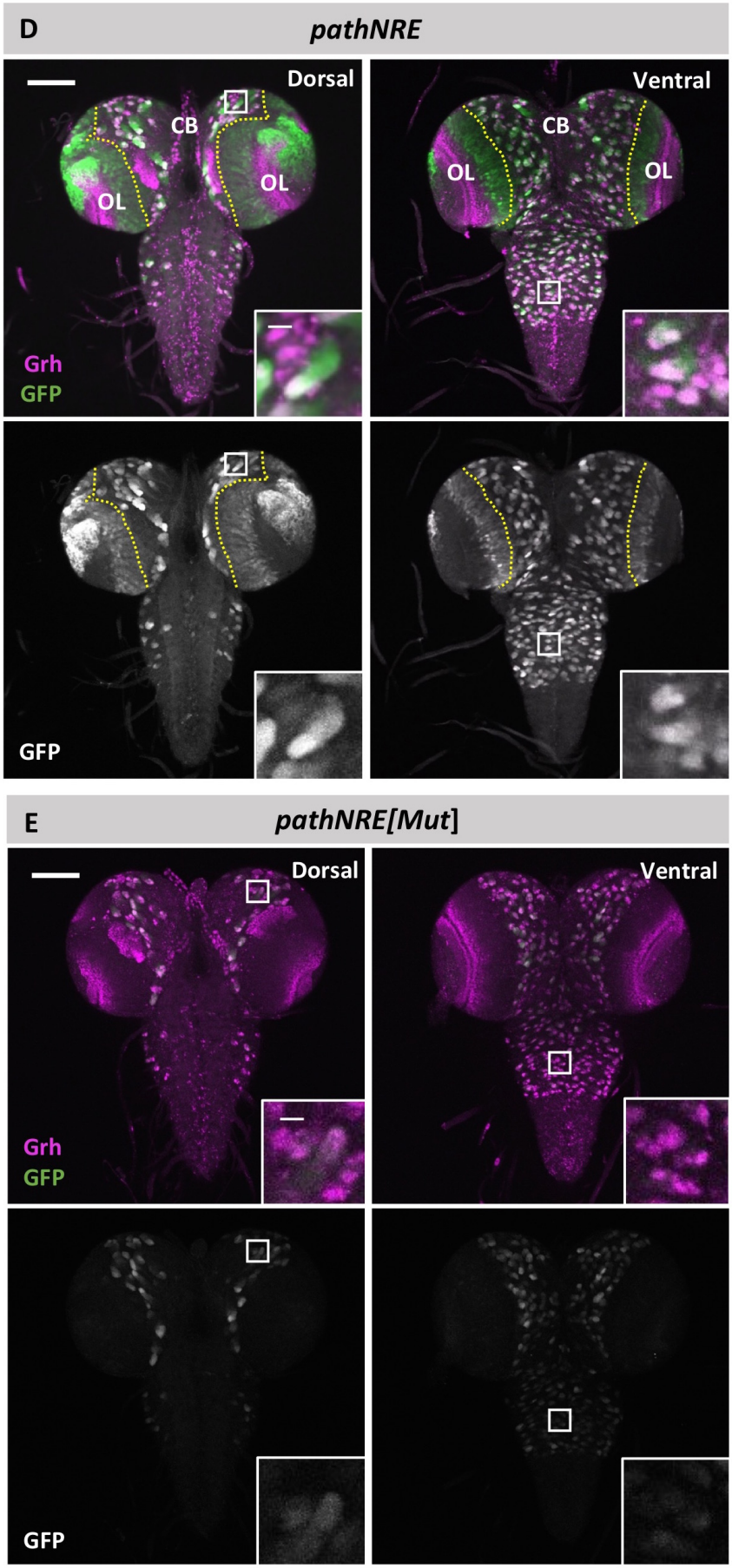
D
pathNRE
Dorsal
Ventral
CB
OL
OL
CB
OL
OL
Grh
GFP
GFP
E
pathNRE[Mut]
Dorsal
Ventral
Grh
GFP
GFP

Fig 3.1. (D&E)

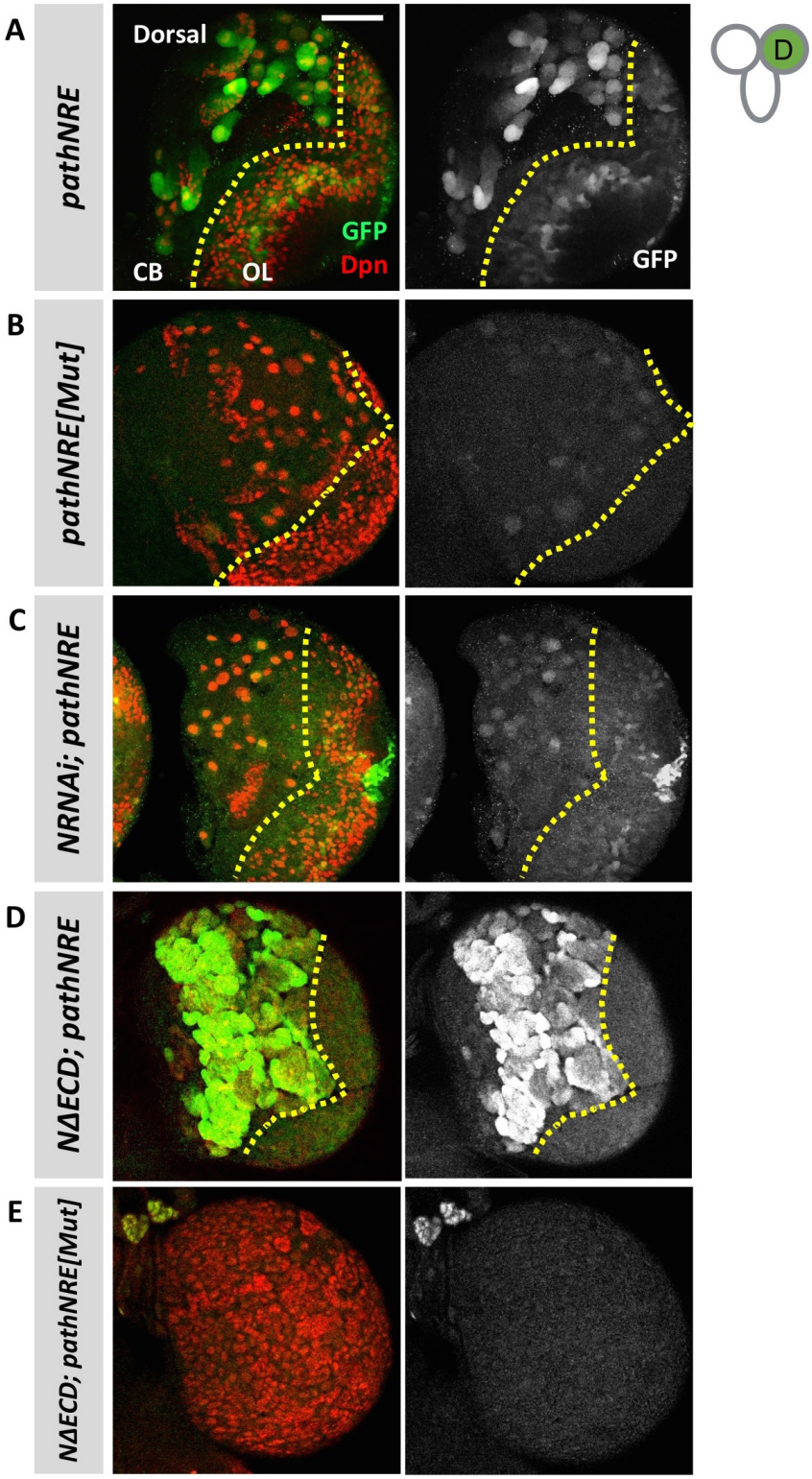

Fig 3.2. *pathNRE* responds to Notch regulation in neural stem cells. (A) *pathNRE* directs GFP (green, grey panel) expression in control dorsal brain lobe. CB, central brain; OL, Optic lobe. (B) *pathNRE[Mut]* GFP loses most of GFP expression. (C) pathNRE (green, grey panel) invokes less GFP expression when Notch is knocked down by RNAi *(insc-Gal4; UAS-NRNAi*) (D) Robust expression from *pathNRE* (green, grey panel) in CB when Notch is overexpressed (*insc-Gal4; UAS-NΔECD*). (E) Mutated pathNRE (*pathNRE[Mut],* green, grey panel) no longer responds to activated Notch (*insc-Gal4; UAS-NΔECD)*. Neuroblasts are marked by anti-Deadpan (Dpn, red). Scale bar, 50 µm.

3.2.3 syp enhancer directs expression in neuroblasts but is not dependent on Notch

Similar to *path*, a peak of Su(H) binding was detected within the first intron of *syp* (isoform A/I/M/H/K). The bound region (*syp-Enh*), which encompasses several conserved Su(H) binding motifs (Fig 3.3A), was cloned into the luciferase reporter pGL3. Subsequently, a mutated version, in which the three sequence matches to high-affinity Su(H) binding motifs were mutated (Fig 3.3B), was also generated. However, the wild-type fragment showed little response towards Notch induction, behaving similarly to a negative control (mutated Enh, *syp-Enh[Mut];* Fig 3.3C). Furthermore, there was no significant increase in activity of either the wild-type or the mutated *syp-Enh* in the presence of activated Notch (Fig 3.3C). These results suggest that the Su(H) bound region of *syp* does not confer Notch response in cell lines.

In vivo, *syp-Enh* was found to direct expression in the NBs and part of the optic lobe (Fig 3.3D). As with *path*, not all the NBs exhibited Syp expression, for example, the mushroom body (MB) NBs consistently lacked GFP expression (Fig 3.3D). However, unlike the situation with *path*, there were no major consequences from mutating 3 of the 5 Su(H) motifs. The mutated enhancer could still direct GFP expression in the NBs (Fig 3.3D & E), and the level of GFP expression was not significantly decreased in comparison to the wild-type fragment (Fig 3.4A & B).

It is possible that the remaining 2 Su(H) motifs could contribute to the NB expression in response to Notch. So the effects of ectopic and compromised Notch activity on *syp-Enh* directed expression was also determined (Fig 3.5). Under NΔECD conditions, *syp-Enh* directed expression in the extra NB-like cells, although in general the expression levels were not higher than in the primary NBs (Fig 3.5C). Furthermore, the expression levels

remained unchanged when Notch was compromised by expression of Notch-RNAi in NBs (Fig 3.5B & D). These results suggest that *syp-Enh* can direct expression in NBs but that it can do so independent of Notch, implying that there are other inputs.

To further explore the potential regulation by Notch, the activity of *syp-Enh* was examined at earlier stages. Notch begins to be active in NBs around the time they exit quiescence and re-enter division (Homem & Knoblich 2012) (NB reactivation: NBs start again to regrow and divide, after a period of mitotic silence from late embryonic stage to L1). If *syp* is a direct Notch target, it might be detectable in NBs as soon as Notch is active, similar to other well-characterised targets (*E(spl)mgamma*-GFP, Zacharioudaki unpublished data). The expression directed by *syp-Enh* at 72hrs, 96hrs, and 120hrs after larval hatching (ALH) was therefore evaluated. At 72hrs ALH, *syp-Enh* directed GFP expression in only 4-5 NBs on either side of the brain (Fig 3.6A). Subsequently, expression in progressively more NBs in both dorsal brain lobes and the ventral nerve cord (VNC) was detected (Fig 3.6B) so that, at 120hrs ALH, syp-EnhGFP was expressed in most of the NBs except MB NBs (Fig 3.6C). This gradual acquisition of expression is different from that of *dpn* and *E(spl)mgamma* (and *pathNRE, see chapter 4*), which appear in most NBs by 24-48hrs ALH and is in line with the assumptions that Notch is not sufficient to confer *syp* expression and that there must be other factors with input into the enhancer.

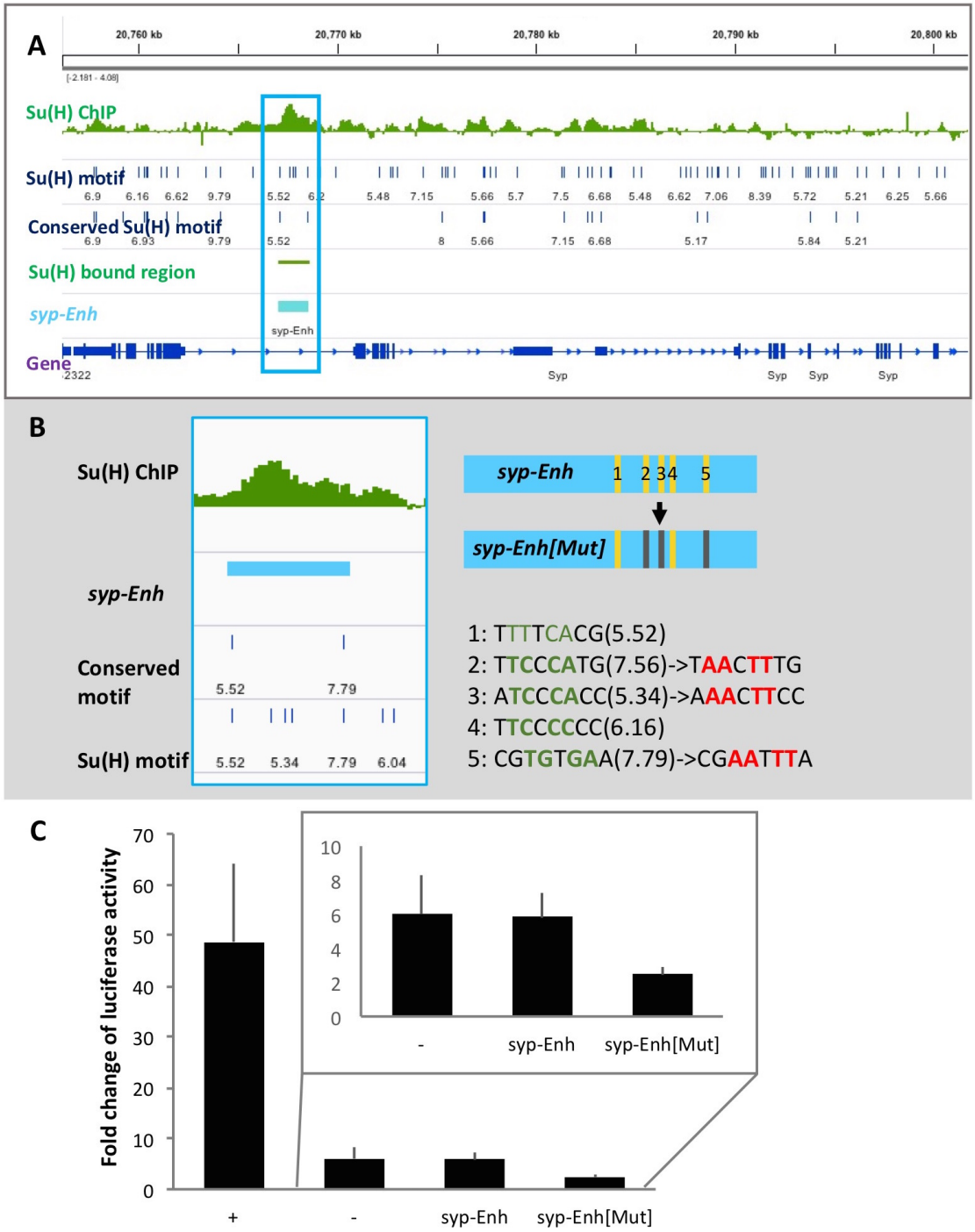

Fig 3.3. *syncrip* enhancer drives expression in NBs but is not dependent on Su(H) motifs. (A) A genomic overview of *syp* gene region shows the Su(H) bound profile (green) , Su(H)motifs/conserved motifs (dark blue), Su(H) bound regions (green), and cloned *syp-Enh* region (cyan). (B) Zoomed in snapshot of the *syp-Enh* region (left) and illustration of how the high-affinity Su(H) binding motifs were mutated (right). (C) Response of *syp-Enh* to a transient activation of Notch in S2 cells. (+): positive control showing response of *m3NRE*; (-): negative control showing response of NME. Error bars represent the SD of three biological replicas. (D&E) Expression from *syp-Enh* (D) and *syp-Enh[Mut]* (E) GFP reporter in L3 larval brains. Reporter expression from the indicated enhancers is detected with GFP (green and grey panel). Neuroblasts and GMCs are detected with Dpn (magenta). Dorsal and ventral sides of the brains are shown. Insets show individual NBs. Scale bar, 100 µm.

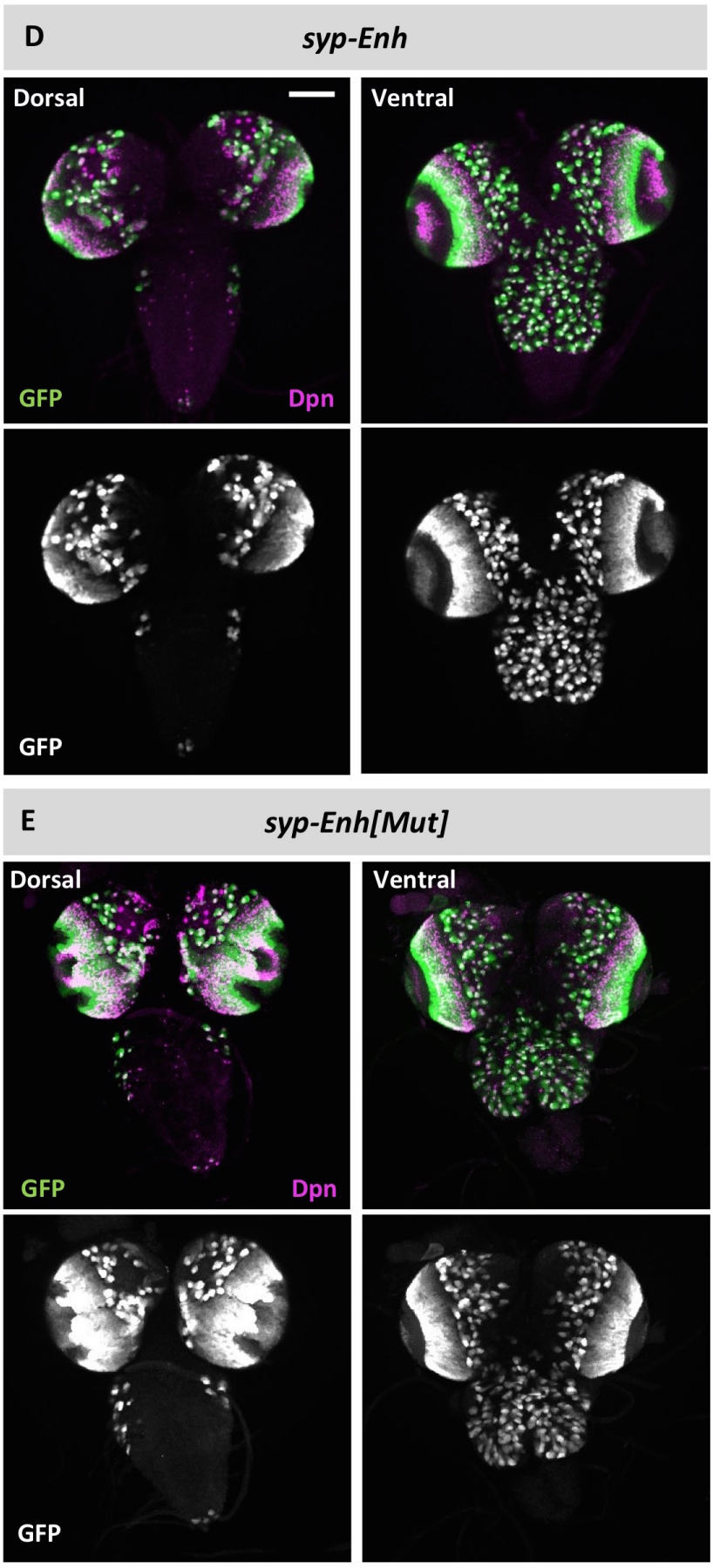
D
syp-Enh
Dorsal
Ventral
GFP
Dpn
GFP
E
syp-Enh[Mut]
Dorsal
Ventral
GFP
Dpn
GFP

Fig 3.3 (D&E)

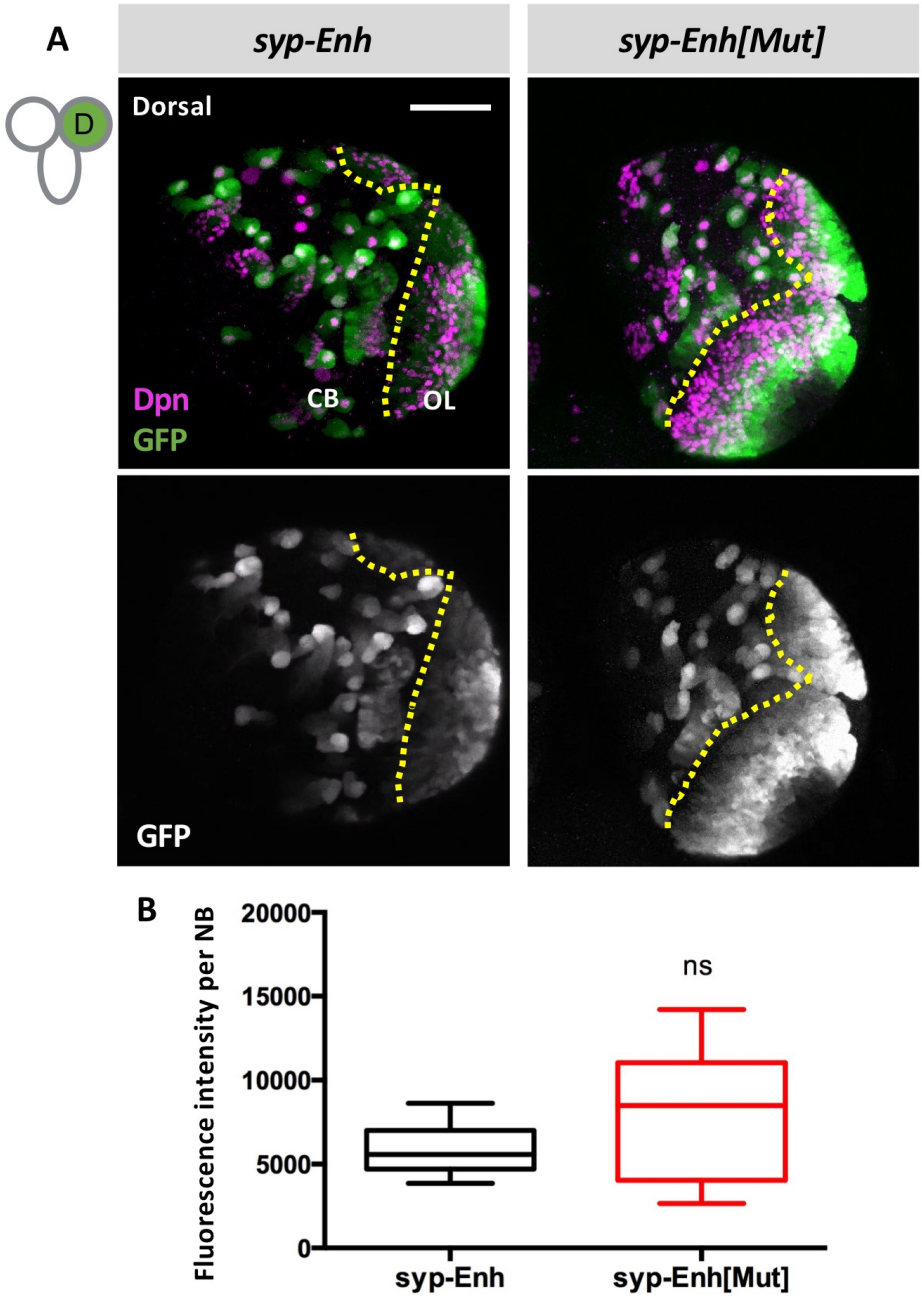

Fig 3.4. *syp-Enh* does not depend on Su(H) binding in neural stem cells. (A) Wild-type *syp-Enh* and mutated *syp-Enh[Mut]* directs GFP expression in NBs and some OL cells. Grey panel shows GFP expression. Green represents GFP; magenta represents Dpn. Scale bar, 50 µm. (B) Quantification of NB GFP intensity. ns, no significant difference, n=5 brains.

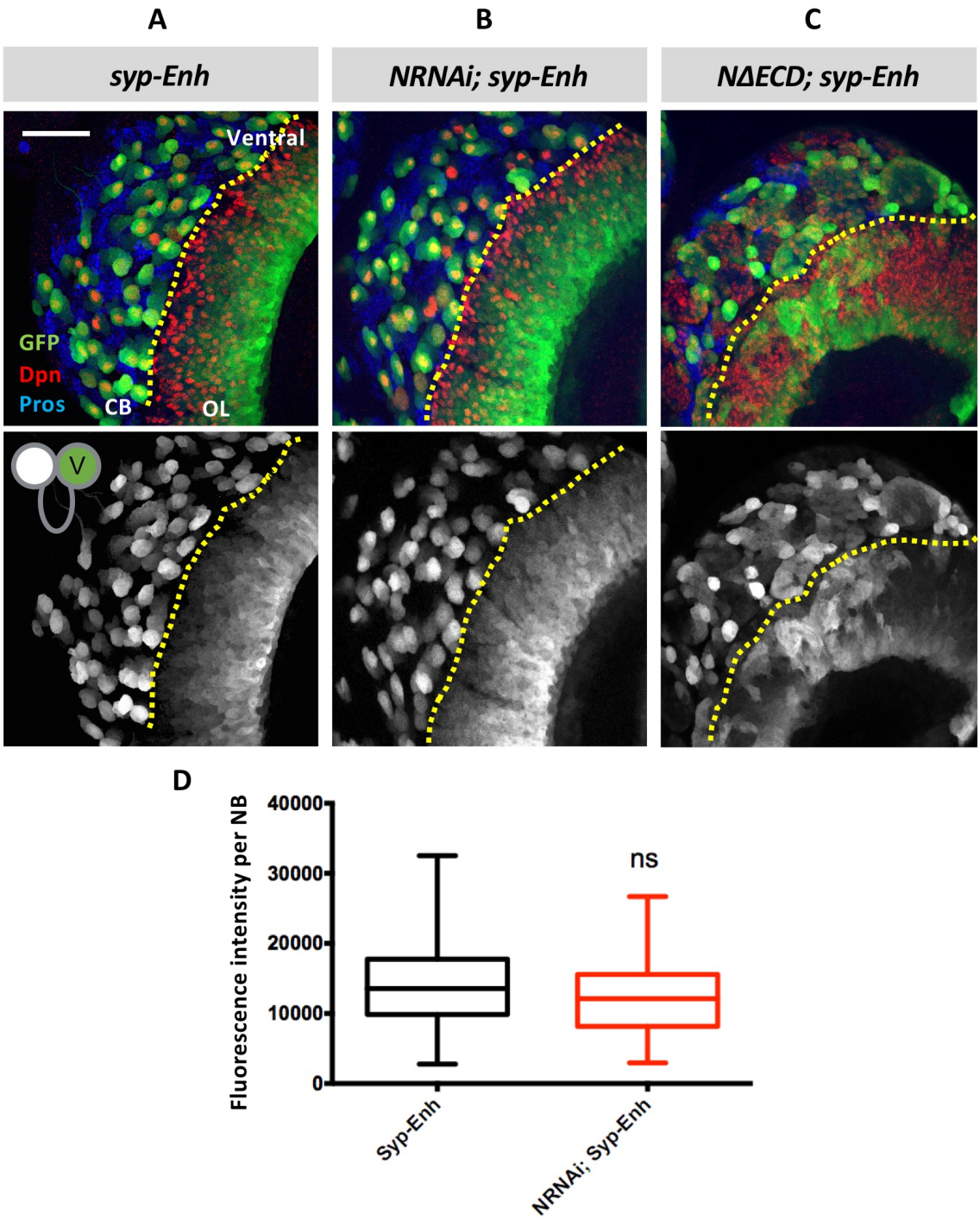

Fig 3.5. Levels of expression from *syp-Enh* are unaffected by changes in Notch activity. (A-C) *syp-Enh* directs GFP (green) expression under control conditions (A) and altered Notch activity: (B) Depleting Notch by RNAi; (C) Hyperactivating Notch with *NΔECD.* NBs are marked with Dpn (red), neurons are marked with Prospero (Pros, blue). (D) Quantification of GFP intensity in indicated genotypes. Scale bar, 50 µm.

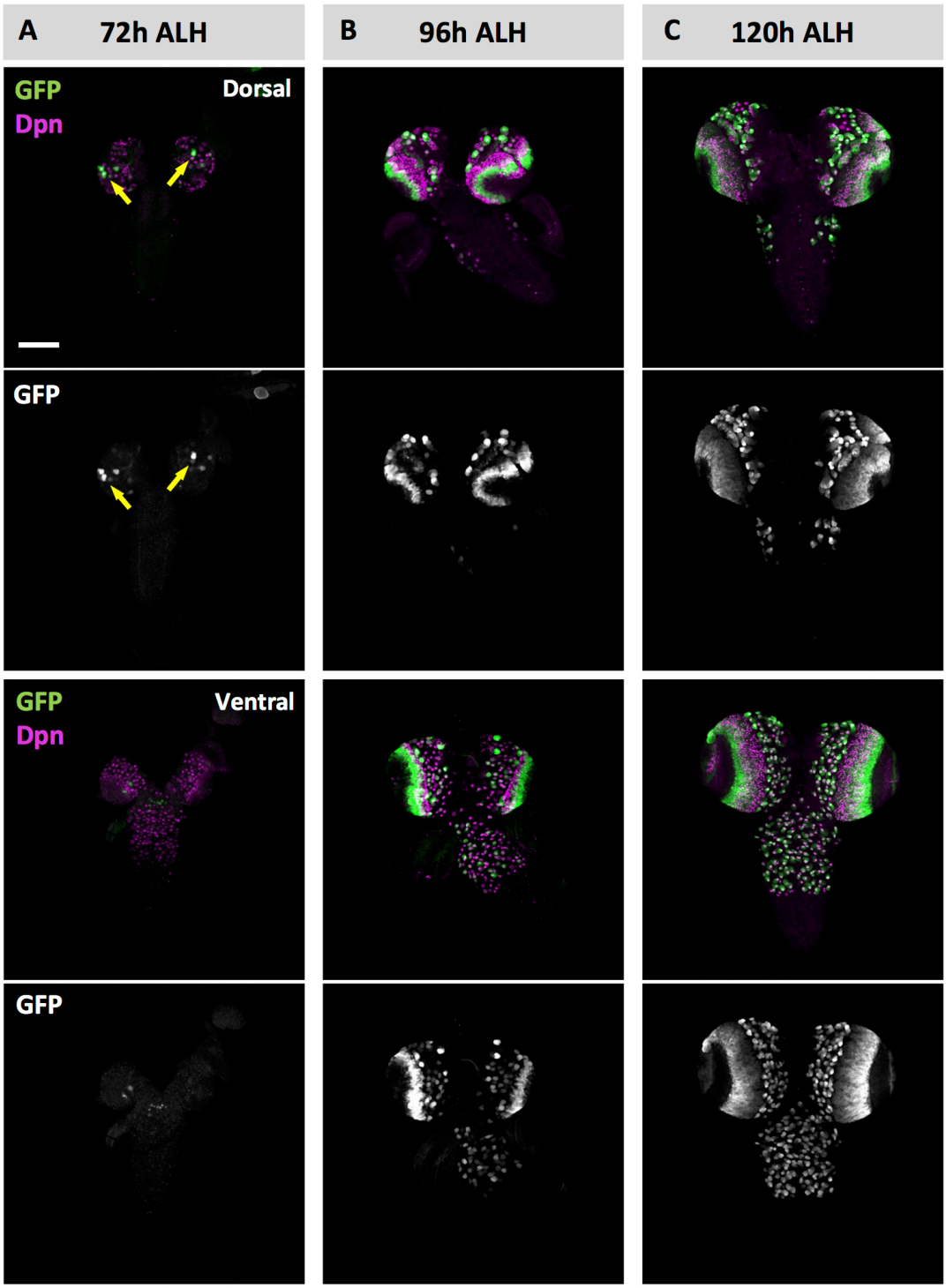

Fig 3.6. *syp-Enh* is progressively more active at older developmental stages. syp-Enh GFP at 72h (A), 96h (B) and 120h (C) after larva hatching (ALH). Dorsal and ventral brain regions are as indicated. Green and grey panels represent GFP, magenta represents Dpn. Yellow arrows in (A) point to mushroom body neuroblasts that first render *syp-Enh* expression. Scale bar, 100 µm.

3.2.3 An enhancer associated with CABLES directs GFP expression in neuroblasts and responds to Notch activity

CG6191 is one of the genes that are up-regulated by Notch hyper-activation in wing discs as well as in brains (Djiane et al. 2013). There are two Su(H) bound regions in the vicinity of *CG6191*: a smaller region within the intron (*CG6191in*) and a robust region with dense Su(H) motifs approximately 13 kb downstream (*CG6191Big*) (Fig 3.7A & B). *CG6191in* had been cloned previously and did not generate expression in the NBs or have a robust response to Notch in cell culture (JJ and Babaoglan unpublished). The distal 3' Su(H) bound region had not been tested in a similar manner because there are several intervening genes making it difficult to discern whether it is indeed directly regulating CG6191 (Fig 3.7A). Therefore, *CG6191Big* was cloned into the GFP reporter vector for *in vivo* assays. *CG6191Big* directed expression in many NBs as well as in part of the optic lobes (Fig 3.7C), exhibiting typical characteristics of a Notch-regulated enhancer. I therefore tested whether Notch input is required for the GFP expression. When Notch was down-regulated by RNAi driven by *insc-Gal4*, the central brain expression of *CG6191Big* was depleted, while the optic lobe expression was retained (Fig 3.8A & B). This region, distal to *CG6191,* thus appears to be dependent on Notch activity in the central brain NBs, suggesting it could be a direct Notch-targeted enhancer. *CG6191Big* also directs expression at the wing disc D/V boundary (Fig 3.7D), a known site of Notch activity, consistent with predictions for a Notch-regulated target in this tissue. Although this fragment has the characteristics of a Notch regulated enhancer, it remains uncertain whether it does indeed act on *CG6191*, a question that will be addressed in Chapter 5 along with analysis of CG6191 function in NBs.

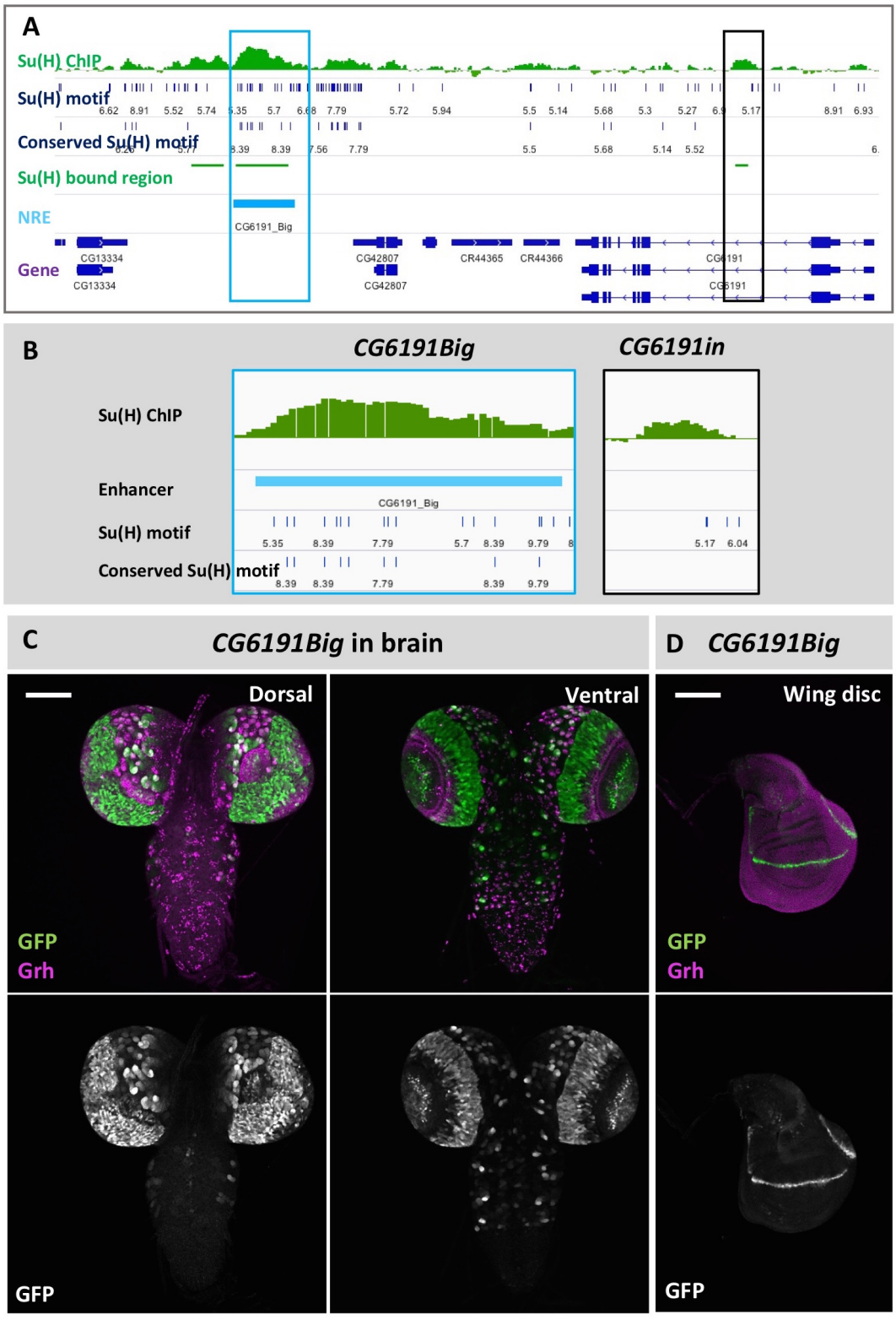

Fig 3.7. A Su(H) bound region 3' distal to *CG6191* directs expression in neural stem cells. (A) A genomic overview of the distal 3' Su(H) bound region (*CG6191Big*) and the *CG6191* gene. The panels show Su(H) bound profile (green), Su(H)motifs/conserved motifs (dark blue), Su(H) bound regions (green), and the cloned NRE region (cyan). (B) Snapshots show *CG6191Big* (left) and an intronic Su(H) bound region called *CG6191in* (right). (C) *CG6191Big* directed GFP expression in L3 larval CNS. Neuroblasts and GMCs are detected by Grh (magenta). Scale bar, 100 µm. (D) *CG6191Big* also directs GFP expression in larval wingdisc. Magenta represents Grh. Scale bar, 100 µm.

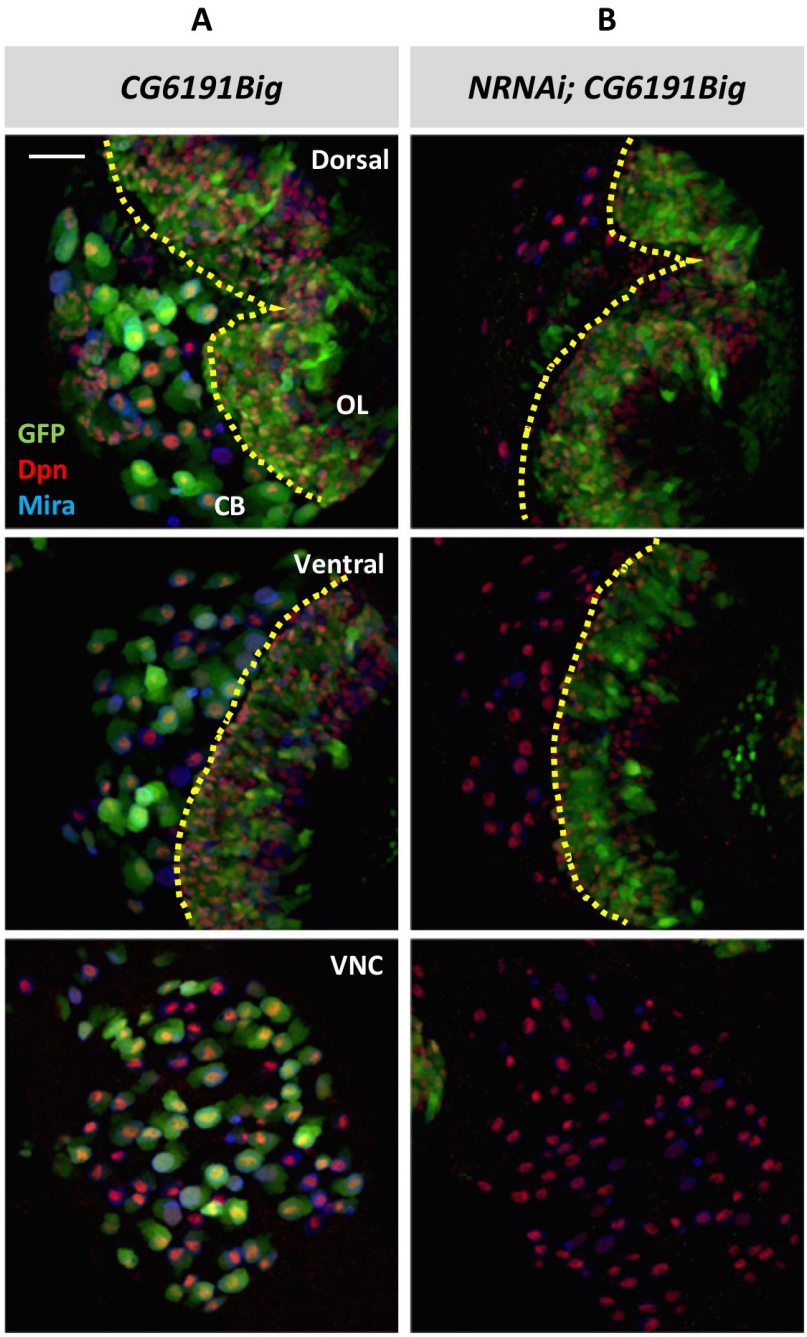

Fig 3.8. *CG6191Big* depends on Notch activity in NBs. (A) *CG6191Big* directs GFP expression in NBs in control larval brains. (B) *CG6191Big* can no longer invoke GFP expression in NBs when Notch is depleted by RNAi. Dorsal, Ventral and VNC view of brain are as indicated. NBs are marked with Dpn (red) and Mira (blue). Scale bar, 50 µm.

3.2.4. Su(H) bound region from *Asph* confers expression in NBs and responds to Notch

The Su(H) bound region of *Asph* is unusual in that it encompasses the promoter region. Furthermore, the conserved Su(H) motif is located at the transcription start site (Fig. 3.9A). To explore whether this fragment can nevertheless confer enhancer-like activity, it was tested in luciferase assays and *in vivo*. Firstly, the fragment could respond to Notch in Luciferase assays, in a manner that was dependent on the Su(H)-motif, since the mutated enhancer had lost the ability to respond (Fig 3.9B & C). Secondly, *Asph-NRE* directed expression in the majority of NBs (Fig. 3.9D). Finally, depletion of Notch activity with *insc-Gal4>Notch-RNAi* caused loss of *Asph-NRE* directed GFP expression in central brain and VNC NBs (Fig 3.9E & F), supporting the notion that it is a direct target in NBs. Thus, similar to *path*, *Asph* fulfils the criteria of a Notch regulated target in NBs although its function has not been explored further.

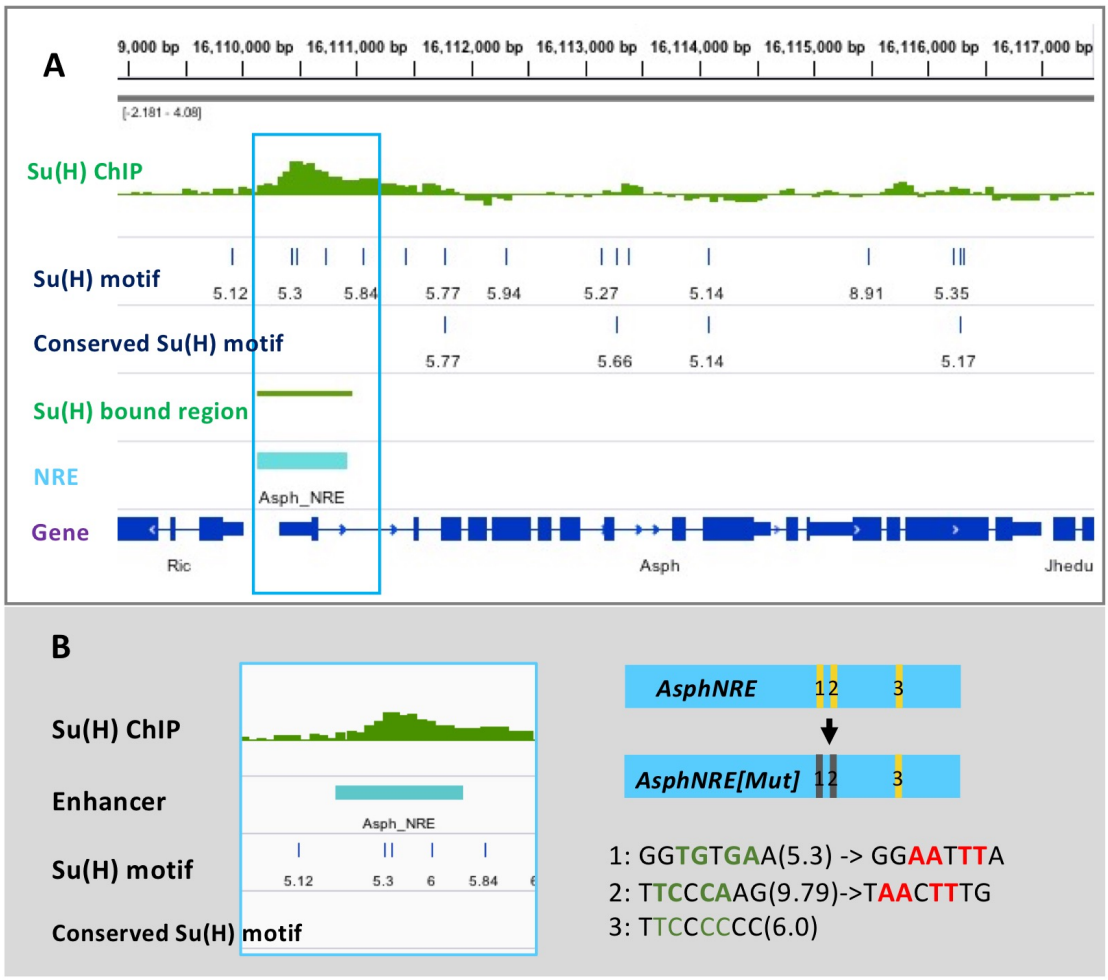

Fig 3.9. *AsphNRE* also responds to Notch regulation. (A) Genomic view of *Asph* gene region showing Su(H) bound region, binding motif and cloned NRE region. (B) Zoomed in view of *Asph* NRE region and the mutated motifs. (C) Luciferase assay of *AsphNRE* and *AsphNRE[Mut]*. (+) positive control, *m3NRE*; (–) negative control, NME. Error bars represent the SD of three biological replicas; *p<0.05. (D) *AsphNRE* directs GFP expression in a varied way in NBs, on both sides of the brain. NBs and GMCs are marked with Grh (magenta). Scale bar, 100 µm. (E&F) *AsphNRE* requires Notch activity *in vivo*. Comparing to AsphNRE-GFP in control condition (E), NB-expressing GFP is depleted in NRNAi condition (F). Green shows NREGFP; red shows Dpn, the NB marker; blue shows Prospero. Scale bar, 50 µm.

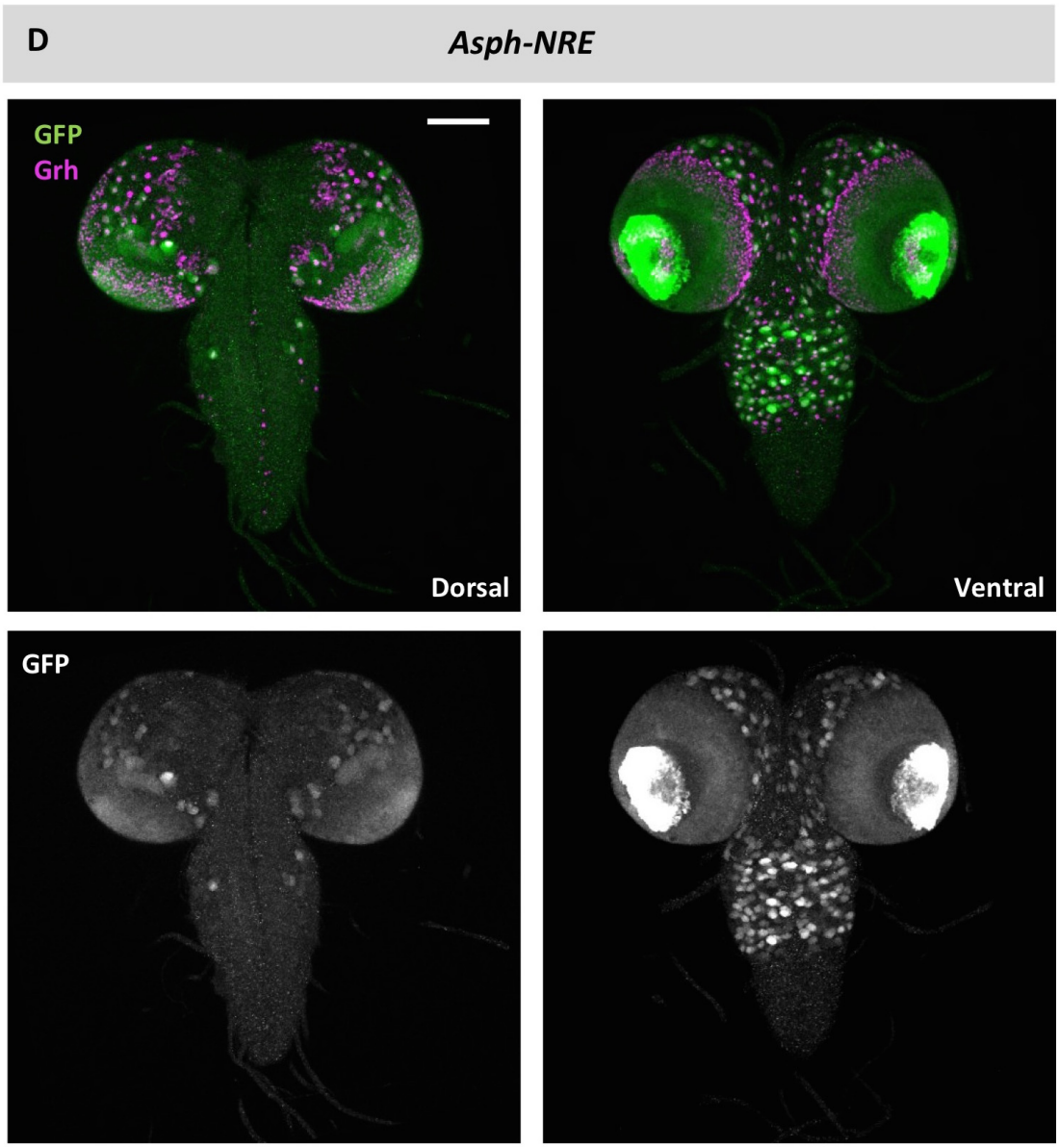

Fig 3.9. (D)

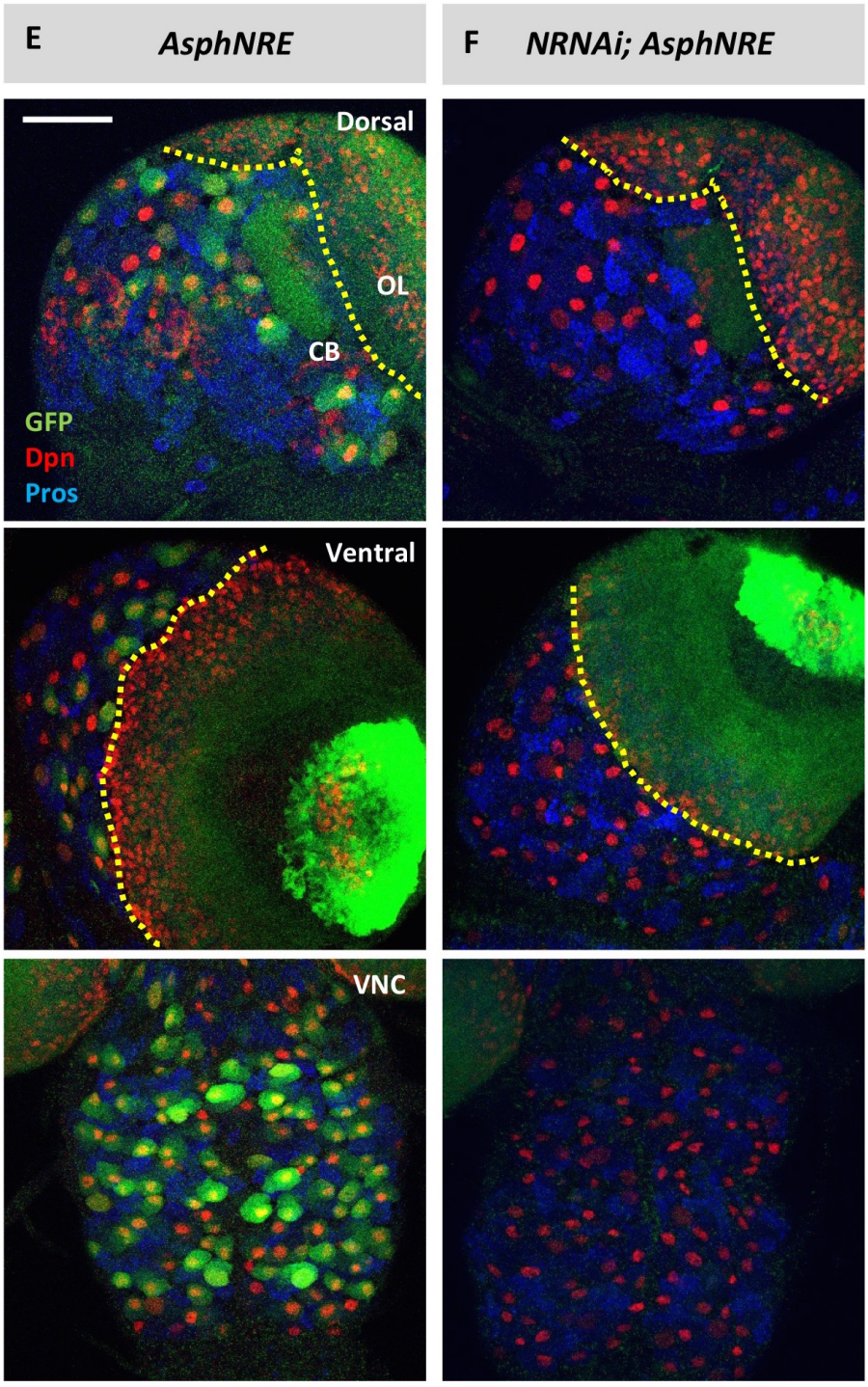
E
AsphNRE
F
NRNAi; AsphNRE
Dorsal
OL
CB
GFP
Dpn
Pros
Ventral
VNC

Fig 3.9. (E&F)

3.2.5 Two *lola-NRE* reporters exhibit different expression patterns in the brain

Two proximal Su(H) bound regions were associated with the *lola* gene, one in the intron (*lola_in*) and the other upstream of the promoter (*lola_beh*) (Fig. 3.10A). Both regions were isolated and their high-affinity Su(H) binding motifs were mutated (Fig 3.10B & C). However, neither of the regions responded effectively to Notch induction in the luciferase assay, nor was there a clear effect from mutating their Su(H) motifs (Fig. 3.10D & E).

Both *lola_in* and *lola_beh* directed GFP expression extensively *in vivo*, including NBs and their progeny, part of neuropil, and part of optic lobe. *lola_in* exhibited ubiquitous expression in NBs and neurons (Fig 3.11A), while *lola_beh* had more enriched expression in NBs compared to neurons (Fig 3.11B). Because *lola_beh* exhibited more specificity in the stem cells, it is more likely to have a function in NB maintenance. Nevertheless, neither expression pattern is strongly indicative of Notch regulation so no further analysis was carried out.

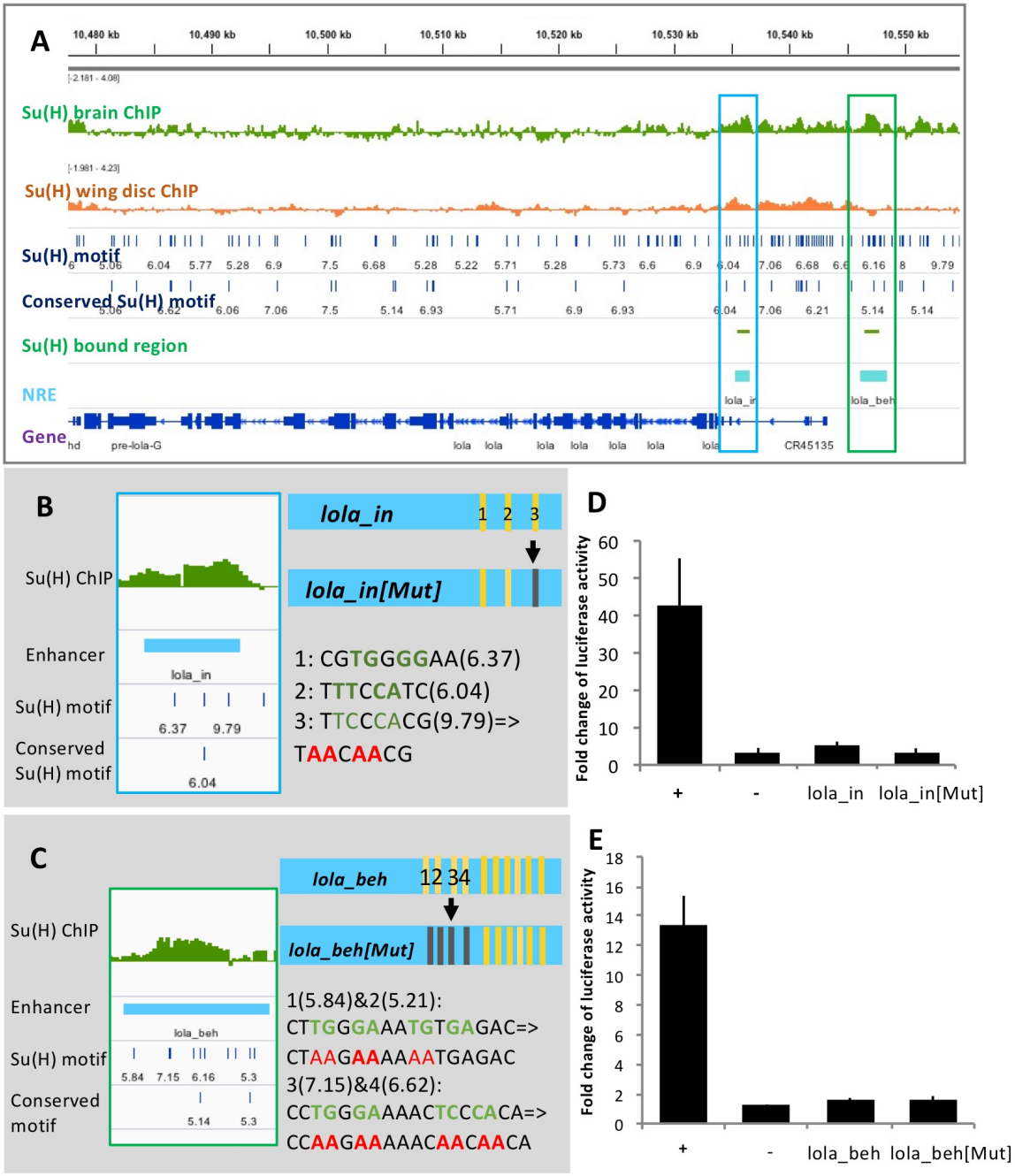

Fig 3.10. *lola* has two NRE, *lola_in* and *lola_beh* that present a low response to Notch activation. Two enhancers proximal to *lola* has expression in larval brains and do not vigorously respond to Notch in S2 cells. (A) *lola* has two nearby NRE regions. Genomic view shows the *lola* gene and the two cloned regions. (B&C) Zoomed in view and the mutated Su(H) binding motifs. (D&E) Luciferase assay of *lola_in* and *lola_beh* and the mutated enhancers in S2 cells. Error bars represent the SD of three biological replicas.

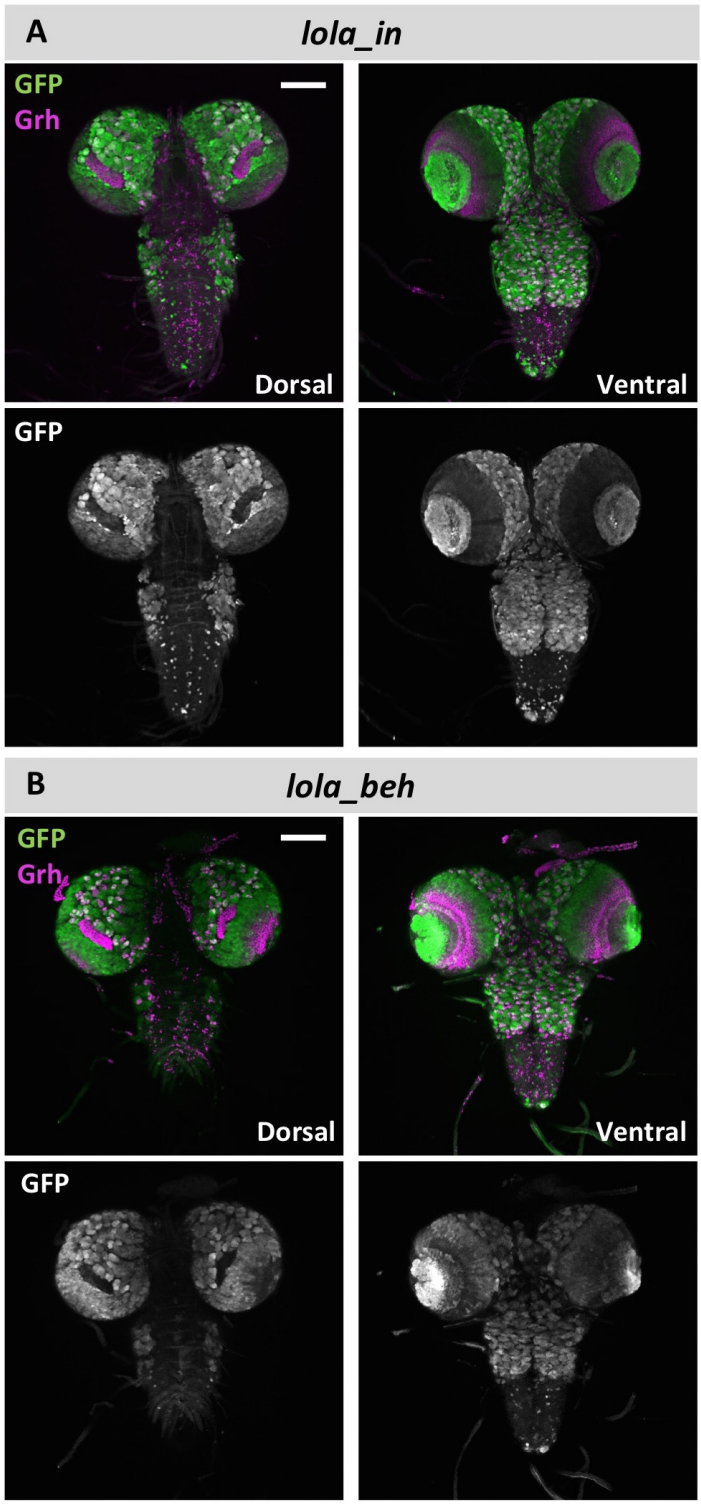

Fig 3.11. *lola_in* and *lola_beh* direct GFP expression *in vivo.* (A) *lola_in* invokes GFP expression in both NBs that are marked by Grh (magenta) and other types of cells in the larval brain. (B) *lola_beh* also directs universal expression in the brain. Scale bar, 100 µm.

3.2.6 *Fer2NRE* directs expression in a subset of neurons

Fer2 was upregulated in Notch-induced hyperplasia, and the gene exhibits one Su(H) bound region located 5' of the promoter (Fig 3.12A). This region has three Su(H) high-affinity binding motifs (Fig. 3.12B) and indeed, *Fer2NRE* exhibited a response to Notch activation in S2 cells. This response was significantly reduced when all three of the Su(H) binding motifs were mutated (Fig. 3.12C).

Despite the Notch regulation in cultured cells, *in vivo Fer2NRE* displayed a completely different pattern of expression from previous enhancers. There was no overlap between the cells where *Fer2NRE* directed GFP expression and expression of the NB marker Grh (Fig 3.12D). In contrast, co-staining with the neuronal marker Elav revealed significant overlaps, showing that *Fer2NRE* directs expression in a subset of neurons (Fig 3.12E). When 3 Su(H) motifs were mutated, fewer of the neuronal cells exhibited expression from *Fer2NRE*, indicating a dependence on Su(H) binding (Fig 3.13A & B).

The *Fer2NRE* directed expression suggests a potential role of *Fer2* in neurons. This is in agreement with a previous study indicating that *Fer2* is enriched in neurons over NBs (Berger et al. 2012). The response of the *Fer2NRE* to Notch in luciferase assays suggests that the expression in neurons could be Notch-regulated.

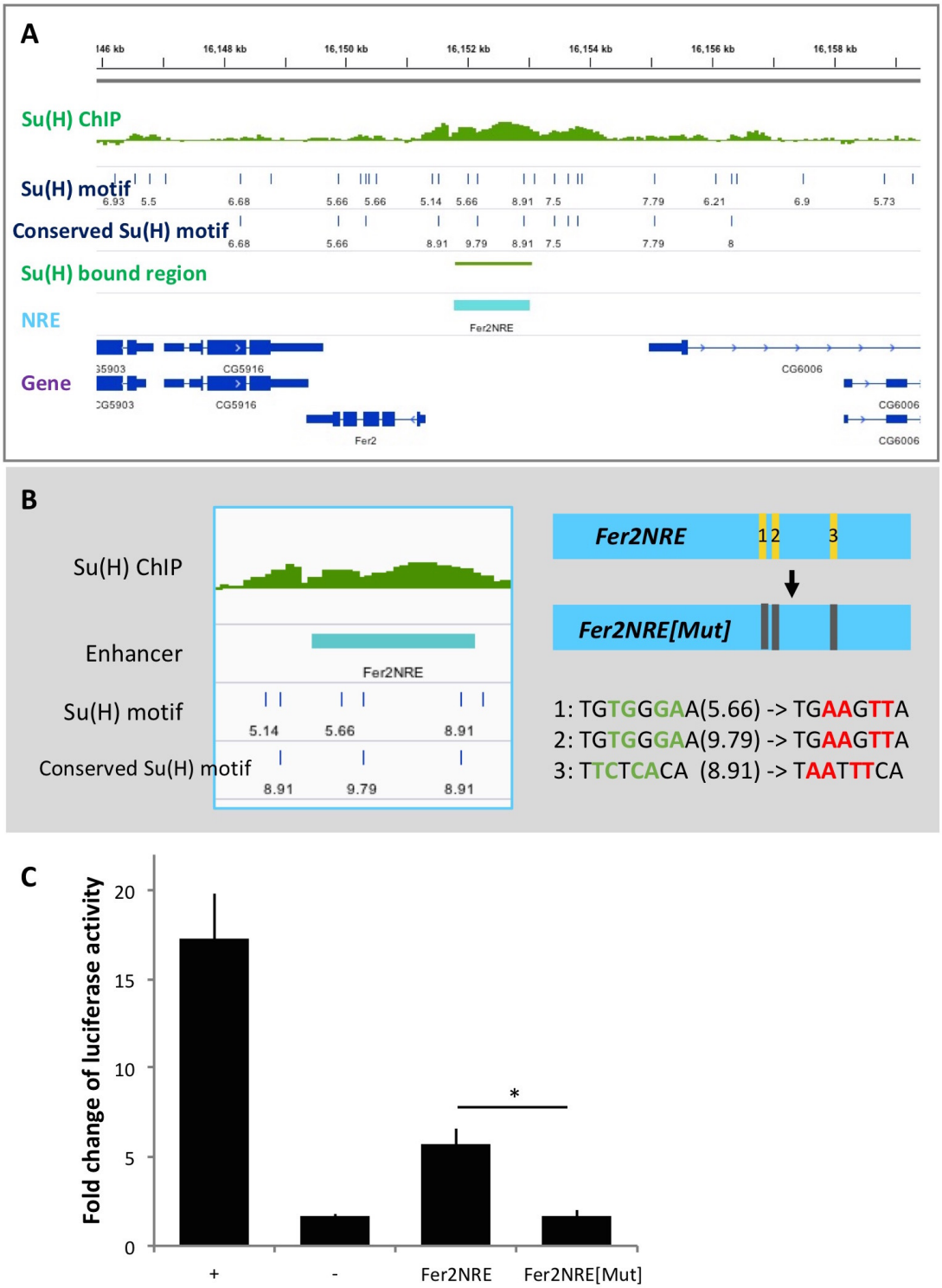

Fig 3.12. *Fer2NRE* directs expression in a subset of neurons. (A) Genomic view of the *Fer2* gene and the cloned NRE region. (B) Zoomed-in view of the *Fer2NRE* and the mutated Su(H) binding motifs. (C) Luciferase assay of *Fer2NRE* and *Fer2NRE[Mut]* in S2 cells.* p<0.05. (D) *Fer2NRE* directs expression in cells that are not NB lineage (no overlap with Grh). Green represents Fer2NREGFP; magenta represents Grh. (E) *Fer2NRE* directs expression in a subset of neurons. Magenta represents Elav, which marks all of the neurons. Scale bar, 100 µm.

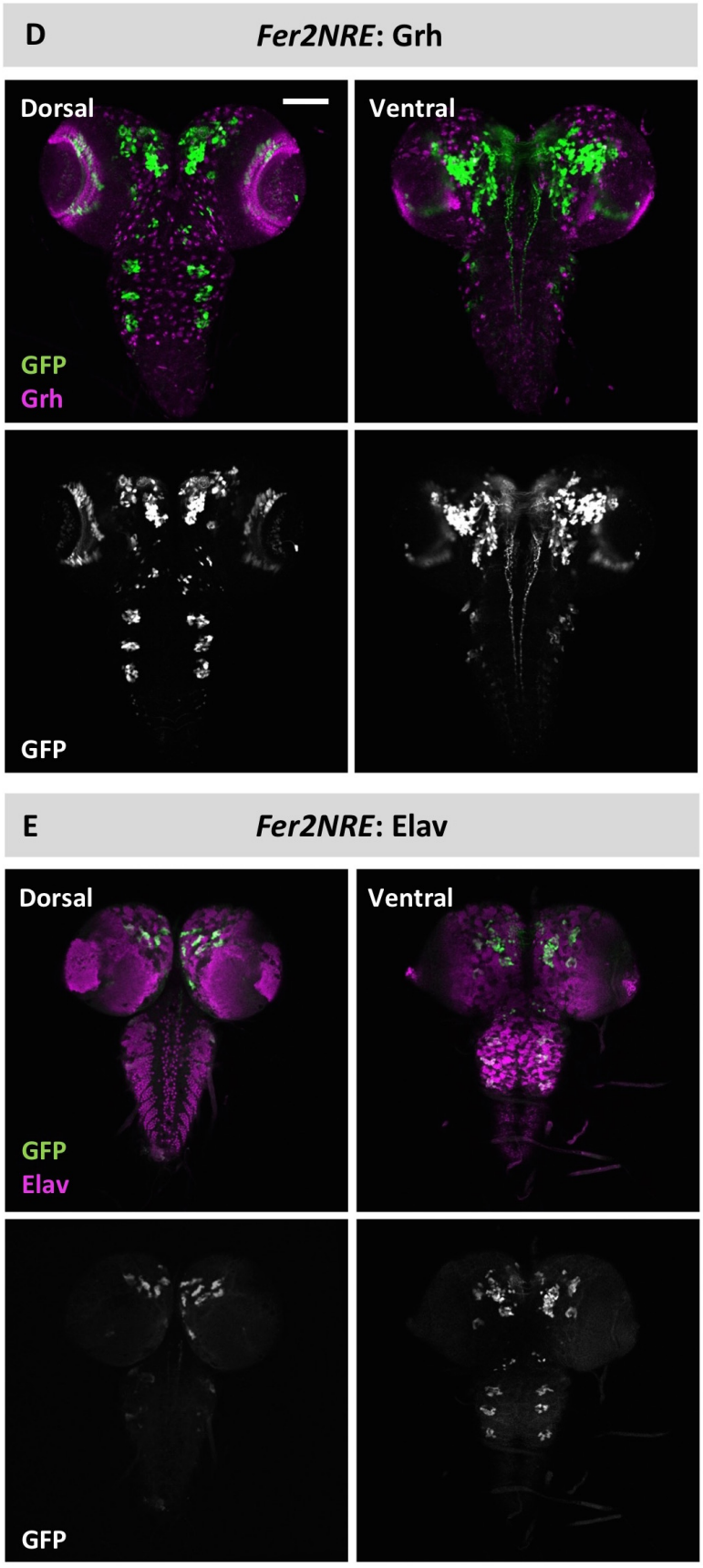
D
Fer2NRE: Grh
Dorsal
Ventral
GFP
Grh
GFP
E
Fer2NRE: Elav
Dorsal
Ventral
GFP
Elav
GFP

Fig 3.12. (D&E)

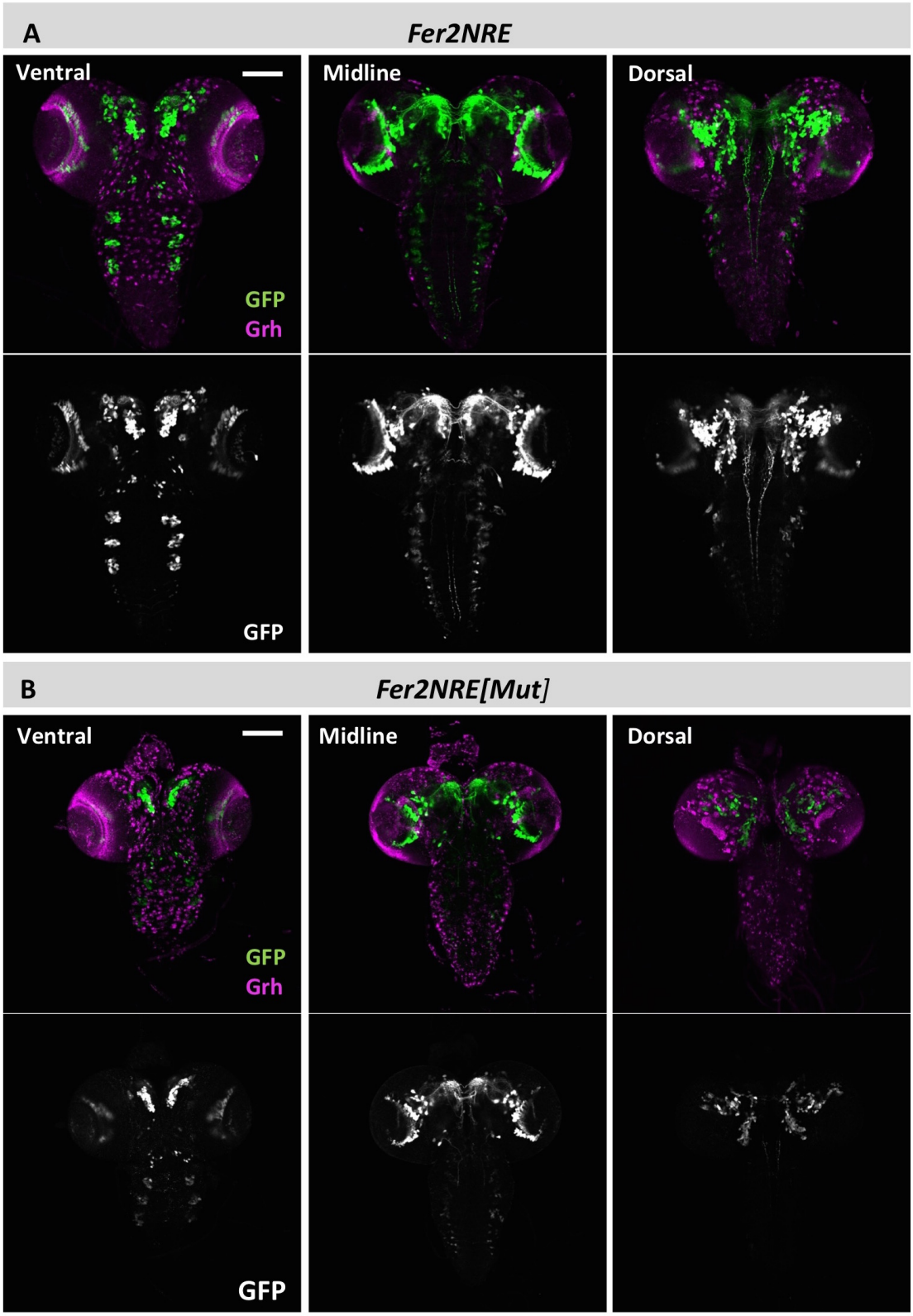

Fig 3.13. *Fer2NRE* is partially dependent on Su(H) binding motifs. (A) Ventral, midline and dorsal sections of Fer2NRE-GFP in L3 larval brain. Green represents Fer2NREGFP; magenta represents Grh. (B) Ventral, midline and dorsal sections of Fer2NRE[Mut]-GFP in L3 larval brain. Scale bar, 100 µm.

3.3 Discussion

NBs in *Drosophila* require multiple contributions to maintain stemness and differentiating ability. One of the major players in NB maintenance is Notch. In different contexts, Notch signalling has various outcomes (Bray 2016) implying that there are varied targets according to tissue specificity/cell type. This chapter focuses on identifying novel targets of Notch in neural stem cells in *Drosophila*, to understand more about the role of Notch in stem cell maintenance. Building on a recent genome-wide study several criteria were applied to select a few candidates for further validation and investigation. The main strategy was to test the activity and Notch responsiveness of enhancers to assess the likelihood that they are direct Notch targets. In this way four of the six genes analysed fulfilled some of the criteria of genuine direct Notch targets with responsive NRE(s). According to the NRE-directed GFP expression pattern, three NREs are responsive in NBs (*path, CG6191, ASPH*), while one is in neurons (*Fer2*). The former are therefore potential targets to enact some Notch functions in NBs, and merit a functional analysis. Two of these are explored in the subsequent chapters (Path, Chapter 4; CG6191, Chapter 5). The third**,** Asph, also has characteristics which suggest that it is directly regulated by Notch signalling, although this would need to be explored further (e.g. by mutating the Su(H) motif). Together with the capability to modify the EGF repeats in Notch and its ligands, it is plausible that Asph could be part of a positive feedback mechanism involved in sustaining Notch pathway activity. Future directions to investigate this would be to (1) generate an ASPH knock-out allele to analyse its function; (2) generate a knock-in GFP-tagged ASPH to further analyse its regulation; (3) investigate ASPH's catalytic ability in NBs and see if Notch/Delta could be the substrate.

The pattern conferred by the *Fer2* enhancer was unexpected since it directs expression specifically in neurons and not in NBs. However this pattern shows some resemblance to that obtained recently with a gene tag, Fer2::GFP, which was shown to be expressed in a group of dopaminergic (DA) neurons (Bou Dib et al. 2014). A staining of anti-tyrosine hydroxylase (TH) in combination with Fer2NRE would help to confirm whether it is directing expression in the DA neurons. If so, it is possible that the role of Notch in DA neuron maintenance is through the regulation of *Fer2*, adding an important link to a recent finding of Notch function in DA neuron differentiation (Trujillo-Paredes et al. 2016).

Based on my analysis, and previous work (Zacharioudaki, et al. 2016), it is evident that many of the Su(H) bound regions identified from brains indeed correspond to Notch regulated enhancers, making this a promising strategy to identify novel targets. However, two of the enhancers tested did not behave accordingly. *syncrip* at first seems like a "classic" Notch target as its enhancer directs expression in the NBs. This pattern fits well with that observed by Syp antibody staining (McDermott et al. 2012), suggesting this enhancer reflects the *syp* gene expression. However, neither the luciferase experiments nor the analysis of *in vivo* regulation supports the idea of it being a Notch target. There was no change in enhancer activity from altering Notch activity levels nor was the expression compromised when the Su(H) motifs were mutated. It is possible that Notch acts redundantly with some other factor, as observed for Deadpan (Babaoğlan et al. 2013) or that it is only required for initiation but not maintenance of Syp expression, so the regulation of Notch on *syp-Enh* is only detectable in a narrow window. However, Syp-Enh expression fits well with the changing profile observed for

Syp during development (Liu et al. 2015), making it less likely that the latter is the case. Given that this enhancer recapitulates well the pattern of Syp expression it will be valuable for exploring further the other regulators. This may then reveal whether there are redundant inputs working with Notch conferring NB expression, or whether the Notch input is only significant in another context. Notably, whatever the mechanism of its regulation, Syp has emerged as a key regulator of NB development, affecting the temporal maturation of the NBs (Liu et al. 2015).

The other enhancers that showed less clear evidence of Notch regulation were those from *lola*. Both of the regions tested exhibited no significant response to Notch signalling. They also displayed a more general expression in CNS. Of the two *lola* enhancers, *lola_beh* directs more specific expression in NB and less in neurons, compared to the more ubiquitous expression from *lola_in,* and thus may have some input from Notch although this was hard to verify. It is also possible that specific Notch responsive patterns can only be achieved in combination with the correct promoter, as *lola* is a gene with multiple RNA isoforms (Goeke et al. 2003; Ohsako et al. 2003). The Su(H) binding profile in the *lola* locus is also complex, which may indicate that specificity is only achieved by combinations of enhancers (Fig3.10A), A more thorough investigation of *lola* enhancers would be needed to distinguish these possibilities.

These examples illustrate some of the pitfalls in the approaches used. First, there is the possibility of redundant/parallel enhancer inputs, as suggested by Syp (and observed for Dpn,(Babaoğlan et al. 2013)), so that the role of Notch is masked. Further analysis would be needed to investigate whether the lack of response from *syp* and *lola* enhancers may be explained by this possibility. Second, because the original strategy used to profile the

Notch-regulated genes involved using whole brains, changes in gene expression in other cell types could have confounded the analysis. Thus, NBs only constitute a very small part (~300 NBs) and there are much larger numbers of other cell types (~10,000 neurons and ~300 glial cells) in the larval CNS (Kang & Reichert 2015). This may explain how *Fer2* was identified, as it's enhancer exhibited characteristics of Notch regulation despite the fact that it directed expression in neurons rather than NBs. Third, the Notch-regulated enhancers may only recapitulate a subset of a genes expression pattern in the CNS. This may explain why *path*, whose enhancer strongly drives expression in NBs in a Notch-dependant way, was not highly up-regulated based on the RNA profiling of brains with activated Notch (Table 3.1). This contradiction can now be explained by the robust expression of Path in the glia (see *chapter 4*), demonstrating the risk/noise in whole tissue experiments. In comparison, the Knoblich data identifies *path* as having NB-enriched expression, because it is based on RNAs isolated from purified NBs (Berger et al. 2012).

Finally, *CG6191Big* enhancer illustrates another complexity with identifying targets based on binding of transcription factors, namely how to match the enhancer to its appropriate transcription unit. The strategy taken by the Bray lab was to match Su(H) bound regions to nearby genes based on their responsiveness to Notch activity. *CG6191* mRNA level was elevated in brains expressing activated Notch (1.89 fold) (Zacharioudaki, et al. 2016) and also in wing discs with similar conditions (Djiane et al. 2013). This led to the suggestion that the Su(H) bound region nearby, here referred to as *CG6191Big*, could be an enhancer for *CG6191*. While some other examples have supported this suggestion, others link the enhancer to more proximal genes such as *CG13334* (T D Southall & Brand

2009). Clearly, it is important to distinguish which gene(s) are directly regulated by *CG6191Big* since it gives robust expression in NBs that is sensitive to Notch activity. Possible strategies would be using Hi-C to monitor the interactions between the gene and its promoter, although this may be challenging given the tissue context. Alternatively, the consequences on mRNA expression from deleting the enhancer would be informative. This is the strategy that has been taken, using CRISPR/Cas9 genome editing, as described in Chapter 5. The results support the hypothesis that *CG6191Big* is a bone fide enhancer for *CG6191*, validating the original strategy taken.

3.4 Summary

In this chapter, I have cloned seven genomic regions, identified on the basis of Su(H) binding, and presented data suggesting that four of them behave as Notch-regulated enhancers. These identified NREs provide the basis for future work examining whether the genes have important functions as Notch targets in NBs. They will also be valuable for future research into how these genes are regulated. Since the validation of these NREs confirmed these genes as putative Notch targets in the brain, the results also add more potential players to explain the regulatory network in neural stem cells.

Chapter IV

The SLC36 transporter Pathetic as a novel direct Notch target is required for protecting neural stem cell proliferation under abnormal conditions

4.1 Introduction

Food shortage is a huge challenge for animals in nature, especially during early development when body growth is more sensitive to nutrition level (Mirth & Shingleton 2012; Prado & Dewey 2014). For thousands of years, organisms have developed different strategies to deal with hunger. Newborns with developmental malnutrition are usually smaller in size, but their brains are similar in size to individuals with normal nutritional status (Lanet & Maurange 2014). Human fetuses in the situation of nutrition deprivation would adapt through maximising oxygen and nutrient supply to the brain (brain sparing) (Malamitsi-Puchner et al. 2006; Flood et al. 2014; Cohen et al. 2015).

There is a similar mechanism in the *Drosophila* late larval stage. During *Drosophila* larval CNS development, the early larval stage (L1-L2) is most sensitive to nutrition fluctuation, with poor nutrition resulting in a much smaller adult (Hietakangas & Cohen 2009). Without adequate nutrition input, larval neuroblasts cannot wake up from quiescence (Sousa-Nunes et al. 2011). This process is regulated by fat body and glia signals (Sousa-Nunes et al. 2011; Chell & Brand 2010). After larvae reach a critical weight (60 hrs ALH),

nutrition levels no longer restrain the ability to pupate (Mirth & Shingleton 2012). As a result, starvation after this stage will result in a smaller larva, pupa and adult with generally smaller organs, except for the brain. Brain growth is mostly protected during this period. After the critical weight time point, starvation gives a brain with a similar size as control counterparts (Cheng et al. 2011). Several pieces of work shed light on different compartments of the CNS response to nutrition restriction (Cheng et al. 2011; Lanet et al. 2013) and indicate that the Alk/Jeb pathway instead of Tor pathway plays an important role in this process. But the underlying mechanism is far from well understood.

Pathetic is a member of the SLC36 transporter family with a classic transmembrane domain. It interacts with Tor pathway components in eye growth and body growth of *Drosophila* (Goberdhan et al. 2005). Recently, a role of *path* has been identified in promoting dendrite growth of C4da neurons (Lin et al. 2015). When the Path transporter was expressed in *Xenopus* oocytes, it exhibited high affinity for alanine and glycine with low transporting capacity (Goberdhan et al. 2005), while the closest mammalian relative, proton-assisted transporter 4 (PAT4 or hPAT4), had high affinity to proline and tryptophan (Muralidharan Pillai & Meredith 2011); notably, although named as proton-assisted transporters (PATs), PAT4 is not proton-coupled.

As for the mechanism of Path/PATs, initially they were proposed to function as amino acid transducers (sensors) that turn on Tor signalling, since they do not transport bulk amino acids and they were found to genetically interact with mutations affecting the Tor pathway (Goberdhan et al. 2005; Muralidharan Pillai & Meredith 2011). SLC38A9 has been validated as an amino acid sensor in the process of mTORC-activation in

mammalian cell lines (S. Wang et al. 2015; Rebsamen et al. 2015). More recently, SLC36A4 was found to be required for promoting proliferation in colorectal cancer through interacting with mTORC1 (Fan et al. 2016). A requirement for SLC36A4 in mice retinal pigmented epithelial cells also involved mTORC-activation (Shang et al. 2017). While these findings link PAT4 to mTORC-activation in different contexts, it is unclear whether its growth-promoting role is adaptive to starvation as in the brain sparing mechanism where the Tor pathway is somehow bypassed in nutrition deprivation.

In the previous chapter, I have demonstrated that the intronic region of *pathetic* contains a Notch-responsive element (Fig 4.1A). This *pathNRE* directs expression in NBs (Fig 4.1B) and in the excess NB-like cells generated by Notch over-activation (Fig 4.1C). A mutated version of the *pathNRE*, in which the Su(H) binding motifs were disrupted (*pathNRE[Mut]),* retained little NB expression and was no longer responsive to Notch over-activation (Fig 4.1D & E). These results suggest that *path* is directly regulated by Notch signalling in NSCs. Previous studies showed that *path* promoted both general and neuron dendrite growth (Goberdhan et al. 2005; Lin et al. 2015). However, its role in NBs and brain growth has not been investigated.

The proposed role of PATs for activating Tor in different contexts raised the question whether *path* is involved in amino acid-mediated regulation of growth pathways in NSCs and in Notch-induced hyperplasia. This study focuses on this question, investigating the function of the novel Notch target *pathetic*. Objectives: (1) to examine Path expression pattern in *Drosophila* larval brain; (2) to explore the role of Path in NSCs through knocking out *path* through mosaic clones and knocking down *path* using RNAi; (3) to examine whether *path* is involved in Notch-induced hyperplasia and its mechanism; (4)

to investigate whether *path* responds to nutrition restriction (NR); (5) to explore *path* function under NR and its mechanism. Results suggest that *path* is required for normal NSC growth and that it also protects the brain from extreme growth conditions.

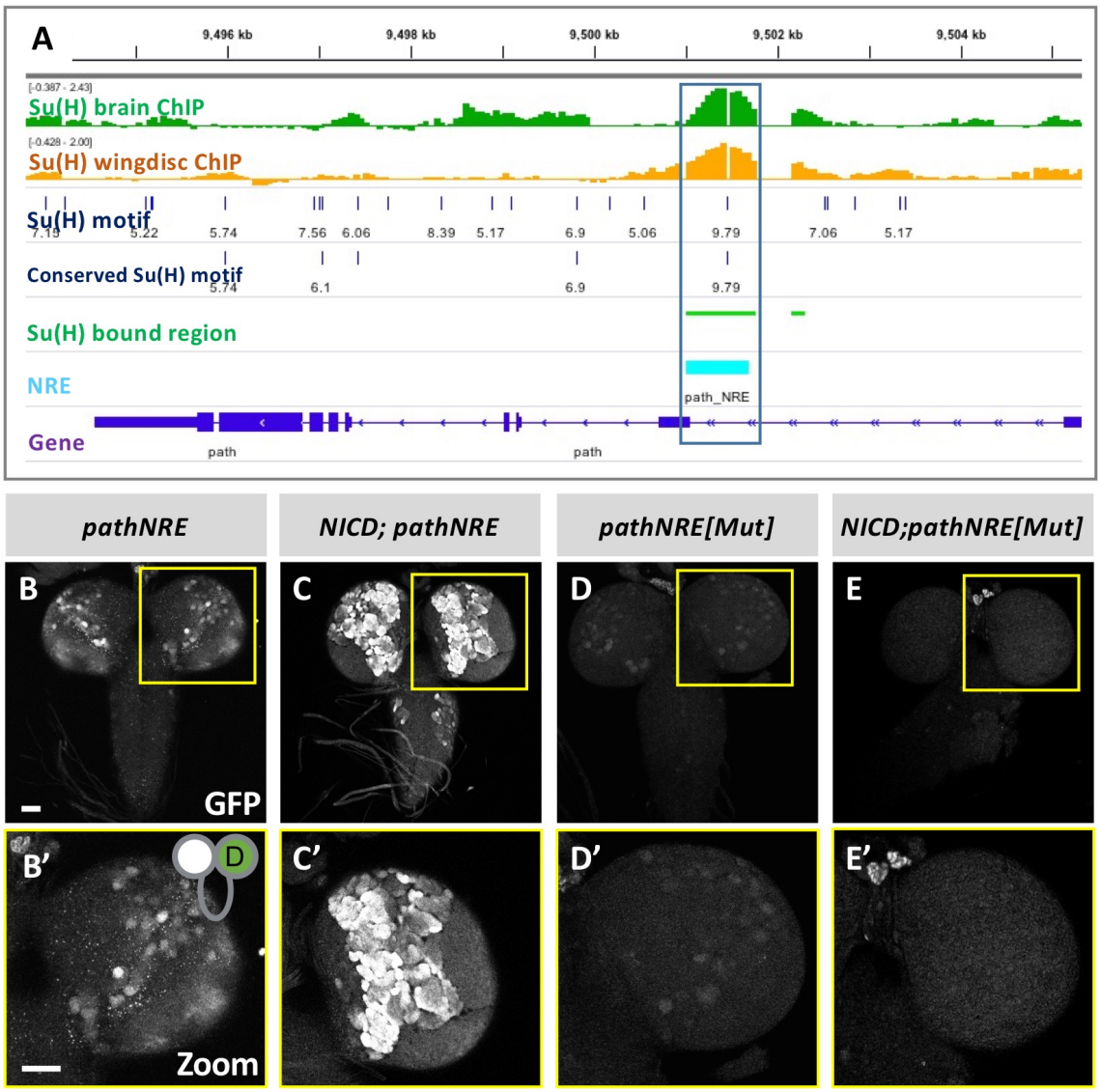

Fig 4.1. *pathNRE* is a Notch-responsive element in neural stem cells. (A) A genomic overview of *path* gene region displays profiles of Su(H) binding in the brain (green) and wing disc (orange) (enrichment relative to input AvgM, log scale is as indicated) along with Su(H) motifs/conserved motifs (blue bars, the numbers indicate its Patser score (Rebeiz et al. 2002)). The blue box outlines the region cloned as *pathNRE*, indicated by the cyan rectangle. (B-E) *pathNRE* responds to Notch regulation in neural stem cells while a mutated version (*pathNRE[Mut]*) has lost expression and response. All images show the dorsal side of the brain. NRE Reporter expression in the indicated genotype is detected with anti-GFP (grey). (B'-E') Zoomed in view of (B-D). Scale bar, 50 µm.

4.2 Results

4.2.1 Path is expressed in neural stem cells and glia

The expression of pathNRE-GFP suggests that the Path protein will be expressed in NBs. To verify this, the expression pattern was analysed using Path[GFP], a functional allele with GFP inserted at the C-terminus, as well as an anti-Path antibody (Gifts from J.Z. Parrish) (Lin et al. 2015). Expression of Path[GFP] was detected broadly in the L3 brain, where it was highly expressed in surface and cortex glia (Fig 4.2A & B). Low levels of Path[GFP] were also present in NBs and their progeny (Fig 4.2A inset). A similar enrichment of Path in the surface glial cells was detected with Path antibody (Fig 4.2C & D; Repo is a glial cell marker). Because of the high level of Path expression in surface glia, it was difficult to ascertain whether there was expression in the underlying NBs. To assess this, I used a glial cell-expressing driver, *repo-Gal4*, to downregulate *path* in glia with RNAi. When the glial expression was suppressed, the stem cell expression of Path was more clearly revealed (Fig 4.2E & F). Furthermore, it was evident that Path expression was enriched in NBs rather than in neurons (Fig 4.2E & F and insets), which is consistent with previous transcriptomic analysis of FACS (fluorescence-activated cell sorting) sorted cells (Berger et al. 2012). These data confirm that Path is expressed in NBs, as suggested by the expression driven by *pathNRE*.

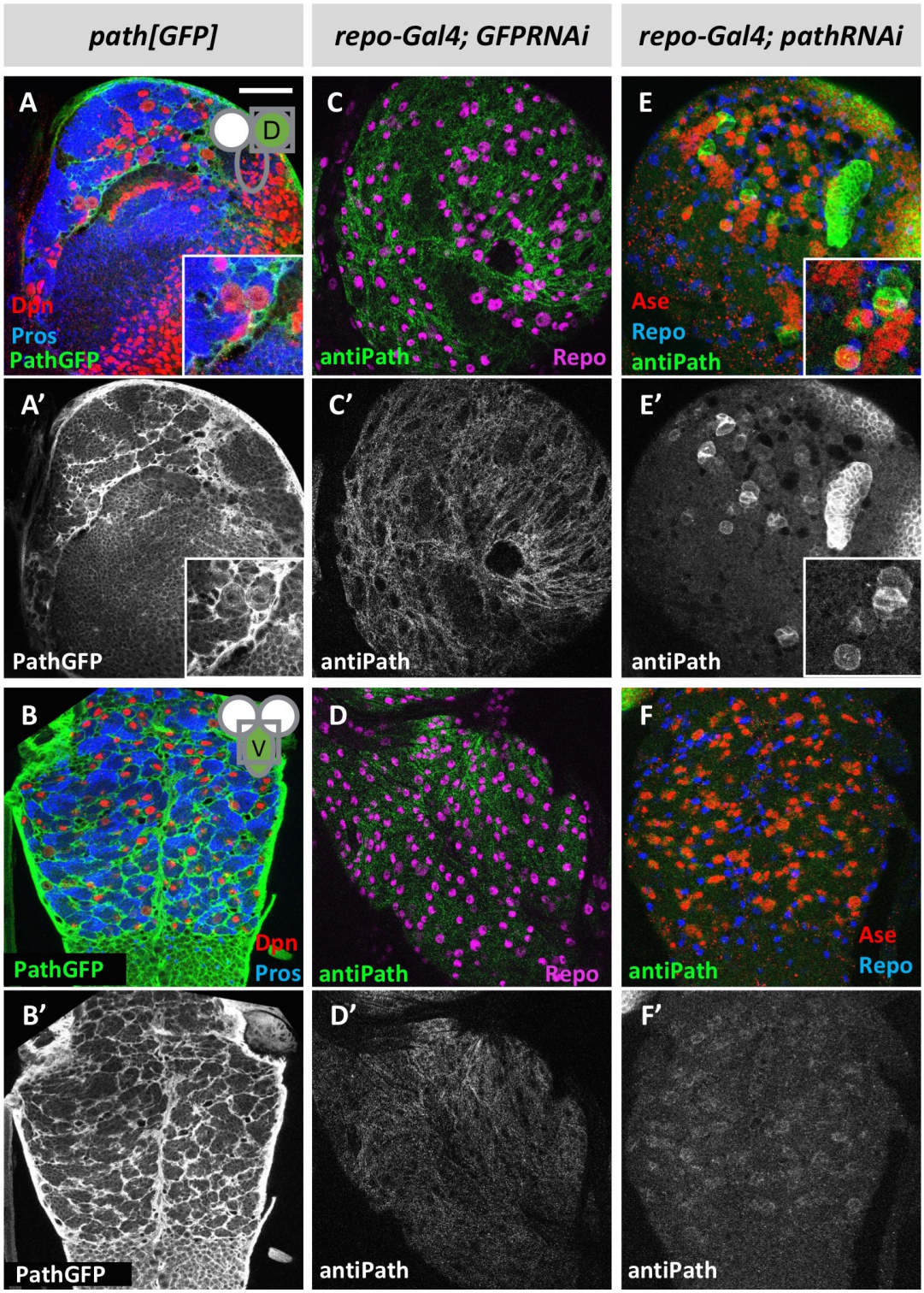

Fig 4.2. Path is expressed in both glia and neural stem cells. (A-B) Path expression pattern revealed by GFP knock-in allele *path[GFP]* (green in A&B, grey in A'&B') in the dorsal brain lobe (A) and ventral nerve cord (B); NBs are marked with Dpn (red), and neurons with Pros (blue), (C-D) Anti-Path staining (green in C&D, grey in C'&D') is enriched at the surface of the brain, as shown on the same surface with glial cells marked by Repo (magenta). (E-F) Anti-Path (green in E&F, grey in E'&F') stains NBs when glial-expressed Path is depleted by *pathRNAi*. TypeI NBs are marked with Ase (red), glia cells were marked with Repo (blue) Scale bar, 50 µm.

4.2.2 Depletion of Path causes an increase in neural stem cell size and a reduction in the number of NB progeny

Given the role of Notch in maintaining NSCs and the evidence that Path is directly regulated by Notch, it is plausible that Path could play an important role in implementing Notch function in NBs. First, I tested the role of *path* in NSC proliferation, using the MARCM system to generate random clones of wild-type and *path* mutant cell lineages marked with GFP (Fig 4.3A). Analysing cell size and cell number revealed that, when *path* is removed, the NB clones contain less progeny, i.e. fewer cells were present per clone (Fig 4.3B, C & D) control clone cell number mean value is 43.88±3.34, n=26; mean of *path* mutant is 30.33±1.89, n=42). At the same time, the mutant stem cells were larger than control ones (Fig 4.3B, C & E, control NB mean size is 8.91±0.07 μm, n=253; mean of *path* mutant NB size is 9.43±0.11 μm, n=120). The increase in NB size was also observed when *path* was depleted specifically in NBs, by driving *path* RNAi with inscutable-Gal4 (Fig 4.4, control NB mean size is 8.71 ± 0.067, n=303; mean size of *path* knock-down NBs is 9.58 ± 0.068, n=340). Some of the brains expressing UAS-*pathRNAi* are slightly smaller than control brains, suggesting there are less neurons/glial cells generated when *path* is depleted. Neuronal defects in the resulting adults need to be further examined. Despite these changes, the *path* mutant NBs retained expression of Deadpan and Miranda, which normally mark these stem cells (Fig 4.3C & C', Fig 4.4C & D).

The reduction in the number of cells per NB clonal lineage suggests they underwent either fewer cell divisions or more cell death after clone induction. Considering that larger stem cell size can also result from a delay/stop in the cell cycle, changes in

proliferation seemed the more likely explanation, especially as Hoechst staining did not show any sign of apoptotic/fragmented nuclei in the mutant clones (data not shown). EdU labelling was therefore used to investigate the number of cells undergoing DNA replication in wild-type and *path*-mutated NBs. EdU is short for 5-ethynyl-2'-deoxyuridine, a thymidine analogue that can be readily incorporated into DNA during DNA synthesis. Therefore, the rate of EdU uptake represents the number of rounds of DNA replication (Salic & Mitchison 2008). During a 4 hr EdU incubation, all cells that went through DNA replication should be labelled whereas non-dividing cells would not. Under these conditions, *path*-/- clones had fewer cells marked by EdU than control clones (Fig 4.5, mean of control EdU-positive (EdU+ve, or EdU+ in figures) cells is 6.0$\pm$ 0.22, n=61; mean of EdU+ve cells in *path* clones is 4.5$\pm$0.25, n=51). This result suggests that the *path* mutant cells divide more slowly. The estimated division rate for control NBs is 84.56 min and for *path* mutant NBs is 111.02 min. In summary, these results indicate a requirement for *path* in maintaining the normal rate of NSC proliferation.

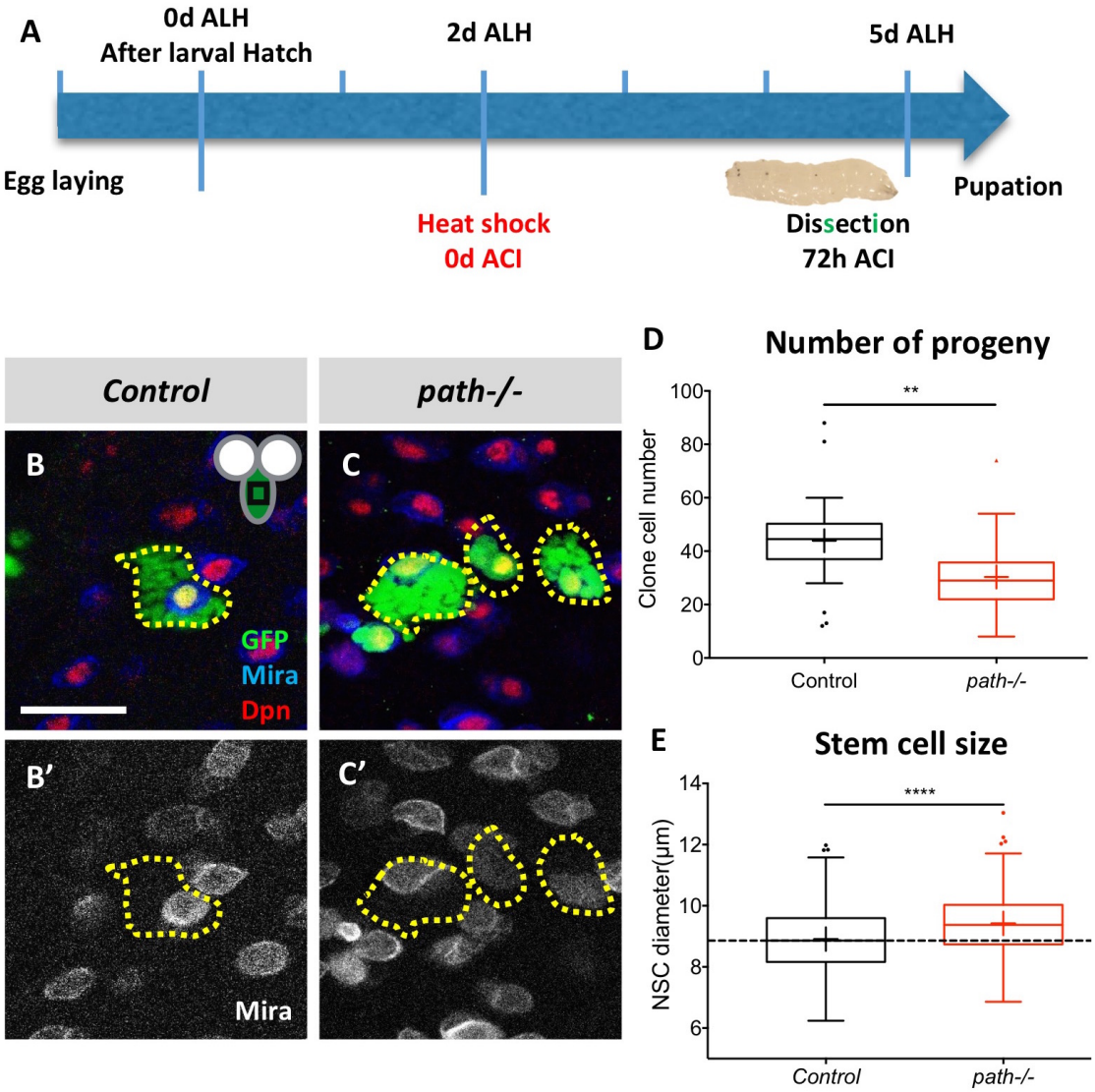

Fig 4.3. Depletion of Path causes an increase in NSC cell size and reduction in lineage number. (A) Scheme for mosaic clone induction. Larvae were heat-shocked 48hrs after larval hatch(ALH) and dissected 72hrs after clone induction (ACI). (B-E) Clonal analysis of *path* mutant NBs 3 days after clone induction (ACI). (B&C) VNC Mosaic clones of control (B) and *path* mutant (C). NBs are marked with Dpn (red) and membrane marker Mira (blue in B&C, grey in B'&C'). GFP-marked NB lineages are outlined with yellow dotted lines. (C) Number of progeny of marked lineages, n=26, 42. (D) Quantification of control and path mutant NB size marked by Mira; n=253, 120. **p<0.01, ****p<0.0001. Scale bar, 50 μm.

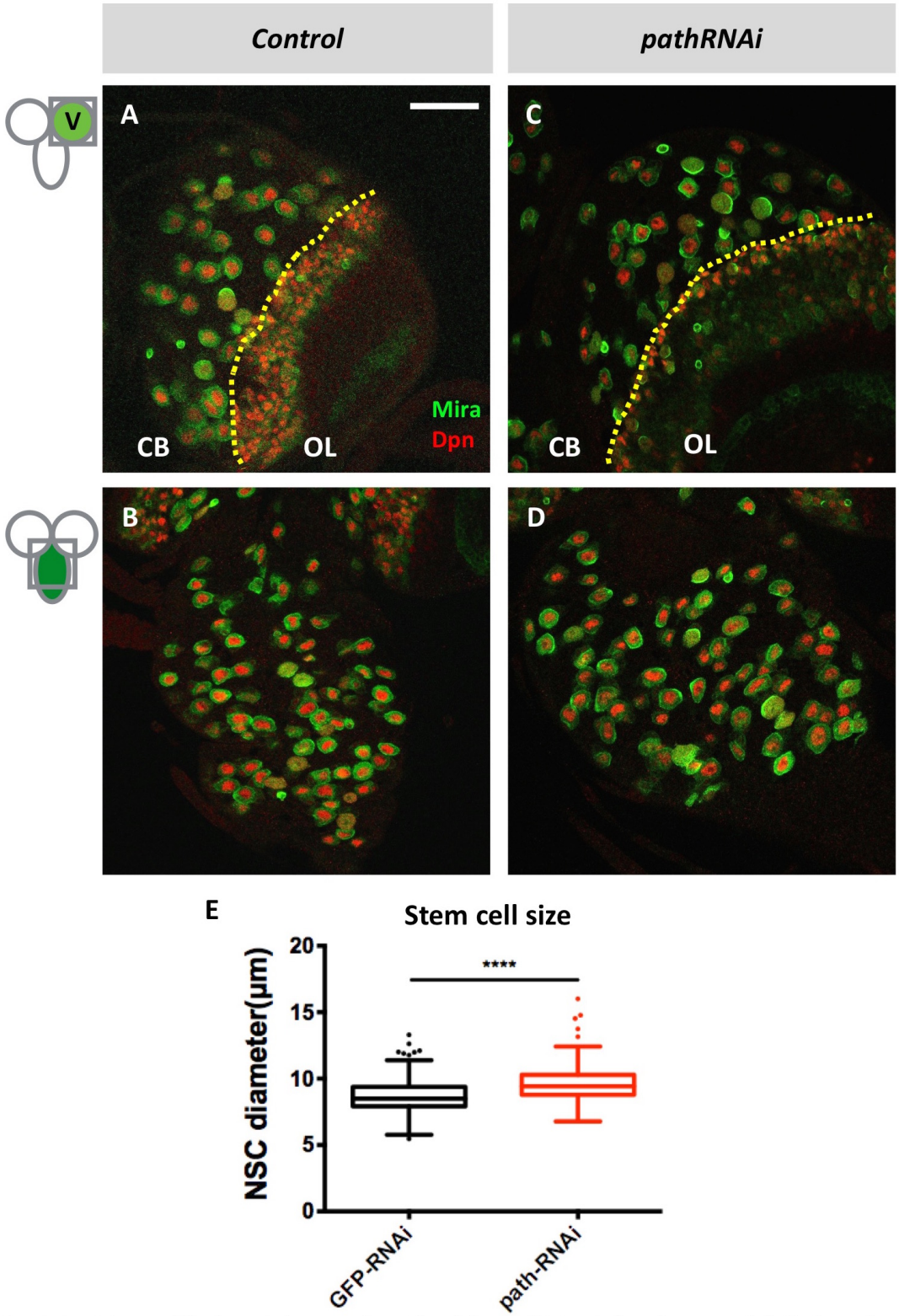

Fig 4.4. NB specific knockdown of *path* with *pathRNAi*. (A-D) Control (A&B) and *path* knockdown (C&D) brains driven by *insc-Gal4,* larvae were incubated at 30°C for 5 days before dissection. Central brain dorsal (A&C) and VNC (B&D) brain NBs are marked with Dpn (red) and Mira (green). CB, central brain; OL, optic lobe. (E) Quantification of NB size with *GFPRNAi* and *pathRNAi*. n=303, 340. ****p<0.0001. Scale bar, 50 µm.

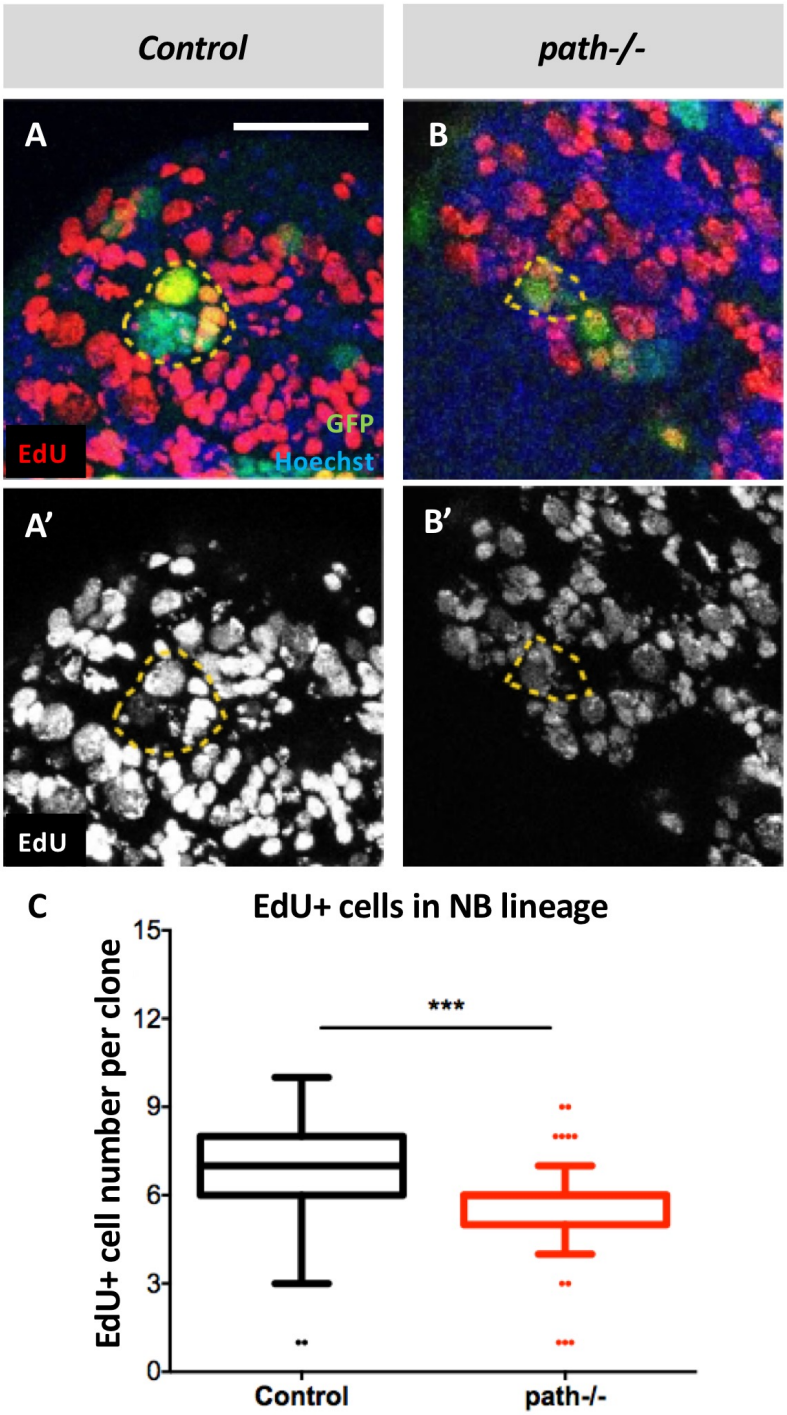

Fig 4.5. Path depletion causes delay in cell proliferation. (A-B) EdU labelling assay of control (A) and *path* (B) mutant NB clones 3 days ACI. Brains were incubated in EdU for 4 hours after dissection and cells undergoing proliferation are marked with EdU (red and grey panels); Nuclei are marked by Hoechst (blue) staining. GFP-marked NB lineages are outlined with yellow dotted lines. (C) Quantification of EdU-positive (EdU+ve, or EdU+ in figures) cells in marked NB lineages; n=61, 51. ***p<0.001. Scale bar, 50 µm.

4.2.3 *path* switches from promoting to restricting proliferation when Notch is over-activated

If *path* is required for normal rates of NB proliferation and its expression is affected by Notch, we anticipated that its depletion would suppress Notch-induced hyperplasia. To investigate this, the consequences of removing *path* from clones of cells expressing an activated form of Notch (NΔECD), were analysed (Fig 4.6). Under conditions where NΔECD expression in MARCM clones resulted in more NB-like cells, evident from their EdU staining, the hypothesis was that removal of Path in NBs would lead to fewer EdU+ve cells. Unexpectedly, the converse occurred. In the *path* mutant NB clones, more EdU+ve cells were produced by constitutive Notch signalling rather than fewer. Thus NΔECD clones lacking *path* contained more cells than those with NΔECD alone (Fig 4.6A-D & E, the mean number of cells per clones for control is 31.24±2.11; for *path-/-* is 17.16 ±1.38; for *NΔECD* is 50.00±3.27; for *NΔECD; path-/-* is 73.77±6.20; n=61, 51, 20, 21). In addition, more cells exhibited EdU labelling indicative of higher rates of proliferation (Fig 4.6A-D & F, the mean number of EdU+ve cells per clones for control is 6.90±0.23; for *path-/-* is 5.53±0.25; for *NΔECD* is 35.83±2.92; for *NΔECD; path-/-* is 50.45±4.34; n=61, 51, 20, 21). In contrast to expectations, the results argue that under Notch over-expression conditions, Path is not promoting proliferation, but rather is restricting it.

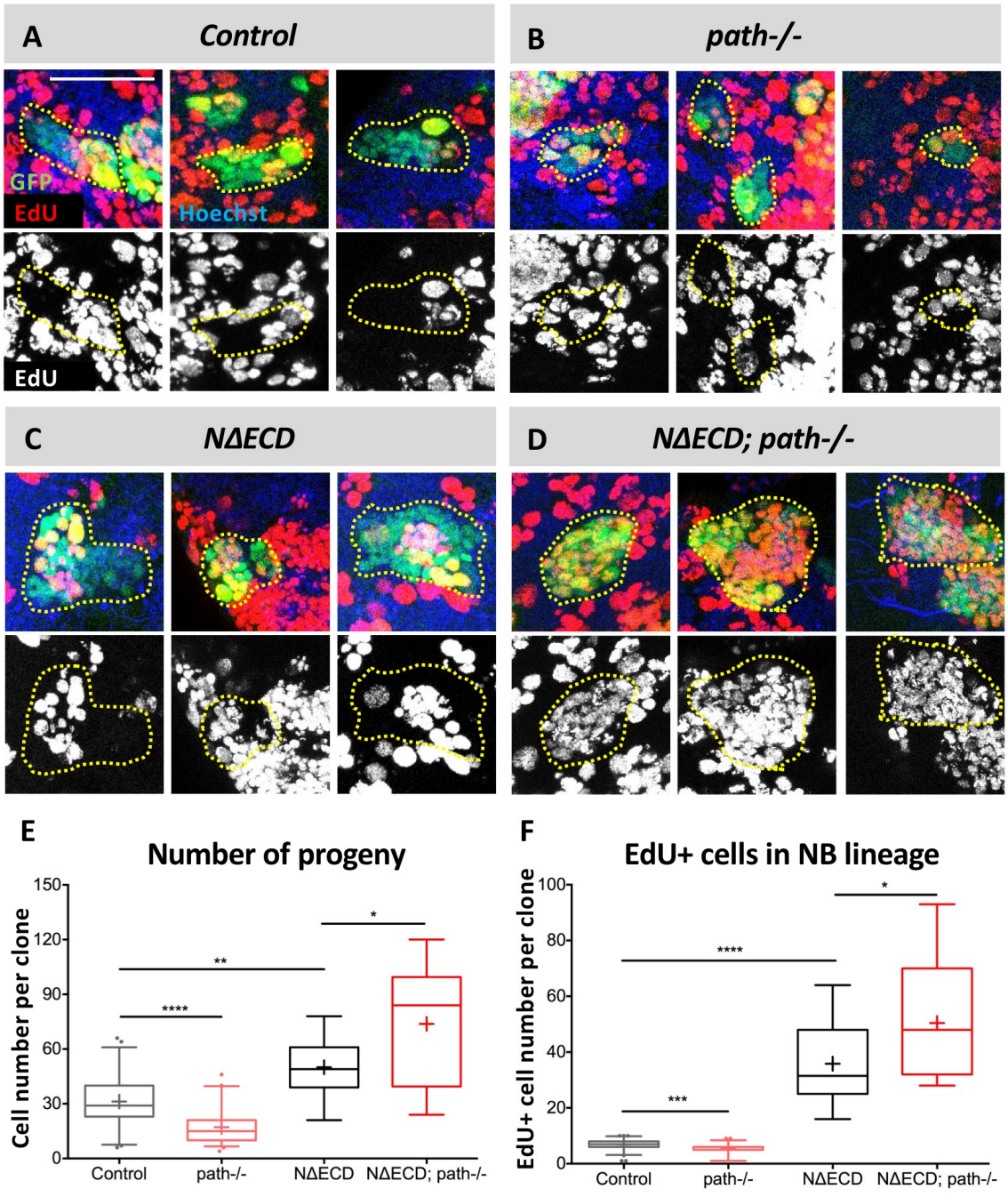

Fig 4.6. Path restricts overgrowth in Notch-induced hyperplasia. (A-D) EdU labelling assay of control (A), *path* mutant (B), Notch overexpression (C) and *NΔECD; path-/-* NBs (D) 3 days ACI. Brains were incubated in EdU for 4 hours after dissection and cells undergoing proliferation are marked with EdU (red); Nuclei are marked by Hoechst (blue) staining. GFP-marked NB lineages are outlined with yellow dotted lines. (E) Number of cells per marked lineage in indicated genotypes; n=61, 51, 20, 21. (F) Quantification of EdU+ve cells per marked NB lineage; n=61, 51, 20, 21. *p<0.05; **p<0.01; ***p<0.001; ****p<0.0001. Scale bar, 50 µm.

4.2.4 Loss of Path promotes 4EBP phosphorylation under conditions where Notch is over-activated

Two major pathways regulate NB cell growth and proliferation at different stages. During the early larval stages, InR/Tor pathway is involved in NB reactivation, growth and proliferation (Sousa-Nunes et al. 2011). However, in L3 NSC growth is regulated by the Alk/Jeb pathway which activates downstream PI3K/Akt signalling, but independent of Tor (Cheng et al. 2011). Despite these differences, the phosphorylated 4E-BP (p4EBP) is a common downstream effector of both InR/Tor and Alk signalling. Therefore, to gain more insight into the mechanisms underlying this switch of *path* function, p4EBP levels were analysed. No change in the number of p4EBP positive (p4EBP+ve, or p4EBP+ in figures) NBs in the dorsal brain was seen when *path* was down-regulated in NBs (*insc-Gal4, path-RNAi*; Fig 4.7A, B & F). Next, *path* was knocked-down in Notch over-expressing NBs. Under conditions with Notch over-expression only, the type II lineages in the dorsal brain were dramatically increased, generating excessive Dpn positive neural stem cell-like cells, as well as more p4EBP+ve cells (Fig 4.7C, E & F). Depleting *path* in this Notch induced hyperplasia resulted in strongly enhanced p4EBP levels (Fig 4.7D & F). Many more cells contained p4EBP and the levels appeared higher (the mean number of cells per brain lobe for control is 37.17$\pm$3.30; for *path-/-* is 36.75$\pm$2.484; for *NΔECD* is 934.7$\pm$54.71; for *NΔECD; path-/-* is 935.5$\pm$60.23; n=8, 9, 10, 6 respectively). The mean number of 4EBP+ve cells per brain lobe for control is 6.875$\pm$1.11; for *path-/-* is 7.56$\pm$1.60; for *NΔECD* is 94.20$\pm$9.92; for *NΔECD; path-/-* is 247.7$\pm$27.80; n=8, 9, 10, 6). The elevated p4EBP is consistent with the increased EdU+ve cells in these conditions, and suggests that *path* suppresses p4EBP in Notch-induced hyperplasia, which may

account for the effects on proliferation. In contrast, *path* does not appear to act through phosphorylation of 4EBP under normal conditions. Notably, anti-p4EBP staining is expected to present in a pattern compatible with cytoplasmic localisation (Cheng et al. 2011), yet in my experiment, in control and *pathRNAi* background, most p4EBP staining in NBs were nuclear. The cytoplasmic pattern emerges when Notch is overexpressed and exaggerates in pathRNAi; NICD brain tumours. Therefore, data regarding p4EBP staining should be interpreted with caution regarding the fidelity of this anti-4EBP antibody. Further experiments would help to validate this antibody, for example, a 4EBP mutant clone that should result in loss of p4EBP staining; or inhibiting mTORC pathway where it is required (e.g. the fat body) should cause loss of p4EBP.

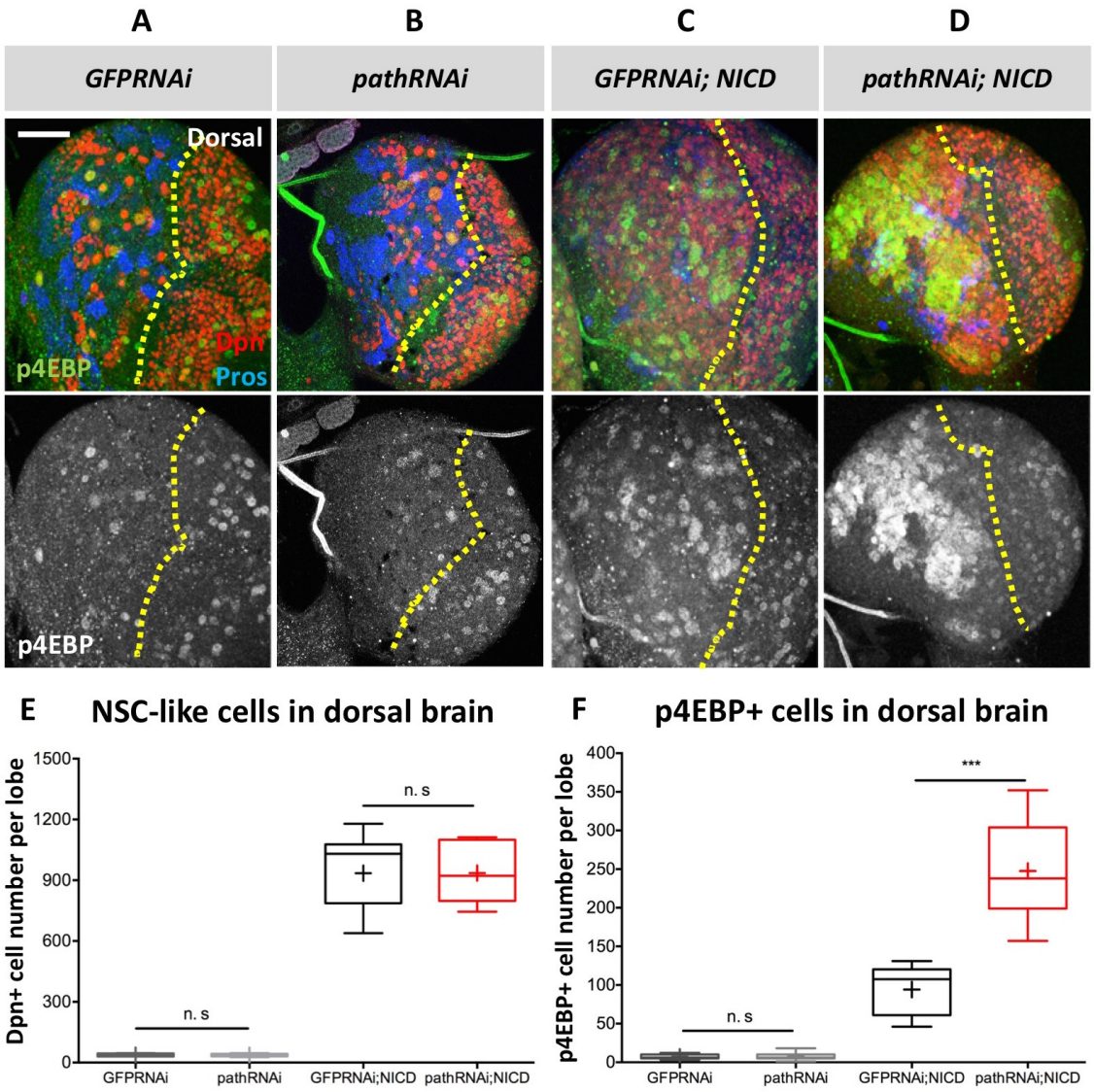

Fig 4.7. Path limits tumour growth in Notch induced hyperplasia through inhibiting p4EBP. (A-D) Dorsal lobe of brains of indicated RNAis driven by *insc-Gal4* at 30°C for 3 days. Notch overexpression (NICD) increases p4EBP expression in NB-like cells (C). *path* knockdown does not change p4EBP expression in NBs (B), yet p4EBP expression increases greatly when *path* is depleted in NICD NBs (D). (E-F) Quantification of NSC-like cell numbers (E) and p4EBP positive (p4EBP+ve, or p4EBP+ in figures) cells (F) in dorsal brain of indicated genotypes; n=8, 9, 10, 6. ***p<0.001. Scale bar, 50 µm.

4.2.5 *path* is not upstream of Alk/Jeb signalling in NBs

Alk/Jeb signalling is the dominant pathway controlling NB proliferation in L3 larval brains and helps to protect against variations in nutrient levels (Cheng et al. 2011). To investigate whether the effects of *path* on proliferation are mediated by changes in this pathway, the expression of Alk and Jeb was analysed in wild-type and *path* mutant MARCM clones. Alk is normally expressed at low levels in NBs and newly born neurons, and at higher levels in late neurons (Cheng et al. 2011). In *path* mutant clones, there was no detectable change in Alk expression in NBs (Fig 4.8, arrows), and the neuronal expression was also similar to control clones (Fig 4.8). Jeb is expressed in glial cells and at low levels in NBs, where it may be taken up from the neighbouring glia (Cheng et al. 2011). No change in NB or neuronal expression of Jeb was seen in *path* mutant clones (Fig 4.9). These results suggest that Path is not functioning upstream of the Alk/Jeb pathway to directly regulate Alk or Jeb distribution. Nevertheless, it remains possible that *path* affects activity of the Alk/Jeb pathway via other mechanisms.

4.2.6 *path* does not alter expression of the temporal factor Broad

Broad, a BTB-zinc finger transcription factor is a temporal factor expressed in late neurons from mid-larval stages (Spokony & Restifo 2009). One possibility for the effects of removing *path* on NB proliferation and size could be that it interferes with the temporal progression of the NBs, arresting them at an early stage. To investigate this possibility, expression of Broad in the *path* mutant NB lineages was examined using anti-Broad (targeting all four isoforms of Broad, Br) was used. Broad expression was still

detectable in the neuronal progeny of the *path* mutant clones, suggesting they had undergone the mid-larval temporal switch in mid-larval stage. Unexpectedly, Broad expression was also detected in some NBs (Fig 4.8, arrows). Although this has not been reported previously, nearby heterozygous non-GFP NBs also had detectable Broad expression suggesting that this is a normal characteristic of late stage NBs. It would be interesting to investigate this further as it suggests that Broad may have a role in regulating NBs at the end of larval development. However, the fact that Broad is detected in both the *path* mutant and the wild-type NBs suggests that it is unlikely to explain the defects in the *path* mutant NBs.

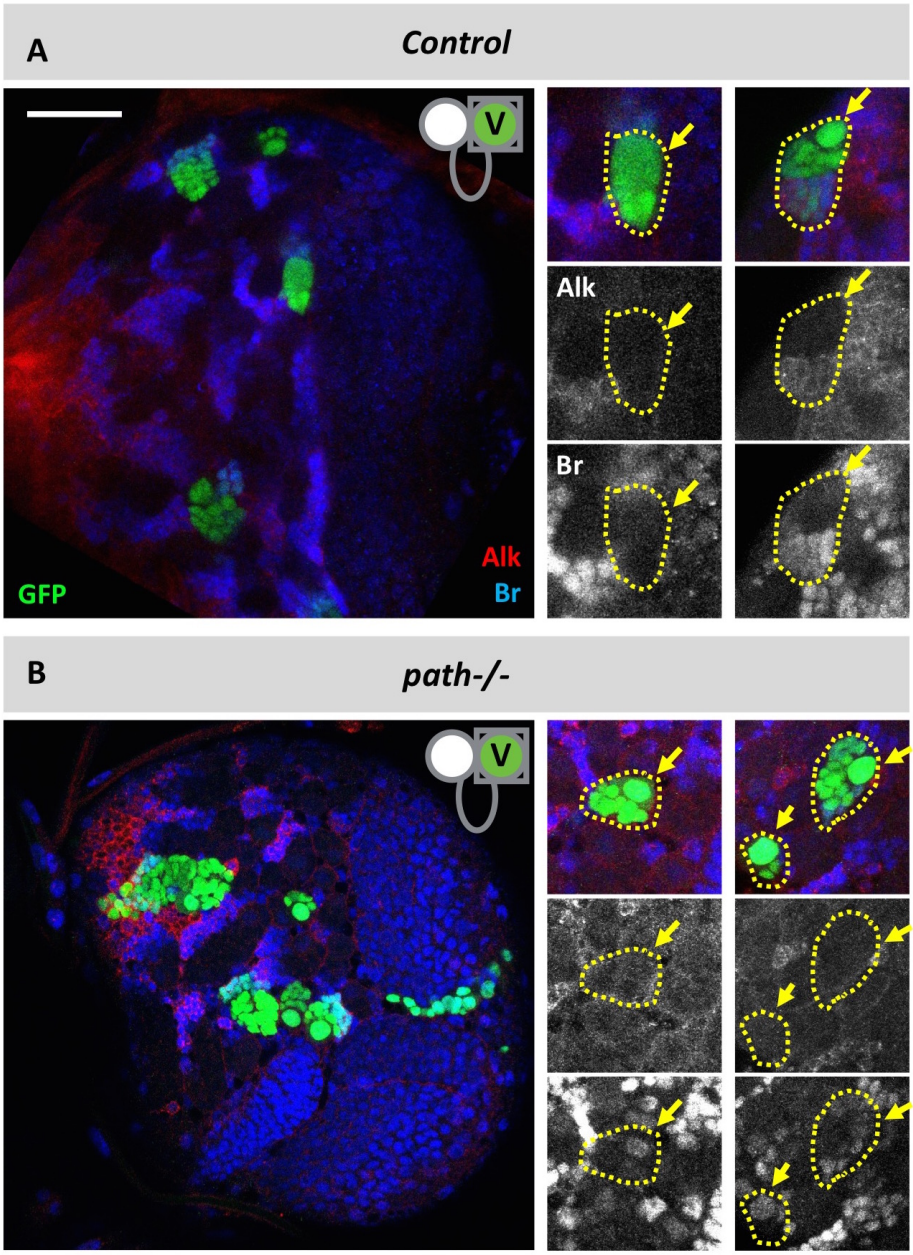

Fig 4.8. Path does not affect Alk and Broad expression in neural stem cells. (A-B) Control (A) and *path* mutant (B) clones are stained with anti-Alk (red) and anti-Broad (Br, blue). GFP-marked lineages are outlined by yellow dotted lines and NBs are marked by yellow arrows (A&B insets). Scale bar, 50 µm.

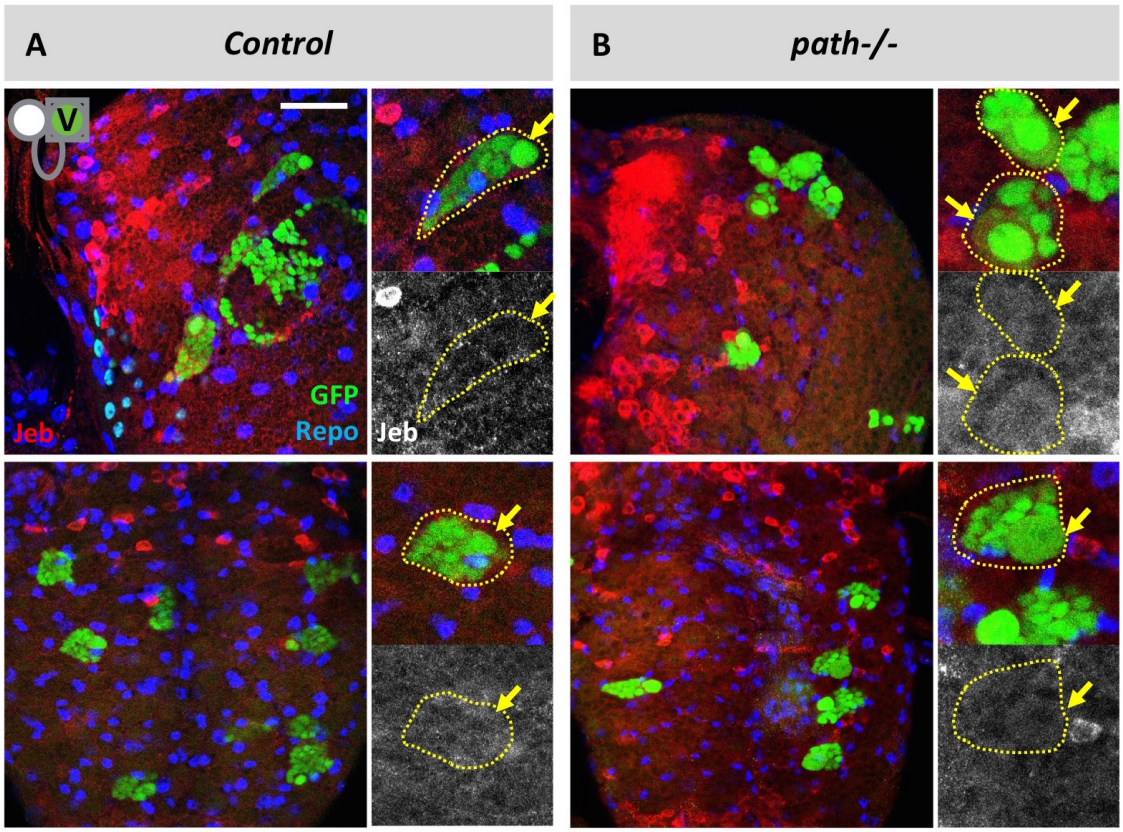

Fig 4.9. Path does not affect Jeb expression in neural stem cells. (A-B) Control (A) and *path* mutant (B) marked linages are stained with anti-Jeb (red) and anti-Repo (blue), outlined with yellow dotted lines; NBs are marked with arrows. Scale bar, 50 µm.

4.2.7 *pathNRE* is a nutrition-dependent enhancer

Once the larva has reached 60 hrs, the critical weight time point, the brain becomes protected from lack of nutrition (brain sparing), while the other parts of the body are still compromised (Cheng et al. 2011). The Alk/Jeb pathway is essential for brain sparing, bypassing Tor and taking the place of InR to activate the PI3K pathway (Cheng et al. 2011). As NBs and neurons need amino acids to grow and survive under nutrition restricted conditions, there must be a mechanism to transport amino acids into these cells from glial cells or elsewhere (e.g. the fat body). As Path has characteristics of an amino acid transporter, it could fulfil this role and might therefore be regulated by nutrition levels.

To investigate whether *path* responds to nutrition challenge, the expression of *pathNRE* was investigated as an indicator. In normal conditions, *pathNRE* expression was low before NB reactivation and then became expressed in all of the NBs during L2 (Fig 4.10B-C). To investigate the effects of nutrient deprivation, larvae were transferred from normal culture medium to a sucrose-only nutrient restrictive (NR) diet at early L3 (72 hrs ALH), after the 60hr ALH critical weight time point. After 48 hrs of starvation, the brains were dissected and *pathNRE* expression was compared with that of fed larval brains of an equivalent age (120 hrs ALH, Fig 4.10A). Strikingly, *pathNRE* expression was significantly reduced upon starvation (Fig 4.10B-E), although the brain size was similar to that of fed larvae indicating that brain sparing was occurring.

To clarify if this change in *pathNRE* expression was because of alterations in Notch activity, expression of *E(spl)mγ-GFP*, a widely used Notch activity indicator, was also examined under NR conditions (Almeida & Bray 2005; Zacharioudaki et al. 2012). Unlike

pathNRE, *E(spl)mγ-GFP* expression levels under NR were similar to fed larvae at 120 hrs ALH (Fig 4.11). This suggests that Notch activity is not changed by NR at this stage of larval life. Therefore, it is unlikely that the reduction of *pathNRE* expression in NR conditions is due to a change in Notch activity, but must rather be due to changes in other sources of its regulation. As *pathNRE* expression is reduced in NR it also suggests that elevated NB *path* may not be required during starvation, although it is possible that an alternate enhancer could operate under these conditions to confer *path* expression.

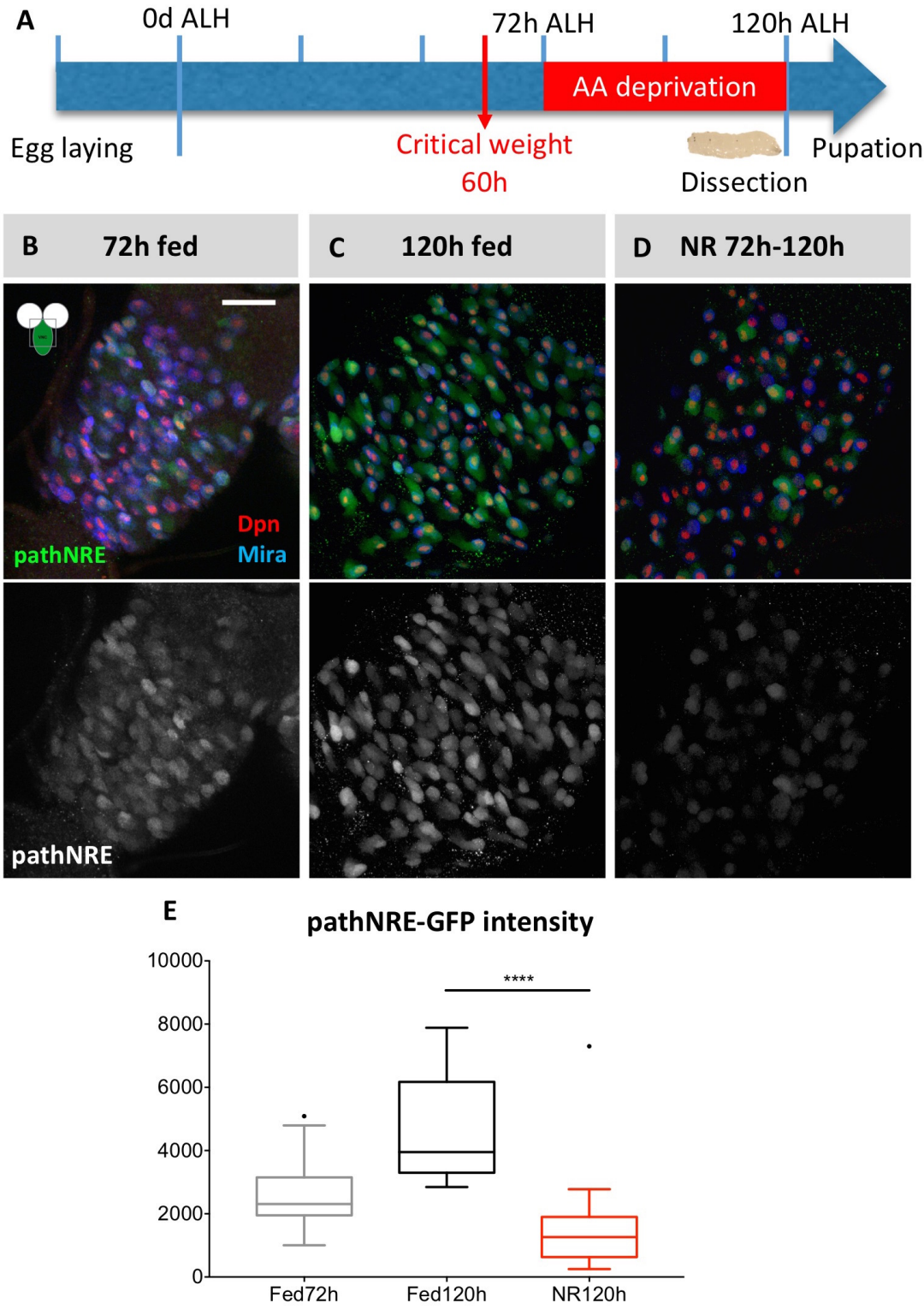

Fig 4.10. *pathNRE* is responsive to nutrition restriction. (A) Scheme for nutrition restriction. Larvae were transferred to amino acid-deprived diet at 72hrs (ALH) and dissected close to 120hrs ALH. (B-D) pathNRE-GFP (green, grey panel) expression in VNC at 72hrs ALH (B), 120hrs ALH fed with yeast-rich food (C) and 120hrs with nutrition restriction (NR) from 72h to 120h ALH (D). NBs are marked with Dpn (red) and Mira (blue). (E) Quantification of pathNRE-GFP intensity in above conditions. ****p<0.0001. Scale bar, 50 µm.

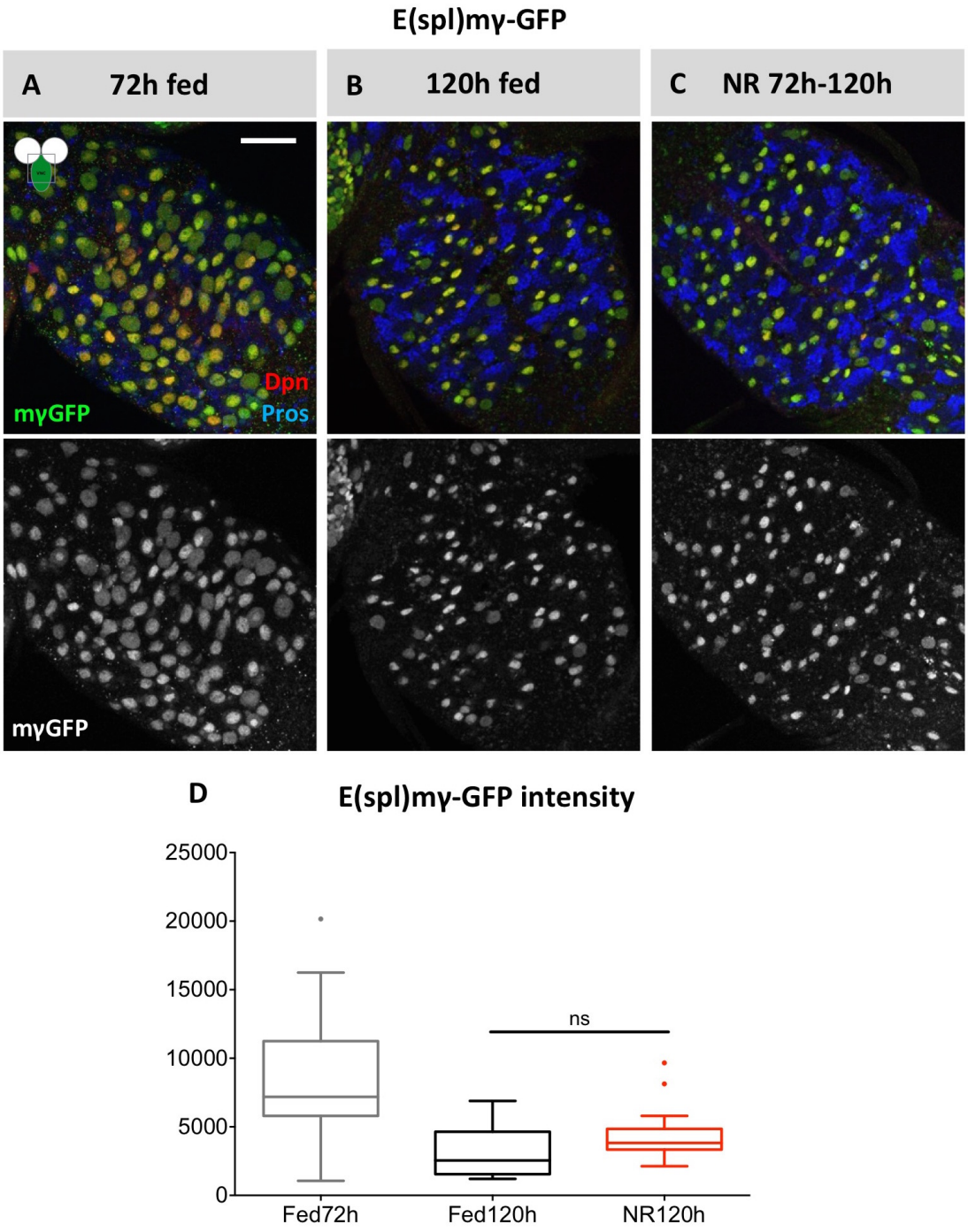

Fig 4.11. Neural stem cells retain Notch activity in response to nutrition restriction. (A-C) Notch reporter E(spl)mγ-GFP (green, grey panel) expression in VNC at 72hrs ALH (A), 120hrs ALH fed (B) and 120hrs with NR from 72h to 120h ALH (C). (D) Quantification of E(spl)mγ-GFP intensity in above conditions. ns, not significant ($p>0.05$). Scale bar, 50 µm.

4.2.8 Glia-expressed Path is required for protecting brain growth under nutrition restriction

To further characterise how Path responds to nutrition alteration, path[GFP] expression was used to examine Path expression pattern. Interestingly, path[GFP] did not decrease after NR from 72-120h ALH (Fig 4.12). Since path[GFP] expression in the brain mostly consists of glial cell expression, including surface glia and cortex glia, it is possible that glia-expressed Path has different behaviours from NB-expressed Path. Since *path* encodes an amino acid transporter, to investigate whether it contributes to brain sparing, I examined whether *path* is required for brain growth under NR condition. Between 72 hrs ALH to 120 hrs ALH (close to puparation), wild-type brains underwent a significant increase in size (Fig 4.13A, B & G), primarily due to an increase in cell numbers produced by the larval NBs. Under nutrition restriction condition, wild-type brains are protected and the brain can grow up to a similar size to those of fed larvae (Fig 4.13B, C & G) (Cheng et al. 2011). In the *path[dg50]* homozygotes (*path[dg50] is* a hypomorphic viable allele of *path*), NR resulted in a greatly reduced brain size, suggesting that path is involved in the brain-sparing mechanism.

To elucidate in which cell type Path is required for brain sparing, *path* was first knocked down specifically in NBs that were subject to NR from 72 hrs ALH onwards. The brain size following NR was comparable with that from fed larvae (Fig 4.14), indicating *path* expression in NBs was not required for brain-sparing during NR.

Second, to explore the function that high expression of Path has in glial cells, *path* was specifically down-regulated in glial cells, using *repo-Gal4*. Path depletion alone did not affect brain size, at 72 hrs ALH or at 120 hrs ALH, as the fed *pathRNAi* brains had a

comparable size to those from fed control larvae (Fig 4.15B, E & G). However, when *pathRNAi* larvae were subject to NR from 72 hrs ALH, the brains did not grow to the same extent as those from fed larvae at 120 hrs ALH, and were more comparable in size to those from 72 hrs ALH larvae (Fig 4.15D, F & G). This suggests that the brain growth is no longer spared when Path is absent from glial cells.

To explore the mechanism through which Path functions in the glia, the expression of the ligand of the Alk pathway, Jeb, was examined in *path[dg50]* homozygous brains. Compromising Path in the whole brain resulted in an overall reduction of Jeb both in glia and in NB lineages (Fig 4.16). These data suggest that *path* is required in glial cells for brain-sparing and that it may do so through regulating Jeb.

The results argue that NB-expressed Path does not participate in protecting brain growth during NR, which is compatible with the reduction of *pathNRE* under these conditions. Strikingly however, the expression of *path* in glial cells does appear to be important for brain sparing and this effect appears to be mediated through the regulation of Jeb.

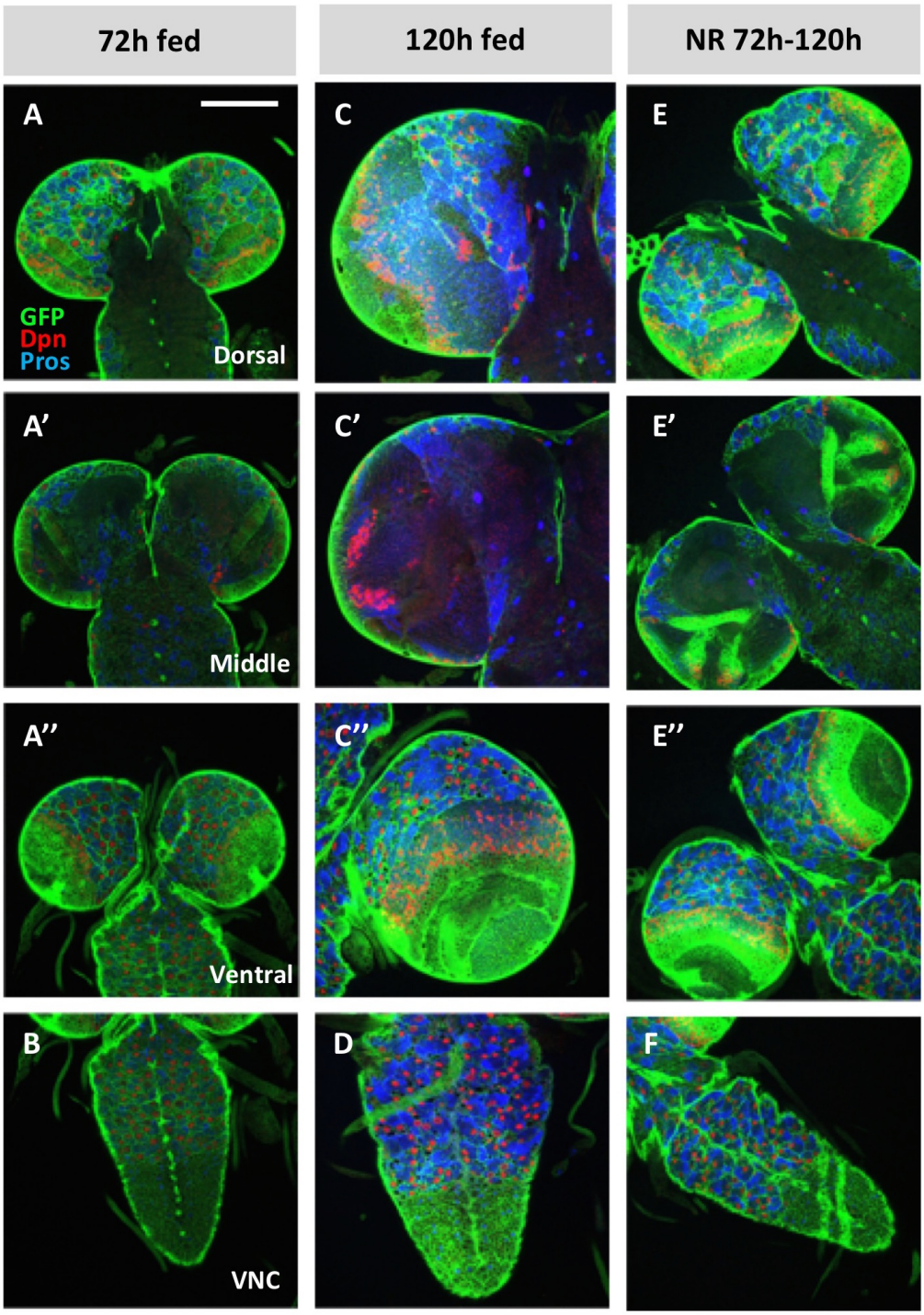

Fig 4.12. Path[GFP] persists under NR condition. Path[GFP] expression under 72hrs ALH fed (A&B), 120hrs ALH fed (C&D) and NR from 72h to 120h ALH (E&F) conditions. (A,C,E) show dorsal side of brain, (A',C',E') show middle section of the brain, (A'',C'',E'') show ventral brain. (B,D,F) show VNC. NBs are marked with Dpn (red), neurons are marked with Pros (blue). Scale bar, 100 µm.

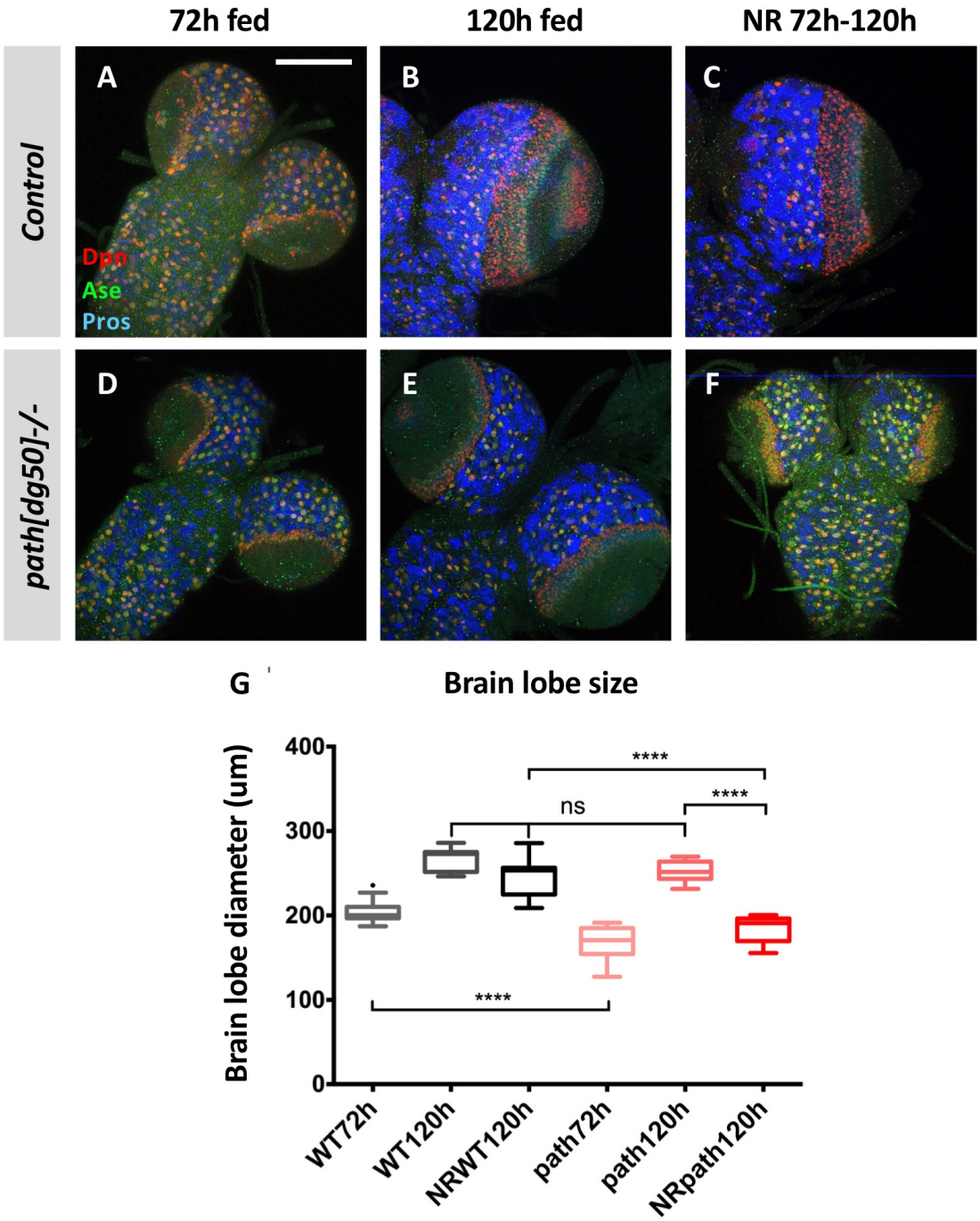

Fig 4.13. Path is required for brain sparing. (A-F) Control (A-C) and *path[dg50]-/-* (D-F) brains under 72hrs ALH fed (A&D), 120hrs ALH fed (B&E) and NR from 72h to 120h ALH (C&F). (G) Quantification of brain lobe diameter under above conditions. n= 6-10 brains. ****p<0.0001, ns, not significant (p>0.05). Scale bar, 100 µm.

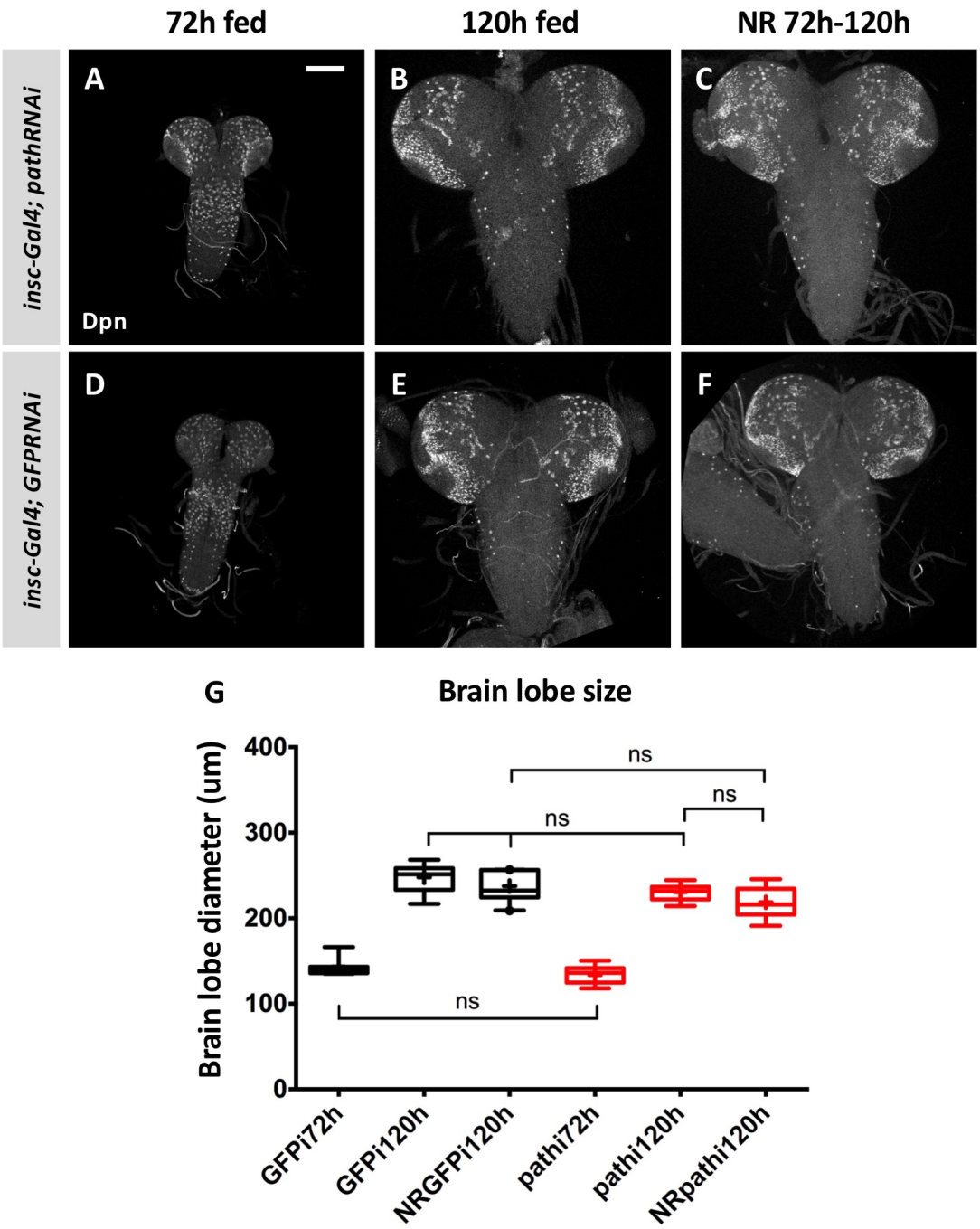

Fig 4.14. NB-expressed Path is not required for brain sparing. (A-F) *insc-Gal4* drives GFPi (A-C) and pathRNAi (D-F) in brains from 72hrs ALH fed (A&D), 120hrs ALH fed (B&E) and NR from 72h to 120h ALH (C&F). (G) Quantification of brain lobe diameter under above conditions. n= 6-10 brains. ns: p>0.05. Scale bar, 100 µm.

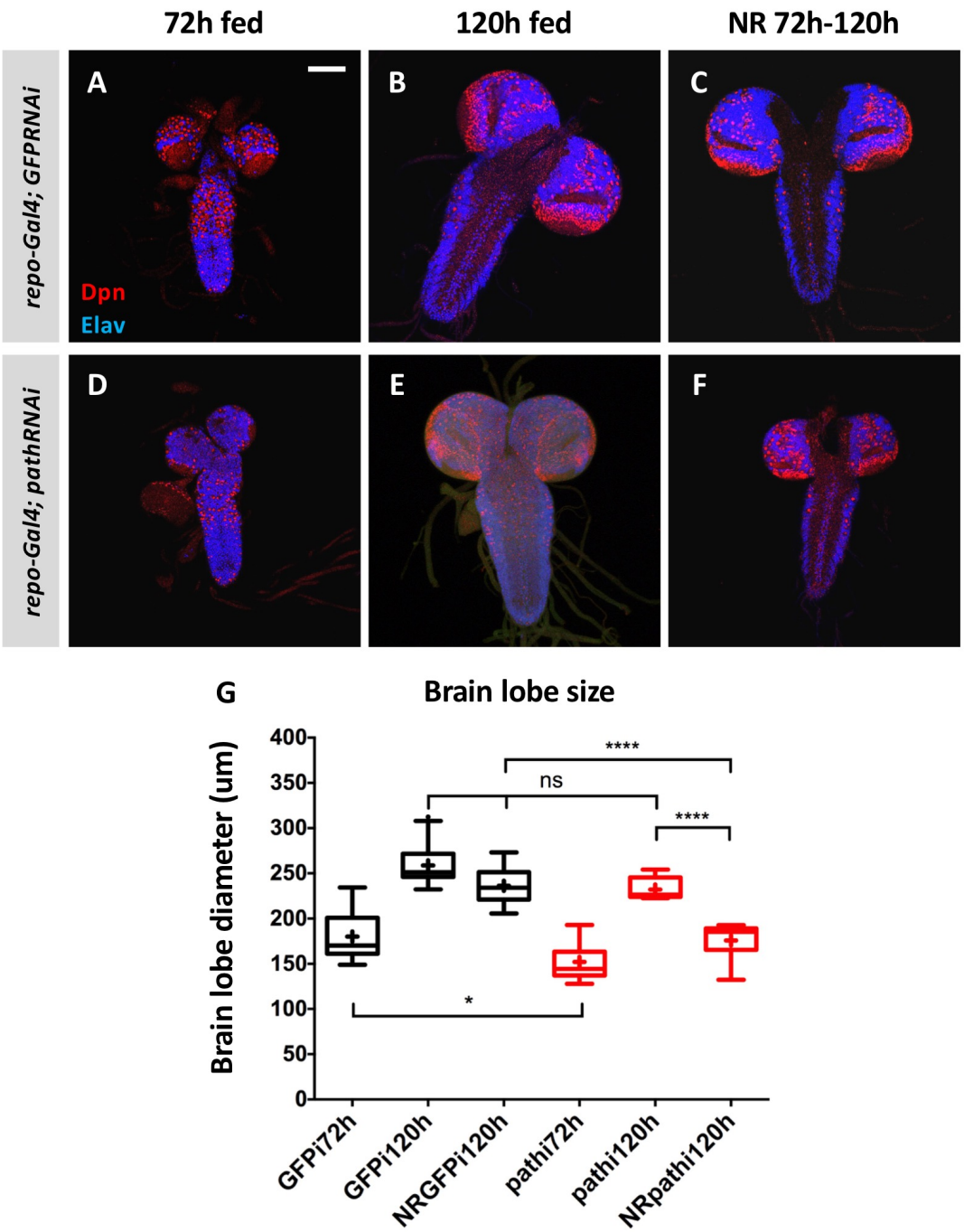

Fig 4.15. Glia-expressed Path is required for brain sparing. (A-F) *repo-Gal4* drives GFPi (A-C) and pathRNAi (D-F) in brains from 72hrs ALH fed (A&D), 120hrs ALH fed (B&E) and NR from 72h to 120h ALH (C&F). (G) Quantification of brain lobe diameter under above conditions. n= 6-10 brains. ****p<0.0001, *p<0.05, ns: p>0.05. Scale bar, 100 µm.

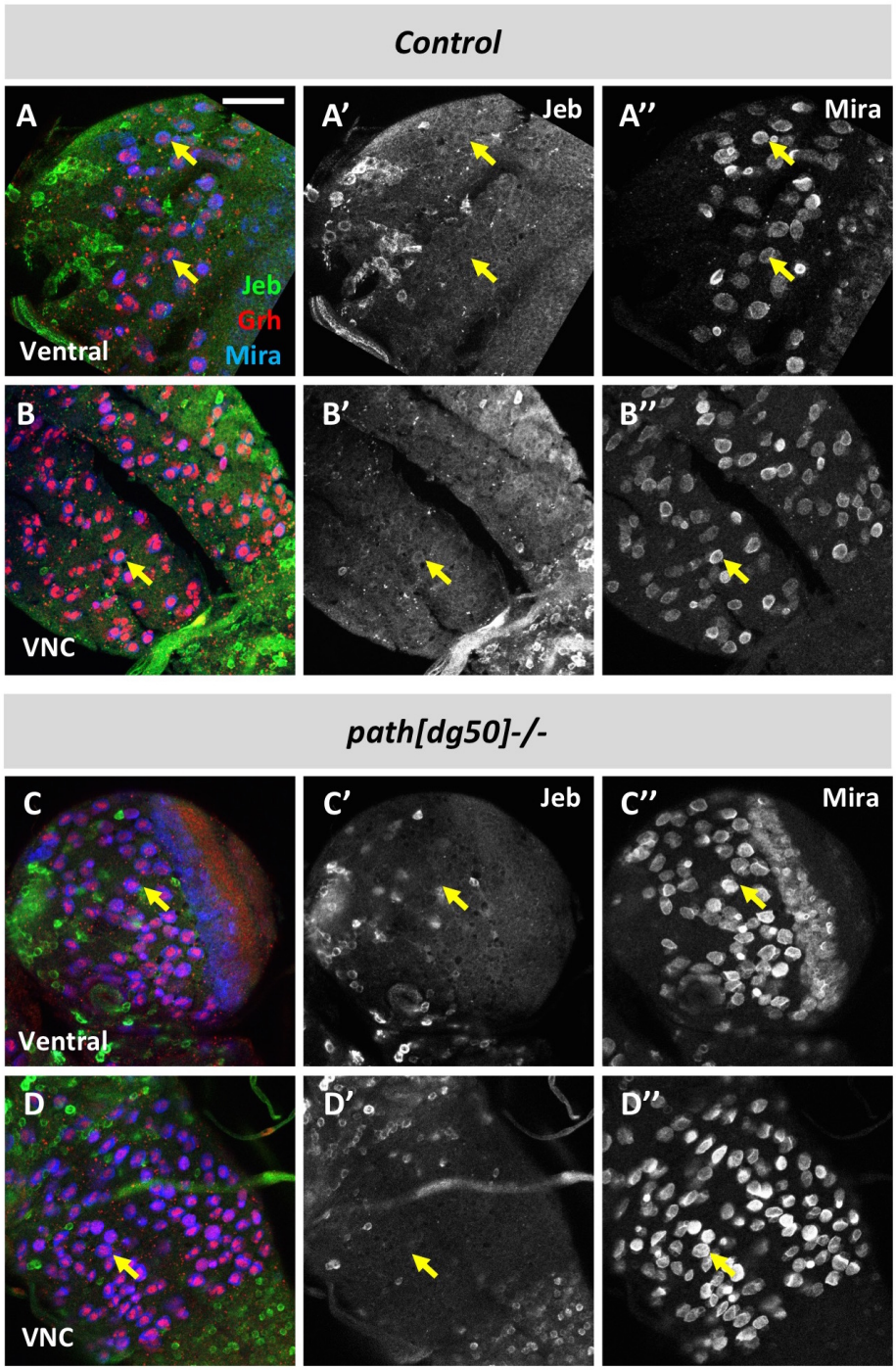

Fig 4.16. Jeb expression is decreased by loss of Path. Control (A-B) and *path[dg50]-/-* mutant (C-D) brains are stained with Jeb (green in A-D, grey in A'-D'); NBs are marked with both Grh (red in A-D) and Mira (blue in A-D, grey in A''-D''); Grh also marks GMCs. (A&C) show ventral brain, (B&D) show VNC. Scale bar, 50 µm.

4.3 Discussion

4.3.1 Function of *path* in neuroblasts

The evidence suggests that *path* is a novel direct target of Notch in NBs. However, its functions appear to differ depending on the conditions. *path* is shown to promote proliferation in normal conditions while in Notch-induced hyperplasia it appears to restrict overgrowth. This suggests that there may be intrinsic differences in the growth regulatory mechanisms in the two conditions as discussed further below.

Path is a potential amino acid transporter with multiple transmembrane domains, but the substrates it transports in NBs have not been confirmed. Indeed, considering Path and PAT4 have different substrates under different cellular conditions and they are orthologues rather than homologues (Goberdhan et al. 2005; Muralidharan Pillai & Meredith 2011), Path might transport different substrates to fit changing growth requirements. In *Xenopus* oocytes, a neutral environment (pH=7.4), Path or PAT4 favoured the transport of non-polar amino acids like Proline and Tryptophan (Muralidharan Pillai & Meredith 2011). A related transporter, SLC38A9 was most active in an acidic pH (5.5-6.5) and was found to transport arginine, contributing to the Ragulator/Raptor machinery that activates the Tor pathway (Rebsamen et al. 2015). The same study excluded the involvement of SLC36, the closer relative to Path, in this process. This fits with results showing that the Tor pathway is activated by charged amino acids like arginine, whereas Path appears to preferentially transport un-charged amino acids. My data also fit with the conclusion that Path function is unlikely to be involved in Tor pathway activation as no change in p4EBP expression was observed after *path* knock down.

One model to explain the current results is that Path functions as a mediator between Alk and the Tor pathway. In L3 larvae brains, most Tor pathway components are dispensable for brain growth and brain size is not changed significantly when Insulin-like peptides (Ilp) levels are manipulated (Cheng et al. 2011). Instead, Alk is required and acts through PI3K/Akt pathway. Though Path was found not upstream of Jeb and Alk in NBs, it is still possible that Path regulates PI3K/Akt signalling. Further characterization of PI3K/Akt expression under Path depletion might address the question. In contrast to the situation in L3, the Tor pathway is activated and required in brains of L1/L2 larvae (Sousa-Nunes et al. 2011), a stage where I also observed higher p4EBP expression in optic lobes and NBs. At 120hrs, p4EBP levels become lower, suggesting a switch-off mechanism of the Tor pathway at later stages. Considering *pathNRE* is upregulated after NB reactivation (Fig 4.10B, C & E), it is possible that *path* helps to keep activity of the Tor pathway at restricted levels at later stages. In this case, the effect of *path* on cell proliferation in NBs would be through nutrient sensing and protein synthesis, similar to its function in C4da neurons (Lin et al. 2015).

As *path* is a direct Notch target, when constitutively active Notch is expressed in NBs, its expression levels would increase. At the same time, *path* seems to help suppress growth in these conditions. The data suggest that it could do so by interfering with Tor activity, since p4EBP is greatly increased when *path* is depleted. Similarly, in both fly wing and HEK293 cell lines, one copy of PAT expression promotes proliferation, while two copies of PATs inhibit proliferation (Goberdhan, Wilson & Adrian L Harris 2016). One model is that increased Path at the membrane could compete with amino acid transporters required by Tor activation, similar to SLC38A9 (which itself has no clear *Drosophila*

orthologue), either by physically displacing them at the membrane or by transporting excess neutral amino acids which cannot activate the Tor pathway and may even suppress it. Therefore, in conditions where less Path is at the membrane, the Tor pathway would be de-repressed, and more p4EBP generated, resulting in more proliferation as I have observed. This result is also consistent with the observation in cell lines that when excessive PATs were expressed, the promoting role of PAT become inhibitive, presumably through a dominant-negative mechanism (Goberdhan, Wilson & Adrian L. Harris 2016).

The resulting model is that, in normal conditions, the activity of the Tor pathway is low (as evidenced by the low levels of p4EBP) and *path* is mainly functioning to promote the Alk/PI3K pathway. In contrast, in Notch over-activated conditions, the Tor pathway becomes activated but is restricted by the presence of *path* (Fig 4.17). The switch in *path* function would be dependent on the relative levels of Alk and Tor pathway activity. This may imply that there is an interplay between Alk (or other growth pathways) and Tor in different cellular context. Also it will be interesting to probe the role of *path* in early larval stages as the model predicts that it would antagonise the Tor pathway during reactivation. It is also possible that the switch in Path, from proliferation-suppressing to proliferation-promoting is brought about by activity of other pathways/conditions that are induced by Notch. For example, when Notch is over-expressed in NBs, the metabolic state of the tumour-like cells might be different so that the energetic consequences of Path-mediated amino acid transport change.

4.3.2 Function of *path* in glia

Besides its function in NB, my experiments also argue that *path* is required in glial cells to maintain brain growth during starvation. Down-regulation of *path* in glial cells did not appear to change the number of glial cells. However, *path* depletion did affect the overall brain size. Although *pathNRE* was down-regulated and dispensable in the NBs following NR, there was no similar effect on path[GFP] in glial cells. Instead path[GFP] expression was maintained under nutrition deprivation. Together the data suggest that *path* is required in glial cells under NR conditions.

During nutrition restriction in late larval stages, the brain keeps growing to achieve a normal size. Whether the growth continues because the supply of amino acids is maintained inside the brain, which is shielded by the glia, or because the NBs have an alternative mechanism to promote growth when they are exposed to an amino acid-deprived environment? The reduction of *pathNRE* expression under NR suggests that the NBs are sensitive to the environmental changes and the brain is not shielded by glia from NR, therefore the latter is more likely to be the case. Alk/Jeb is the major pathway that has been linked to brain growth under NR conditions. Jeb expression in glia and NBs seems to rely on glial-expressed Path (Fig 4.17), which is consistent with the results showing that glial knockdown of Jeb (*repo-gal4>jebRNAi*) resulted in smaller NB-clone size as well as lineage number (Cheng et al. 2011). It is possible that Path at the membrane of surface glial cells could detect the environmental amino acid levels and in turn regulate Jeb expression or transportation. In normally fed conditions, there could be other sensors or signalling to redundantly activate Jeb. For example, in NR condition, much less amino acids exist and only the high affinity Path might be capable of sensing

them; without Path in glial cells, Jeb expression would be compromised and therefore brain growth no longer protected.

It seems unlikely that Path would regulate brain sparing via the mTor pathway in glial cells because (2) there is no detectable p4EBP activity in these cells; (2) losing single mTor pathway components (Tor, Raptor, eIF4E or S6K) did not change glial cell number or morphology but could rescue glioma induced by activating EGFR and PI3K pathway together, suggesting a requirement for mTor pathway only in hyperplasia (Read et al. 2009). As glial cells produce Ilps that stimulate the InR pathway in NBs, Path might regulate the production of Ilps. However, brain sparing can occur in the absence of Ilp2 and InR, suggesting there must be an alternate mechanism (Cheng et al. 2011). As changes in autophagy and lipid droplets have been proposed to contribute to NR sensing, the effects of *path* depletion on these structures in glial cells could be investigated.

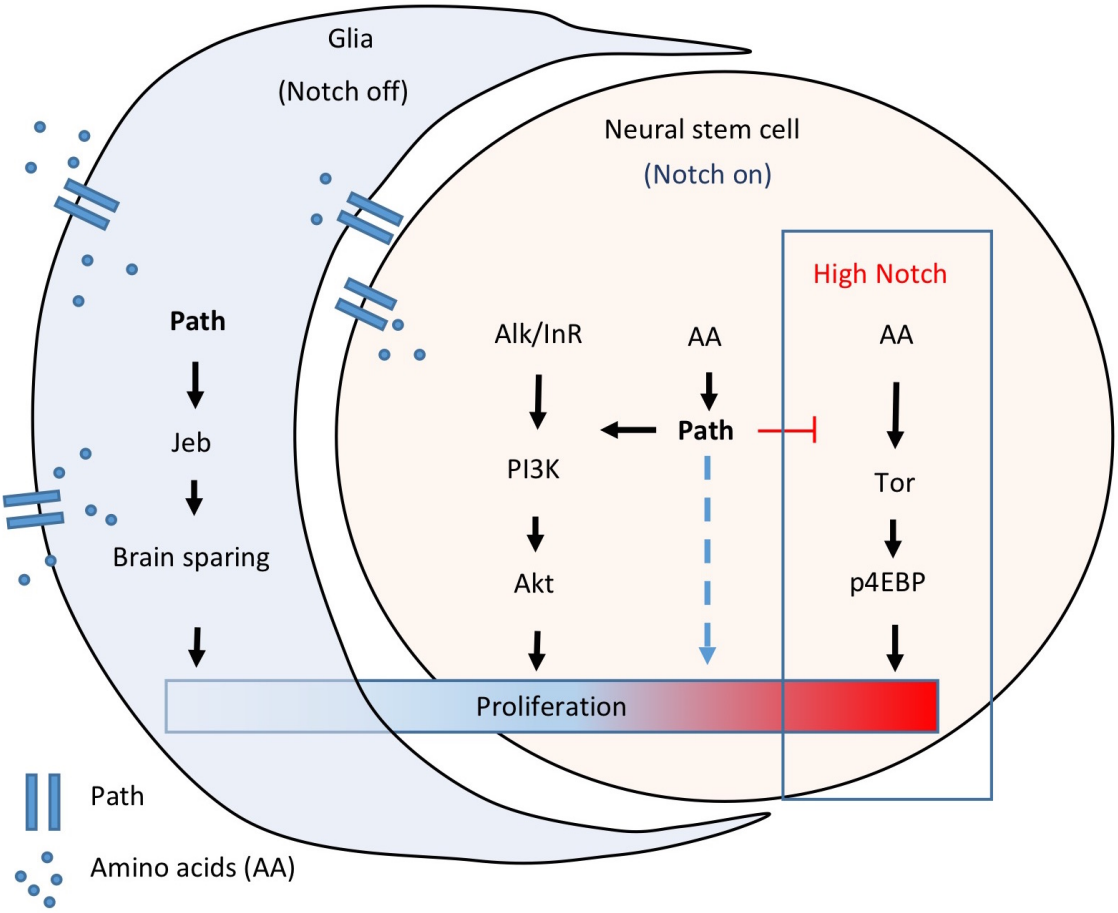

Fig 4.17. Model of *path* function.

4.4 Summary

In this Chapter, the function of a novel Notch target, *pathetic* has been studied in larval brain. Although the expression of Path is broadly distributed in NBs and glial cells, the function of Path appears to be different in these two cell types. NB-expressed Path is required for NB lineage proliferation while restricting growth in the case of Notch-induced brain tumour, potentially through mediating the relative levels of the Alk and Tor pathways. Glial-expressed Path is essential for protecting the brain growth under nutrition restriction, potentially through regulating Jeb expression. Thus the different roles of Path in distinct parts of the brain would together enable the larval brain to proliferate and grow both in normal and in abnormal conditions.

Chapter V

A remote NRE is required for *cables* expression in neural stem cells

5.1 Introduction

The putative enhancer *CG6191Big* was, like *path*, identified in Notch-induced brain tumours by ChIP with Su(H). Indeed this was one of the most robust Su(H) bound regions across the genome and contains an unusually high density of Su(H) bound motifs (Rebeiz et al. 2002). *CG6191Big* is a common region of Su(H) binding between wing discs and brain (Fig 5.1A) and is conserved between close *Drosophila* species (Fig 5.2). It also directs expression in both tissues (Fig 5.1B & C). As shown in Chapter III, *CG6191Big* is responsive to Notch regulation in NSCs (Fig 5.1C & D) and in this chapter, results from investigating its role and function in NSCs will be discussed. The first aim was to find out which genes the enhancer regulates because *CG6191Big* is in an intergenic region (Fig 5.1A), and expression of several nearby genes was upregulated when Notch was over-activated (Table 5.1). Among those, *cables* (*CG6191*) was thought to be a likely candidate regulated by the Notch-dependent enhancer, because it has a small Su(H) bound region in the intron (Fig 5.1A), raising the possibility of forming a regulatory loop with the *CG6191Big* enhancer.

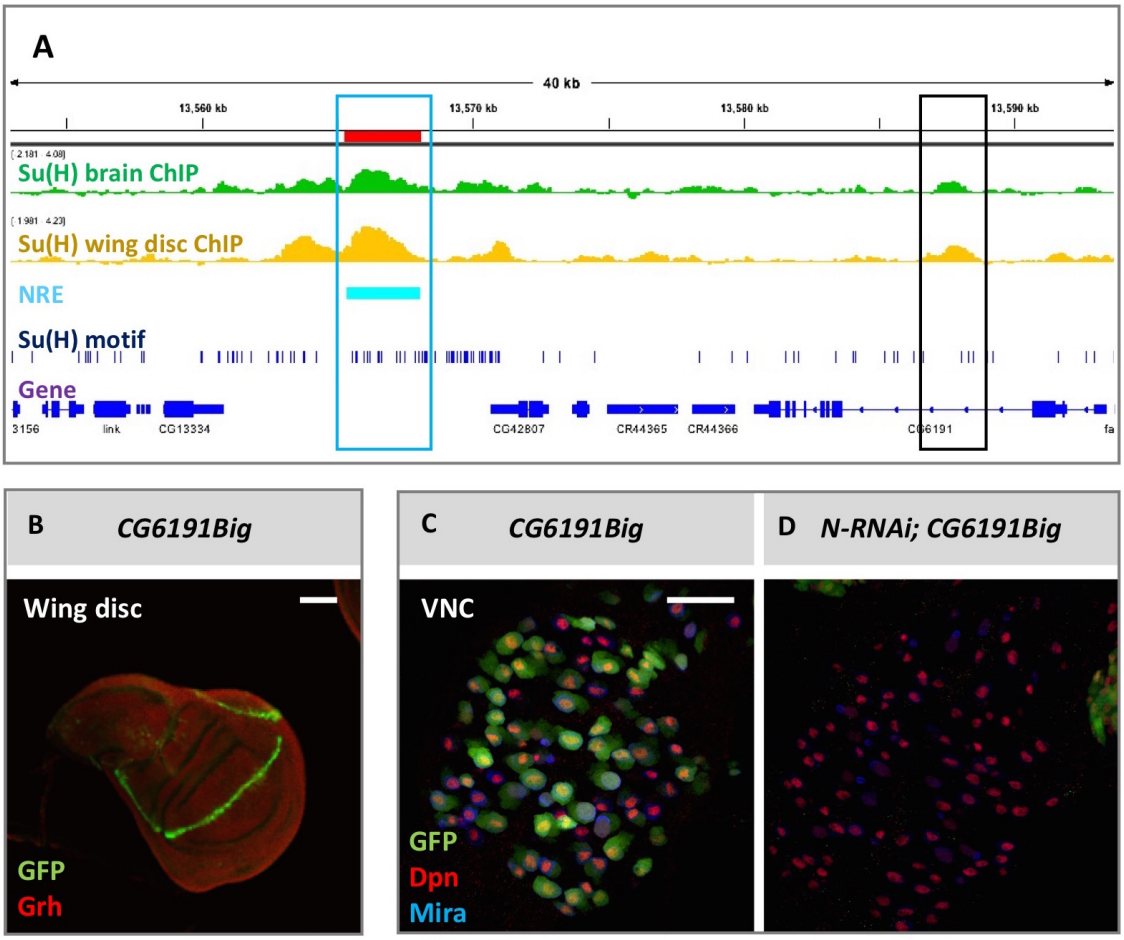

Fig 5.1. An enhancer distal to *CG6191* is responsive to Notch regulation. (A) Genome view of *CG6191Big* and *CG6191* nearby region shows Su(H) binding profile in brain (green) and wing discs (orange) (enrichment relative to input AvgM, log scale is as indicated), *CG6191Big* region (cyan), and Su(H) binding motifs (blue). Su(H) bound regions are outlined with blue (*CG6191Big*) and black (*CG6191in*) box. (B) *CG6191Big* directs GFP expression in wing discs, red represents Grh. (C&D) *CG6191Big* directs GFP expression in L3 larval brain (C) and responds to Notch knockdown (D). Green represents NREGFP; NBs are marked with Dpn (red) and Mira (blue). Scale bars, 50 µm.

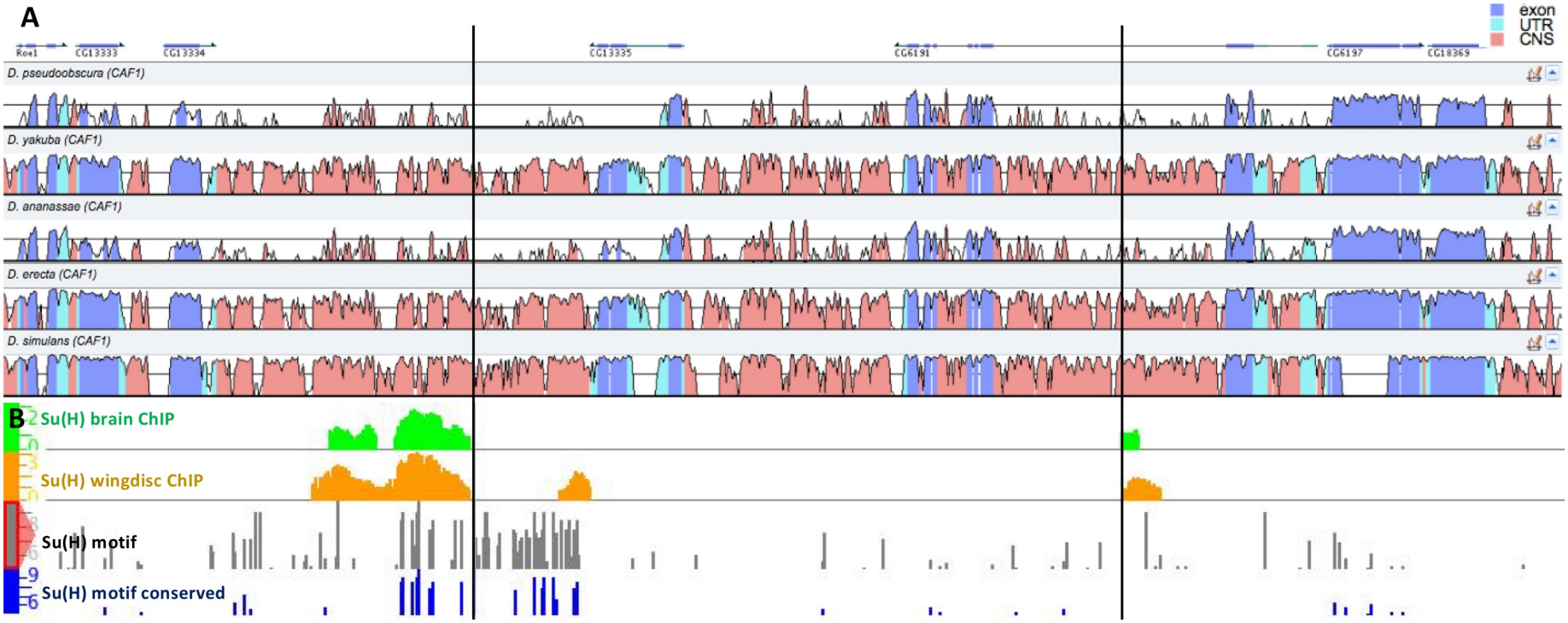

Fig 5.2. Sequence conservation of *CG6191Big* to *CG6191* gene region between *Drosophila melanogaster* and close *Drosophila* species. (A) Conservation map of *CG6191Big* to *CG6191* gene locus between *D. melanogaster* and 5 close species (*D. pseudoobscura, D. yakuba, D. ananassae, D. erecta* and *D. simulans*). Blue represents exon; cyan represents UTR (untranslated region); red represents CNS (Conserved non-coding sequence). (B) Corresponding genomic map to the locus in (A). Su(H) bound regions in both brain (green) and wing disc (orange) are displayed, with enrichment relative to input AvgM, scale $\log_2$ 0-3), as well as the Su(H) binding motifs (grey and blue).
Conserved sequence website:
http://pipeline.lbl.gov/tbrowser/tbrowser/?pos=chr2L:50000-150000&base=droMel_caf1&run=1220#&base=598&run=1220&pos=chr2R:9069585-9116663&genes=refseq3&indx=0&cutoff=50

Gene name	CG number	Distance to *CG6191Big* (bp)	mRNA change in Notch over-activated brains
Roe1	CG6155	10.6k	**2.49**
link	CG13333	8.3k	0.64
CG13334	CG13334	4.9k	**1.35**
CG6191Big		0	
CG42807	CG13335 in Release5	2.7k	**1.71***
CG42808	CG13335 in Release5	5.8k	
cables	CG6191	12.5k	**1.89**
fand	CG6197	25.8k	0.93
S-lap5	CG18369	28.8k	**1.10**

Table 5.1 Genes within 50kb of the *CG6191Big* locus.
* Probing CG13335 in *Drosophila* Genome Release 5, while in Release 6 it is annotated as CG42807 & CG42808.

The second aim was to investigate the functional role of *cables* in NBs. *cables* is the sole *Drosophila* orthologue of human CABLES1/2(CDK5 and ABL enzyme substrate1/2), proteins which are characterised by a conserved C-terminal cyclin-type domain (Fig 5.3A). CABLES1 and CABLES2 both interact with CDK3 and CDK5, as well as with c-Abl (Sato et al. 2002). In human tumour cells, CABLES1 often appears to serve as a negative regulator of the cell cycle. For example, loss of CABLES1 has been recorded in many kinds of cancers, including human colon, lung, ovarian and endometrial cancer, as well as corticotroph adenomas (Dong et al. 2003; Zukerberg et al. 2004; Zhang et al. 2005; Sakamoto et al. 2008; Park et al. 2007; Roussel-Gervais et al. 2016). In mice, CABLES1 also regulates intestinal tumour progression, through effects on the Wnt signalling

pathway (Arnason et al. 2013). In many of these tissue-types, suppression of CABLES1 led to over-proliferation, consistent with it inhibiting the cell cycle. The role of CABLES1 in regulating the cell cycle may be mediated by forming a complex with the Cdk inhibitor p21 in the nucleus and stabilising it (Shi et al. 2015). Degradation of p21 activates CDK2 and CDK4, resulting in enhanced cell cycle progression. By stabilising p21, CABLES1 could keep cells from over-proliferating. The levels of CABLES1 may in turn be regulated by Akt phosphorylation, followed by recruitment of 14-3-3, to neutralise its role as a tumour suppressor (Shi et al. 2015) (Fig 5.3B).

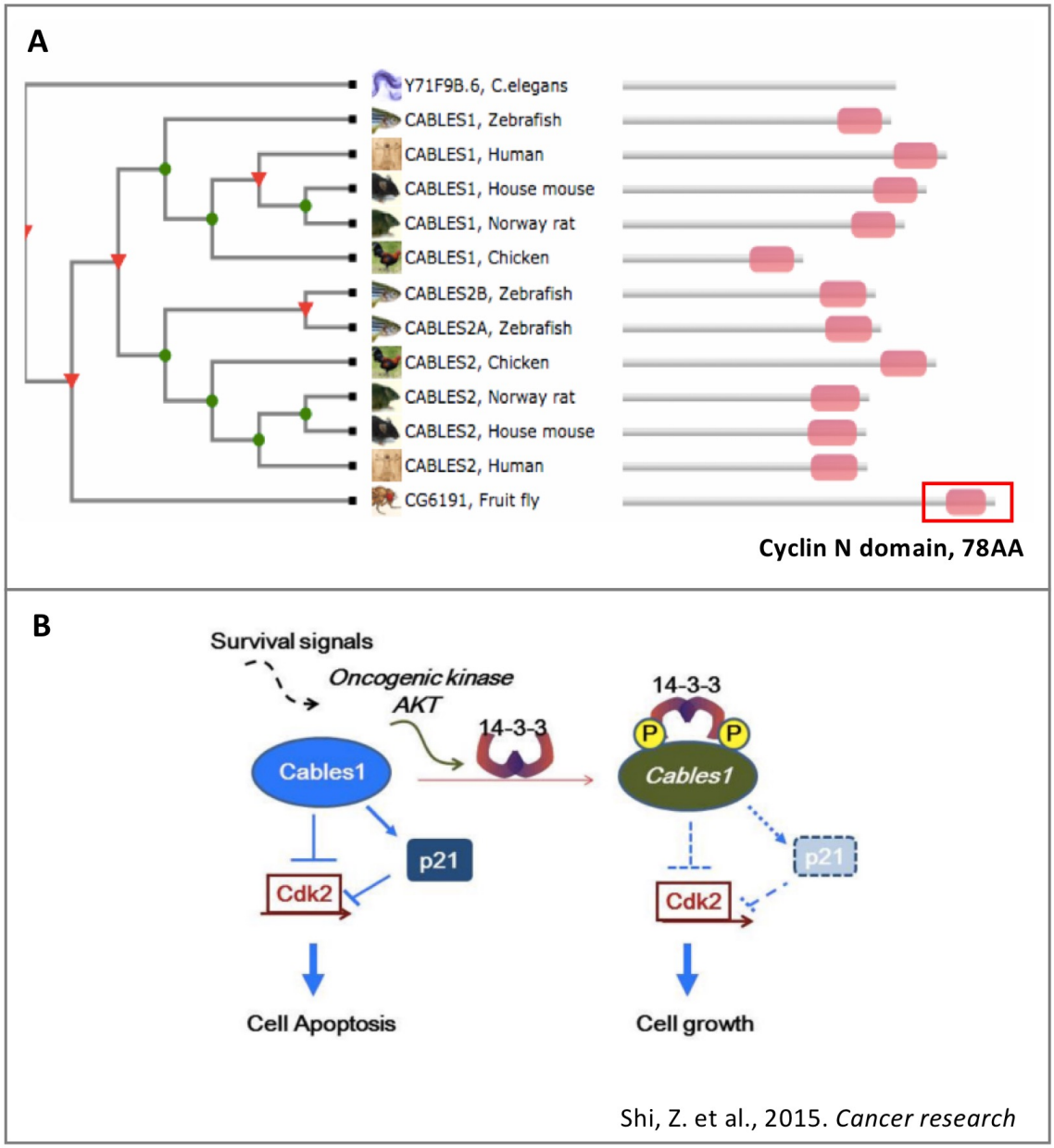

Fig. 5.3. CG6191 is the *Drosophila* homologue of CABLES. (A) Gene tree and conserved domain of Treefam TF323936, showing CABLES orthologues in model organisms. Pink squares represent Cyclin-related domain (outlined by red box). The whole family has 145 members from 89 species. Alignment was conducted with MCoffee, resulting a 1554 AA long alignment with 53% conservation on average. The gene tree was built by TreeBest. (Ruan et al. 2007; Guindon et al. 2010) (B) A working model summarizing functional roles of Cables1 according to previous research in mammals (Shi et al. 2015).

http://www.treefam.org/family/TF323936#tabview=tab1

Conversely, elevated levels of CABLES1 and CABLES2 in some contexts appears to result in increased apoptosis and senescence (Pu et al. 2017). For example, CABLES1 can bind to p53 and p73 while protecting p63 from degradation, to apoptose cells under genotoxic stress (Tsuji et al. 2002; Wang et al. 2010). Likewise, ectopic expression of CABLES2 induced apoptosis in mouse embryonic fibroblasts in both p53 dependent and independent ways (Matsuoka et al. 2003). A hint that this function may be conserved comes from the observation that *Drosophila cables,* together with other cell death regulatory genes like reaper and hid were induced by γ-ray treatment (Zhang et al. 2008).

The few studies that have explored Cables function in developmental contexts have proposed a role in regulating neuronal morphology. For example, in mouse primary cortical neurons CABLES1 was shown to be essential for neurite outgrowth (Zukerberg, Patrick, Nikolic, Humbert, C. Wu, et al. 2000). In Zebrafish CABLES1 was required for normal neural development where it was suggested to link the axon guidance cue protein Slit to cadherin-mediated adhesion and gene transcription (Rhee et al. 2007; Groeneweg et al. 2011). No studies have yet been performed in *Drosophila*, although *cables* is a potential target of chromatin insulator protein BEAF-32, whose mutation causes neoplastic growth in wing discs and increased glial numbers in the CNS, linked to slight overgrowth (Gurudatta et al. 2012). Whether *cables* has a function in *Drosophila* CNS and/or in glial cells is however not known.

Because of the association with the *CG6191Big* enhancer and the up-regulation of *cables* mRNA in Notch-induced brain tumours my initial hypothesis was that Cables has a role in these tumours, perhaps via interactions with CDKs and tumour suppressors. Mammalian CABLES appears to function primarily to inhibit the cell cycle, however in

Drosophila cables was up-regulated in both brain and wing disc hyperplasia induced by Notch over-activation (A Djiane et al. 2013; Zacharioudaki et al. 2016), suggesting a role for *cables* in promoting proliferation. To find out whether *cables* is suppressing or promoting NB proliferation, a functional analysis of CG6191 is necessary. Objectives: (1) to generate *CG6191Big* deletion and *cables* deletion through CRISPR; (2) to explore which genes are regulated by *CG6191Big*; (3) to compare phenotypes of *CG6191Big* deletion and *cables* gene deletion; (4) to investigate the function of *CG6191Big* and *cables* in NSCs and their mechanisms.

5.2 Results

5.2.1 Generation of CRISPR deletions of the remote NRE and *cables*

To investigate the regulatory characteristics of *CG6191Big*, a deletion of this NRE region was generated using CRISPR/Cas9 technique. Fig 5.4 shows the genomic region encompassing the *CG6191Big* enhancer (Fig 5.4A) and *CG6191/cab*les (Fig 5.4B) transcribed region and illustrates the gRNA targets and HDR repair template regions used. The reagents were designed so that the region encompassing the *CG6191Big* peak was deleted, and replaced with a DsRed-expressing module. Fig 5.5 illustrates the CRISPR workflow and the quantification for the success of each step. The deletion and insertion of DsRed was confirmed by PCR genotyping and subsequently by sequencing (Fig 5.6 & 5.7, primers used are listed in Table 2.5 & 2.6). The enhancer deletion allele was named *ΔCG6191Big*. A deletion of *cables*, covering most of the gene coding region from the second exon to the end of the gene was also generated in the same manner

(Fig 5.4B & 5.7), so that the phenotypes could be compared with those of *ΔCG6191Big*.

This allele was named *Δcables*.

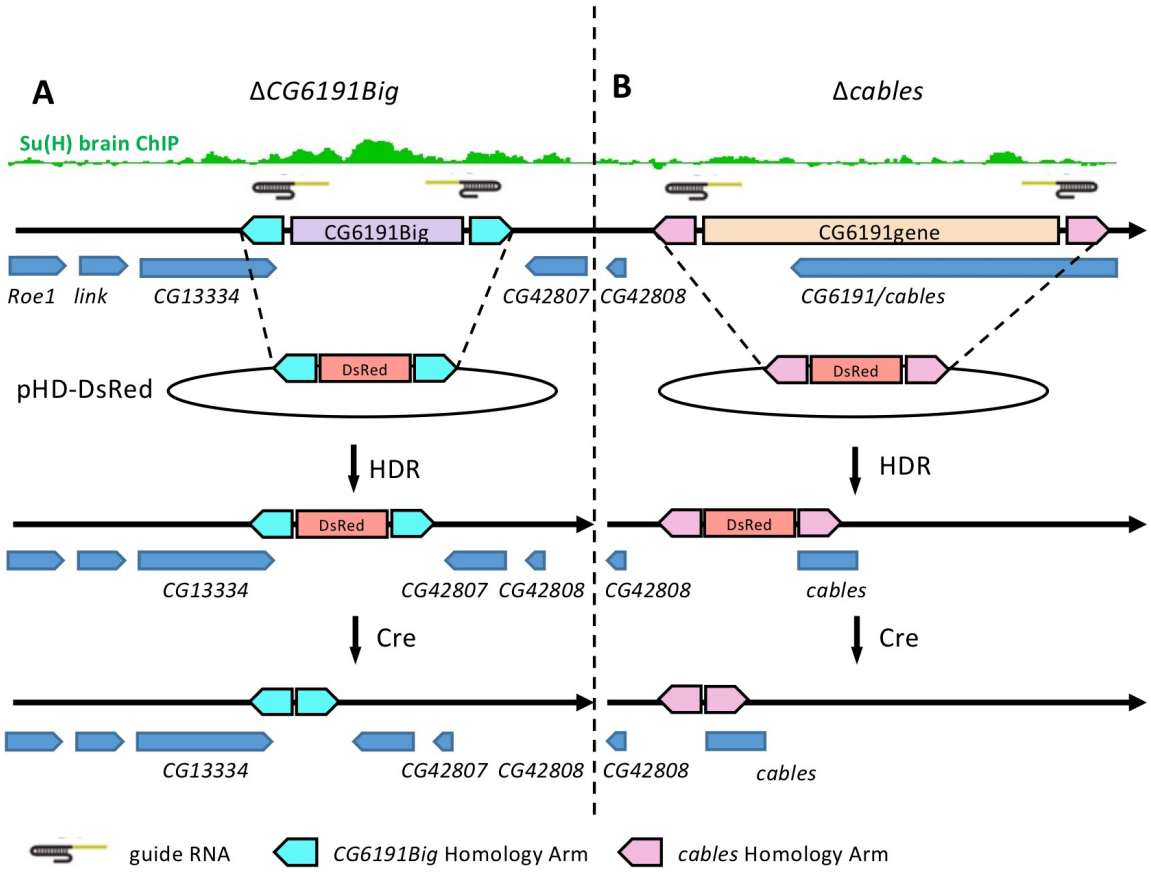

Fig 5.4. CRISPR/Cas9-induced HDR of *CG6191Big* locus and *cables*. Schematic of the *CG6191Big* (A)/*cables* (B) locus and the HDR strategy utilized to replace targeted regions with an DsRed expressing module (red). pHD-DsRed-attP contains an attP ΦC31 docking site for subsequent access to a targeted locus and a 3xP3-DsRed marker, flanked by loxP recombination sites for its removal. Homology arms (Cyan in A and pink in B) of ~1 kb immediately flanking the cleavage sites were cloned into pHD-DsRed-attP. Plasmids for guide RNAs and homology repair were co-injected into Cas9-expressing embryos. Upon HDR, the DsRed module is inserted into the deleted loci, allowing visual selection of genome-edited flies. With a final step of crossing to Cre stock, the DsRed module with flanking loxP sites could be removed.

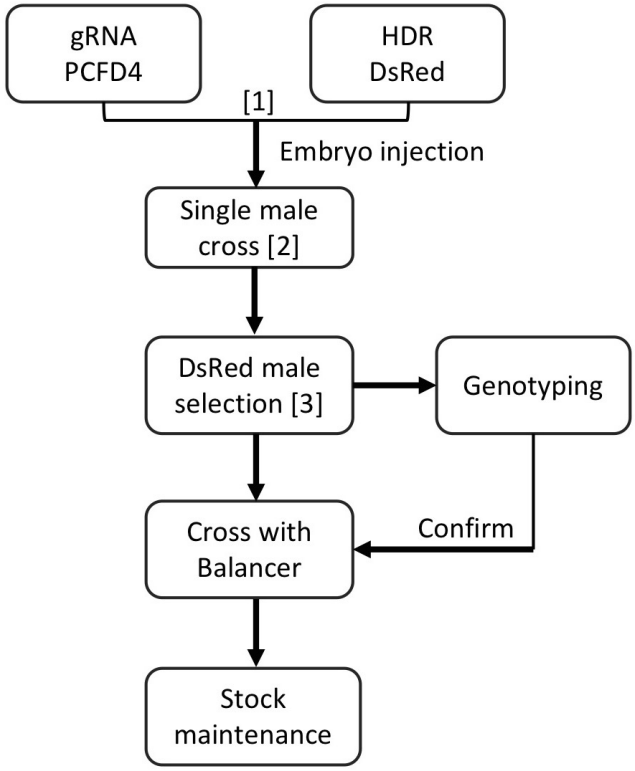

	[1] gRNA:HDR (ng/ul)	[2] larvae hatch rate	[3] DsRed stock ratio
CG6191Big	80:480	40% (230/570)	12.5% (6/48)
CG6191Big	160:480	22% (92/413)	10% (2/20)
CG6191gene	80:480	30% (175/586)	7.5% (3/40)

Fig 5.5. Work flow of CRISPR and relative quantifications in each steps. The flow diagram shows the procedure of CRISPR. The final concentration ratios of gRNA and HDR [1], the hatching rate after embryo injection [2], and the ratio of fertile crosses that expressed DsRed [3] are listed in the table.

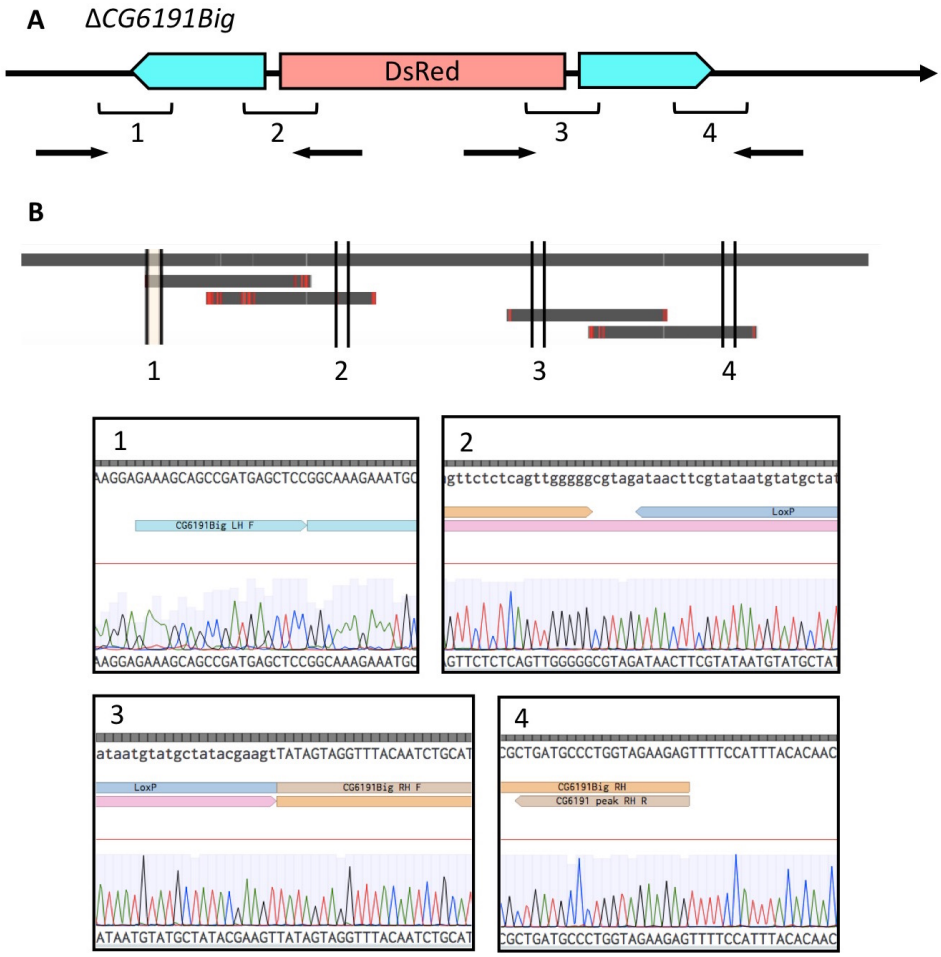

Fig 5.6. Genotyping results of *CG6191Big* CRISPR. (A) Schematic of the regions analysed to confirm Δ*CG6191Big* genotype, arrows indicate the direction of sequencing reads in each of the numbered regions. (B) Sequencing results of region 1-4 in (A) Upper, overview; Lower, zoomed in to show deletion endpoints corresponding to the numbered regions.

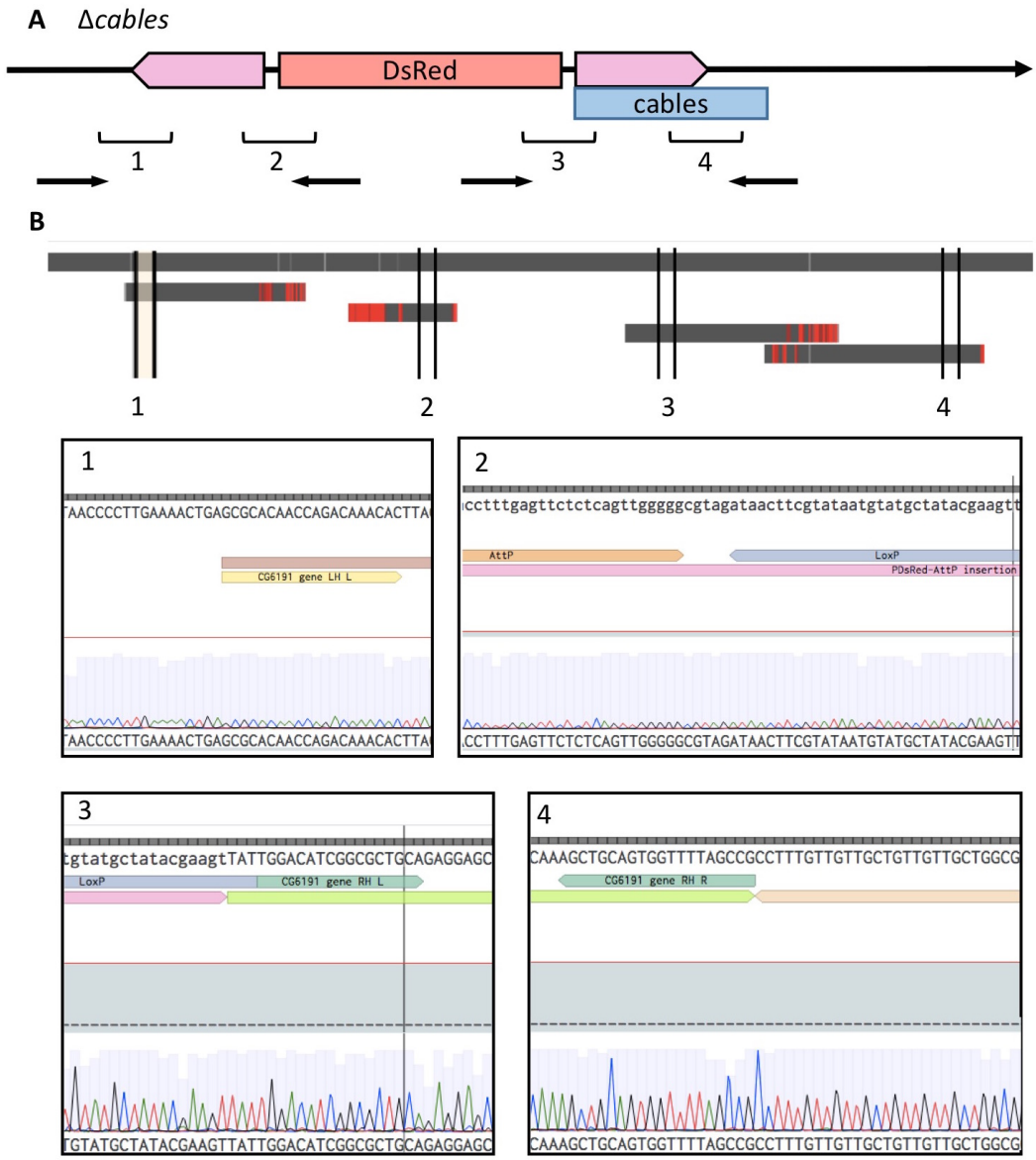

Fig 5.7. Genotyping results of *cables* gene CRISPR Schematic of the regions analysed to confirm Δ*cables* genotype, arrows indicate the direction of sequencing reads in each of the numbered regions. (B) Sequencing results of region 1-4 in (A) Upper, overview; Lower, zoomed in to show deletion endpoints corresponding to the numbered regions.

5.2.2 Identification of *CG6191Big*-regulated genes

To further explore the function of the *CG6191Big* enhancer, real-time PCR was performed using L3 larval brain tissue from wild-type and Δ*CG6191Big*-/- flies to identify which of the neighbouring genes were affected. Eight nearby genes (within 50kb) were selected (Table 5.1) and at least 2 sets of primers were designed for each gene (Table 2.7). The results show that among the tested genes, *cables* mRNA level is significantly reduced in *ΔCG6191Big* brains (Fig 5.8), compared to control. Other flanking genes were not significantly downregulated, even though some were closer to the enhancer than *cables* (Fig 5.8). This result indicates that *cables* is specifically regulated by the *CG6191Big* region, and is consistent with it responding to an enhancer that responds to Notch through Su(H) binding. One other gene, CG42807, exhibited changes in expression in *ΔCG6191Big* flies. However, CG42807 was upregulated rather than down-regulated and although the fold-change in expression was 3.8, the absolute levels of expression were extremely low (Fig 5.8). The *ΔCG6191Big* deletion may render this transcription unit more sensitive to influence from the surrounding chromatin, so that CG42807 is less efficiently silenced. Nevertheless, the real-time PCR results indicate that *CG6191Big* is required for normal levels of *cables* mRNA transcription in the larval brain, supporting the hypothesis that the *cables* gene is directly regulated by this remote NRE in the brain.

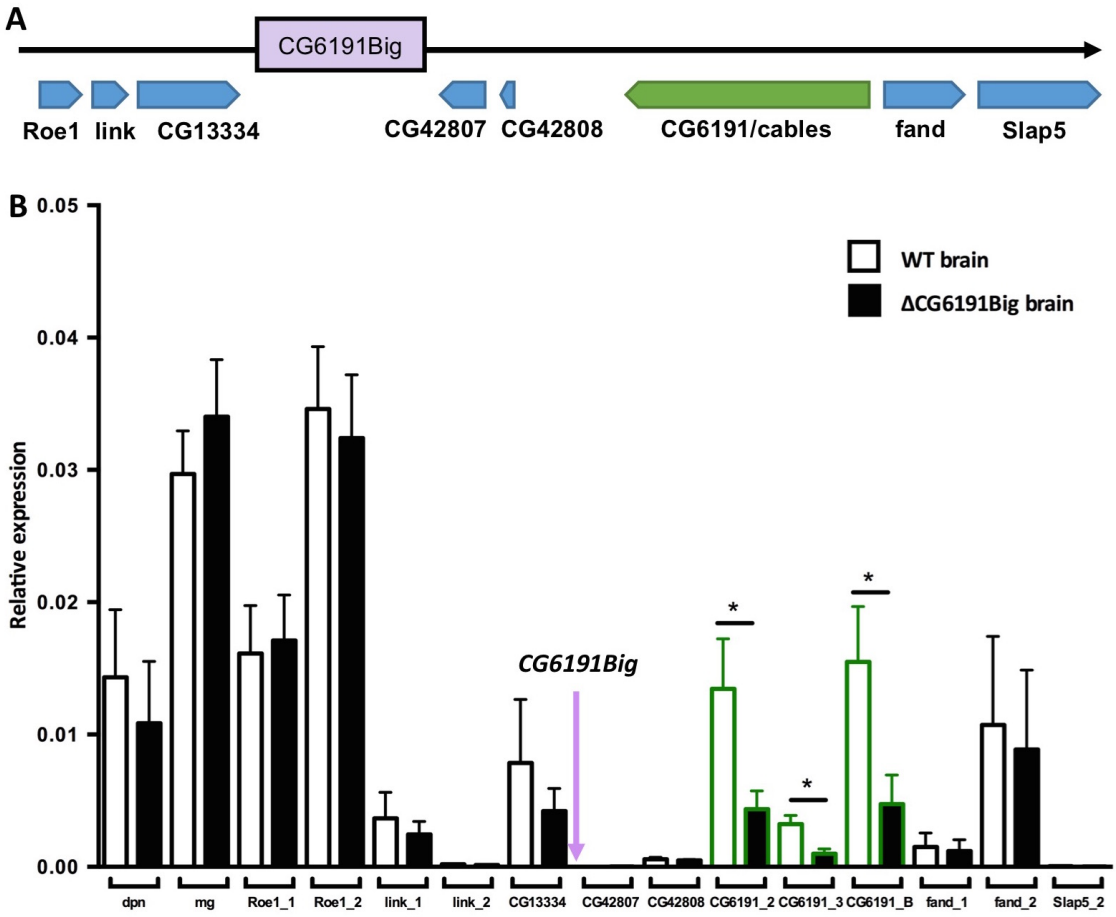

Fig 5.8. RT-PCR result showing mRNA level of *CG6191Big* deletion comparing to wild type control. (A) Schematic of genomic region corresponding to the measured genes. Purple bar shows *CG6191Big* and green bar shows *CG6191/cables*. (B) shows relative genes expression in wild-type (white columns) and Δ*CG6191Big* (black columns) brains normalized to *rp49*. Purple arrow indicates position of *CG6191Big;* CG6191_2, CG6191_3 and CG6191_B are different primer sets targeting different exons; *dpn* and *mg (E(spl)mγ)* are NB representing genes. *p<0.05.

5.2.3 *CG6191Big* and *cables* are both required for normal NB proliferation

To further investigate the relationship between *cables* and its regulatory enhancer, *CG6191Big*, the phenotypes from the deletion alleles were characterised. Firstly, both of the homozygous flies were viable, indicating a non-essential role under standard conditions. Second, the homozygous flies did not have classic Notch phenotypes, such as notched wings, or other wing defects, suggesting that this enhancer on its own is not essential for major Notch downstream effects during wing development.

However, *ΔCG6191Big* homozygous flies from homozygous parents appeared to be infertile. When homozygous females and homozygous males were mated, no eggs hatched. The fertility phenotype raised the possibility that *CG6191Big* may function in the reproductive system. Strikingly, the infertility was only seen when both parents were homozygous mutant (Table 5.2A). Homozygous alleles of Δ*cables* also resulted in lower fertility (Table 5.2B), consistent with the enhancer being linked with *cables* gene function. Because the emphasis was on the NB-related functions, the effects on the fertility phenotype were not analysed further.

Even though the *ΔCG6191Big* and *Δcables* flies were viable, they may nevertheless have altered NB regulation, as in some cases, mutations that specifically affect the NBs do not cause lethality. For example, hypomorphic mutation of *worniu*, such as *wor1/wor1* can alter NB regulation but does not cause lethality (Ashraf et al. 2004; Lai et al. 2012). To evaluate whether there was a change in the proliferation of NB lineages, larval brains from both *ΔCG6191Big* and *Δcables* were incubated with EdU. This nucleotide analogue is incorporated into the DNA during replication and can be detected with a fluorescent probe (Salic & Mitchison 2008). The number of NB progeny cells that had incorporated

EdU during the incubation period was then assessed as an indication of the proliferation rate. Larval brains from both alleles had less NB progeny with EdU incorporation than wild-type brains (Fig 5.9), suggesting that there was a reduced rate of cell division.

Surprisingly, when a second method to analyse cell division was used, the results were the converse. Phosphorylation of histone H3 (pH3) occurs during mitosis. The levels of pH3 in larval brains from *ΔCG6191Big* and *Δcables* were therefore analysed. Both *ΔCG6191Big* and *Δcables* had more NBs containing pH3 compared with controls (Fig 5.10A), indicating more NBs were in mitosis. In both cases, the ratio of pH3+ve NBs to total NBs was increased (Fig 5.10B). This contrasts with the decreased EdU incorporation, which measures the S-phase and can best be reconciled by the cells having a prolonged mitotic phase. Live imaging of *ΔCG6191Big* or *Δcables* NBs would help validating this possibility. Furthermore, as relatively few samples were analysed the experiments should be repeated to confirm this disparity.

A **Egg hatching rate**

ΔCG6191Big	+/- male	-/- male
+/- female	91.40% (53/58)	67.20% (39/58)
-/- female	51.70% (30/58)	0% (0/58)

B **Egg hatching rate**

Δcables	+/- male	-/- male
+/- female	91.93% (57/62)	58.10% (36/62)
-/- female	54.84% (34/62)	1.61% (1/62)

Table 5.2. Embryo viability phenotype of *ΔCG6191Big* and *Δcables*.
Numbers of eggs producing hatched larvae from the crosses are indicated.

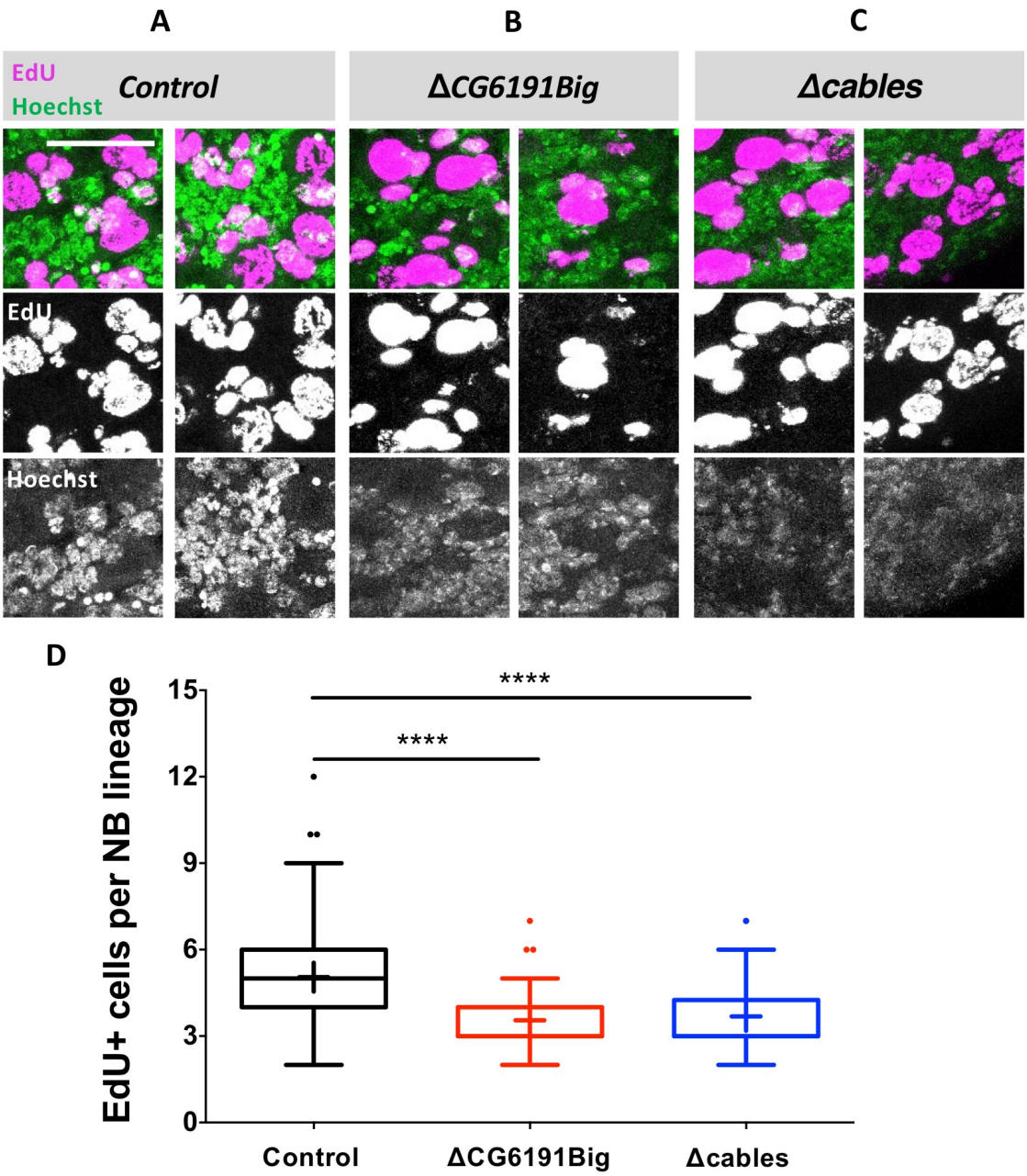

Fig 5.9. Decreased proliferation labelled by EdU in *ΔCG6191Big* and *Δcables* NB lineages. (A-C) EdU labelling of control (A) Δ*CG6191Big* (B) and *Δcables* (C). Magenta represents EdU and green represents nucleus-staining Hoechst. (D) Quantification of EdU+ cells in counted NB lineages, n=104, 70 and 66 (each from 5 brains). ****p<0.0001. Scale bar, 25 µm.

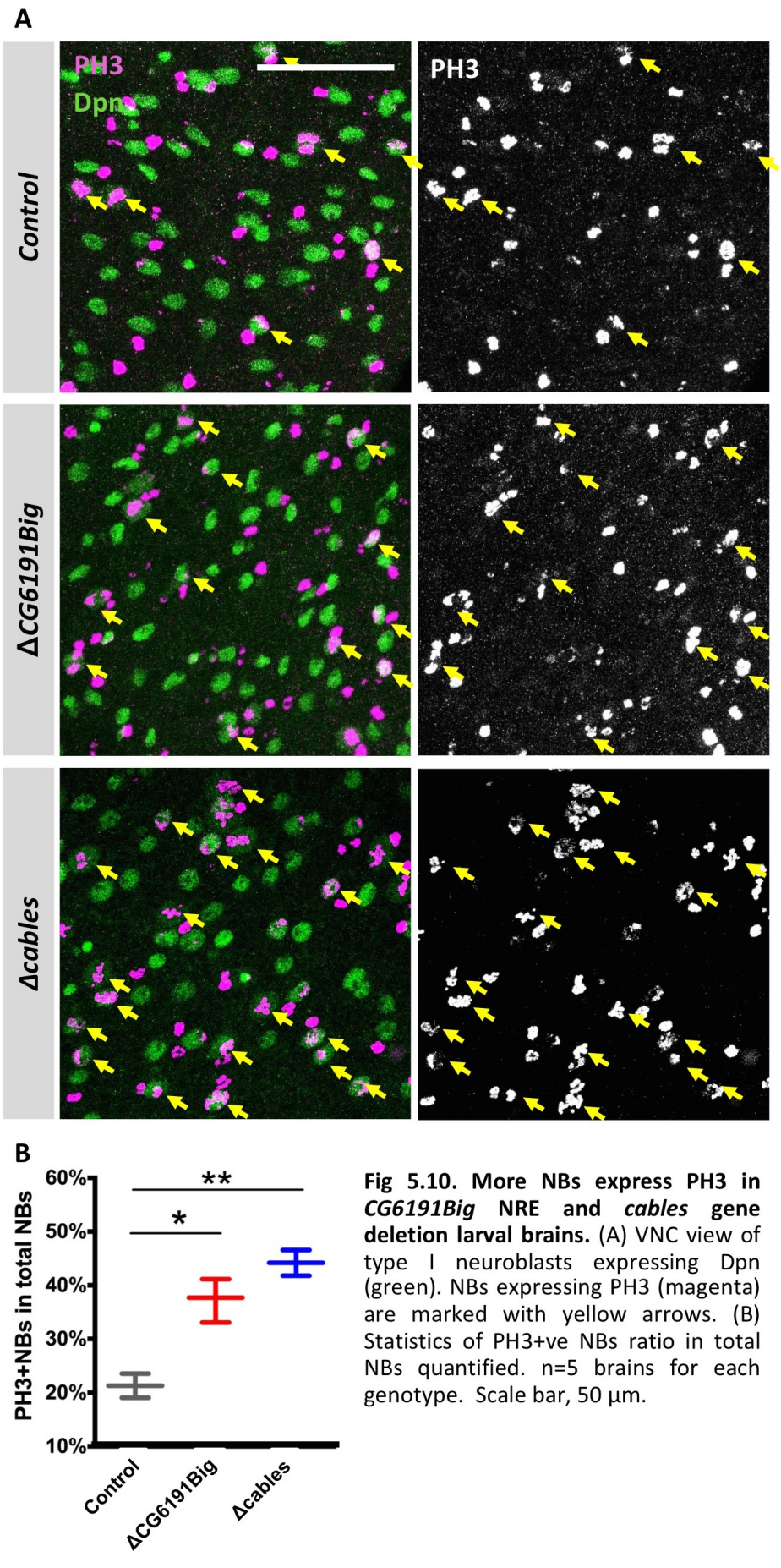

Fig 5.10. More NBs express PH3 in *CG6191Big* NRE and *cables* gene deletion larval brains. (A) VNC view of type I neuroblasts expressing Dpn (green). NBs expressing PH3 (magenta) are marked with yellow arrows. (B) Statistics of PH3+ve NBs ratio in total NBs quantified. n=5 brains for each genotype. Scale bar, 50 µm.

5.2.4 Neither E2F nor Dap expression are affected by ∆CG6191Big

To further investigate the proliferation defects in *ΔCG6191Big* the effects on two cell cycle markers, E2F and Dacapo/p21 (Dap) were analysed. E2F is synthesised during G2, and degraded in S phase so that NBs where no E2F is present would be in S-phase (Zielke et al. 2014). The effects of *ΔCG6191Big* on E2F levels in the NBs was analysed in homozygous mutant NB lineages using the MARCM approach. There was no difference in the proportion of E2F+ve NBs between *ΔCG6191Big* and control lineages (Fig 5.11). This result suggests that the S phase of the NBs is not affected in *ΔCG6191Big*. Due to time constraints, it was not possible to perform the same analysis on *Δcables* mutant lineages.

Dacapo is the *Drosophila* homolog of p21, a Cyclin-dependent kinase inhibitor of the CIP/KIP family that binds to CycE-Cdk2 complexes and inhibits their protein kinase activity. Normally p21 is upregulated in the NB progeny where it arrests them in G1/G0 before terminal differentiation. In mammalian cells, CABLES was reported to form a complex with p21 in the nucleus and stabilise it. If this mechanism is conserved in *Drosophila*, Dap/p21 should be degraded if CABLES is removed. To test this possibility expression of Dap was examined in *ΔCG6191Big* clones. However, staining with an anti-Dap antibody failed to give the expected pattern, even in wild-type (Fig 5.12), little or no protein was detected in the NB progeny in either wild-type or *ΔCG6191Big*. Thus it is not possible to conclude whether Dap is affected when Cables expression is compromised.

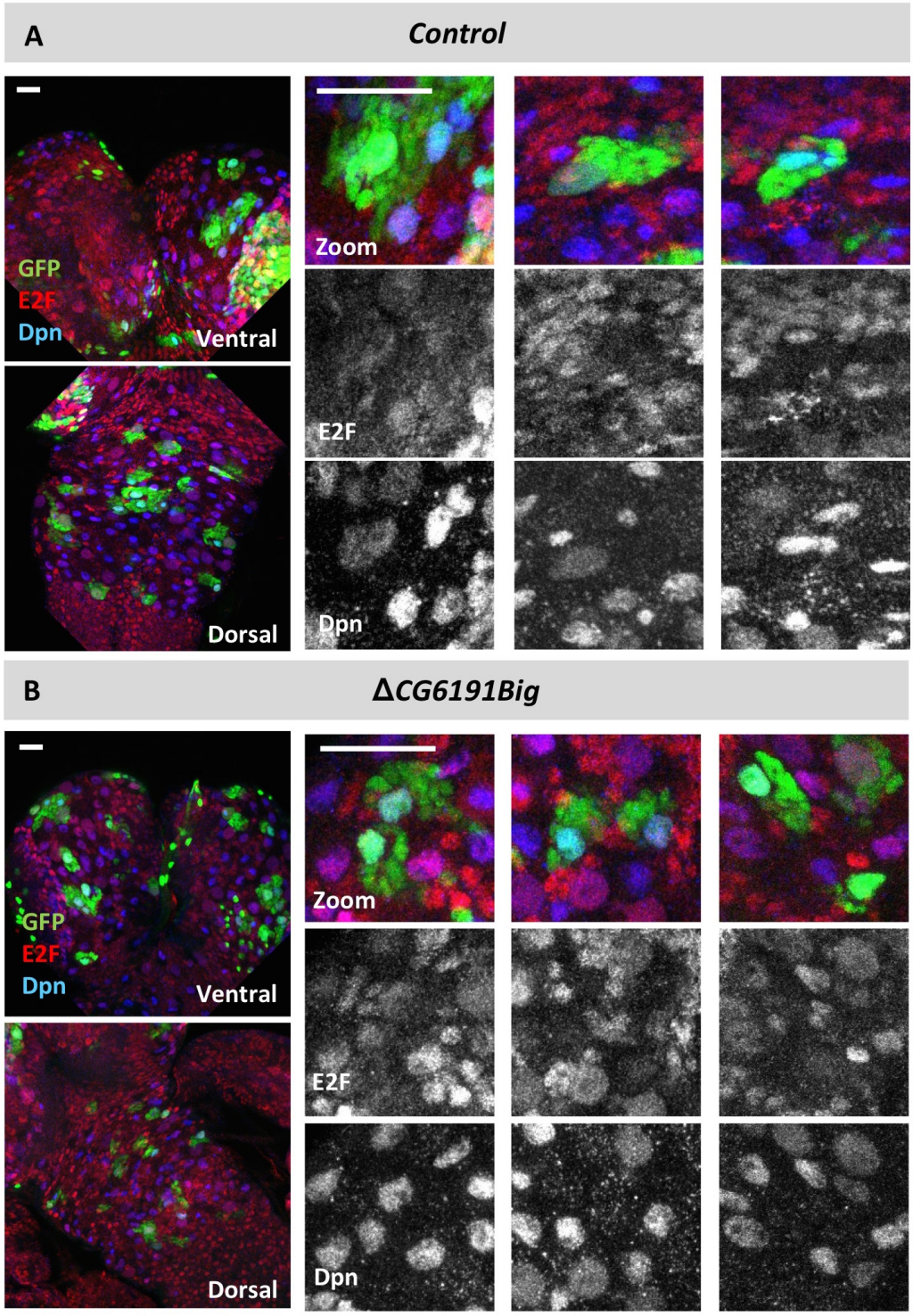

Fig 5.11. E2F expression in control (A) and Δ*CG6191Big* (B) mosaic clones. Clones were marked with GFP and stained with E2F(red and grey) and Dpn (blue and grey). Scale bar, 25 μm.

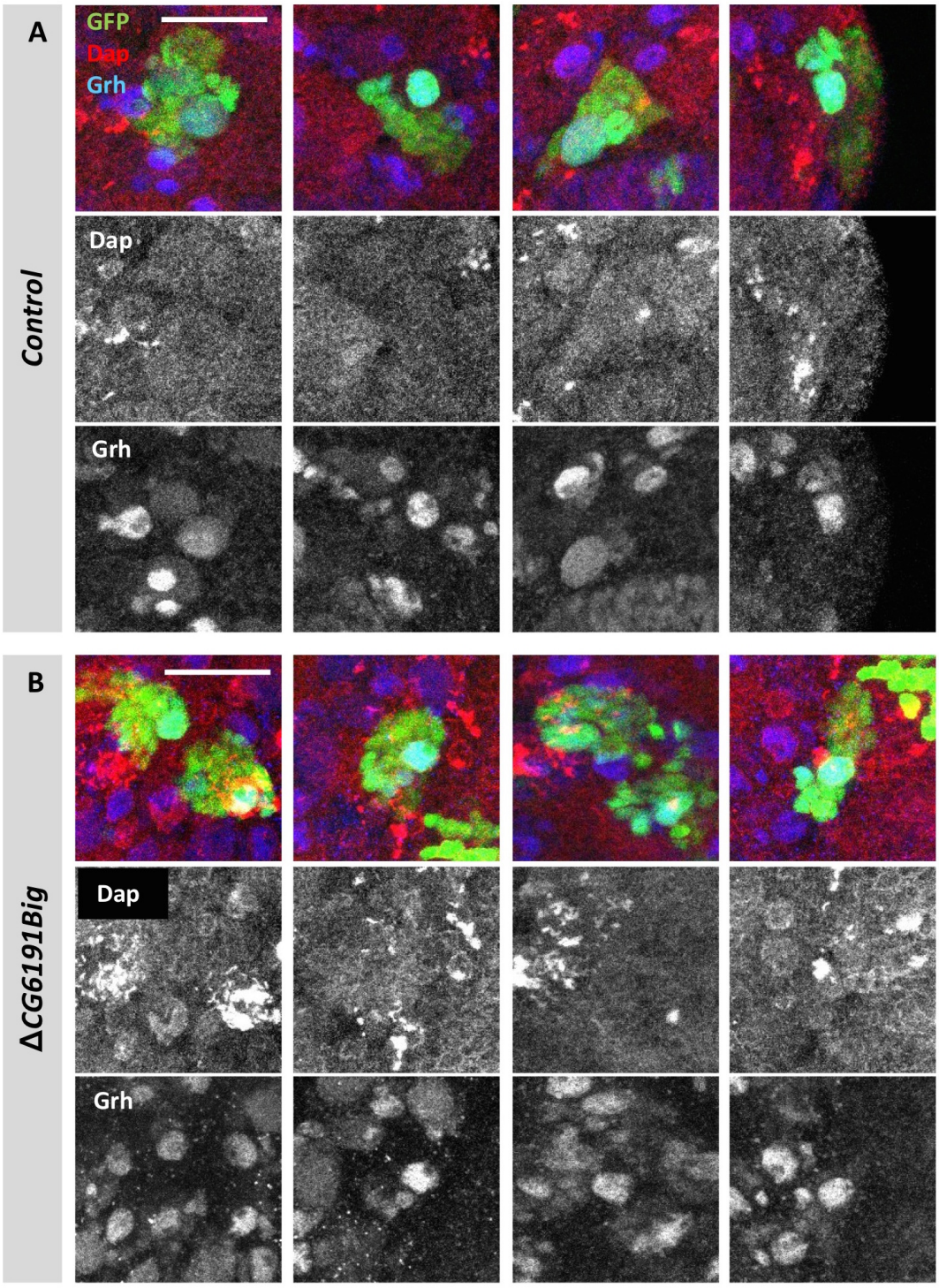

Fig 5. 12. Dacapo expression is not altered in *CG6191Big* mutant NBs. Mosaic clones of control (A) and Δ*CG6191Big* (B) are marked with GFP and stained with Dap (Red and grey) and Grh (blue and grey). Scale bar, 25 µm.

5.4 Discussion

CG6191Big encompasses one of the regions in the genome that is the most highly enriched regions for Su(H) motifs (Rebeiz et al. 2002). As demonstrated in Chapter 3, this region functions as an NRE, being responsive to Notch regulation both in cell lines and *in vivo*, and it directs GFP expression in the larval CNS with a specific NB-enriched pattern. Furthermore, in wing discs *CG6191Big* directs expression at the wing disc D/V boundary, a known site of Notch activity. However, it remained unclear which gene was the target of this NRE. The Bray group considered *CG6191/cab*les as the potential Notch target of this NRE in wing discs (Alexandre Djiane et al. 2013) whereas other groups assumed that *CG6191Big* was associated with *CG13334* because it is the closest gene to it (Tony D Southall & Brand 2009a; Slaninova et al. 2016). By making a deletion of *CG6191Big*, I have confirmed that *cables* is the primary target of this enhancer, as its expression was severely compromised by this deletion. No significant changes in *CG13334* expression were detected and among the 8 genes that were analysed by real-time PCR, only one other gene in the region, besides *cables* showed any change in expression. This was *CG42807* which had a significantly increased mRNA level, although the absolute expression levels were very low (Fig 5.8C). This suggests either that there is an inhibitory element within the region that was removed in *ΔCG6191Big*, or that by preventing the long range interactions between *CG6191Big* and *cables*, insulators such as BEAF-32 are no longer associated with the region so that CG42807 is de-repressed. Despite the effects on CG42807, both the reduction in *cables* mRNA levels and the similarity between the phenotypes from deleting *CG6191Big* and *cables* itself, suggest that this region is a distal Notch -esponsive element that acts on *cables,* regulating it

from a distance. While it is very likely that *CG6191Big* interacts with *cables*, possibly via the other Su(H) bound region *CG6191in*, to prove this a method like chromatin conformation analysis (3C) would need to be used to measure the long range interactions between these two enhancers. Effects on expression levels in other tissues should also be confirmed.

Besides being bound by Su(H) in different contexts (brain and wing disc (Fig 5.13)), *CG6191Big* is also bound by multiple TFs (Ase/Pros/Dpn/Snail) in embryonic NBs as shown in Fig 5.13 (Tony D Southall & Brand 2009b), suggesting that *CG6191Big* is a "universal" regulatory region, or super-enhancer. It is also likely subject to Polycomb regulation, since this region has H3K27me3 activity in L3 larva while nearby regions do not (Fig 5.13) (Schertel et al. 2015). Overall, chromatin profiling suggests *CG6191Big* could be a docking site for multiple regulatory inputs, which makes it perplexing that there are so few consequences from deleting it or its putative target *cables*.

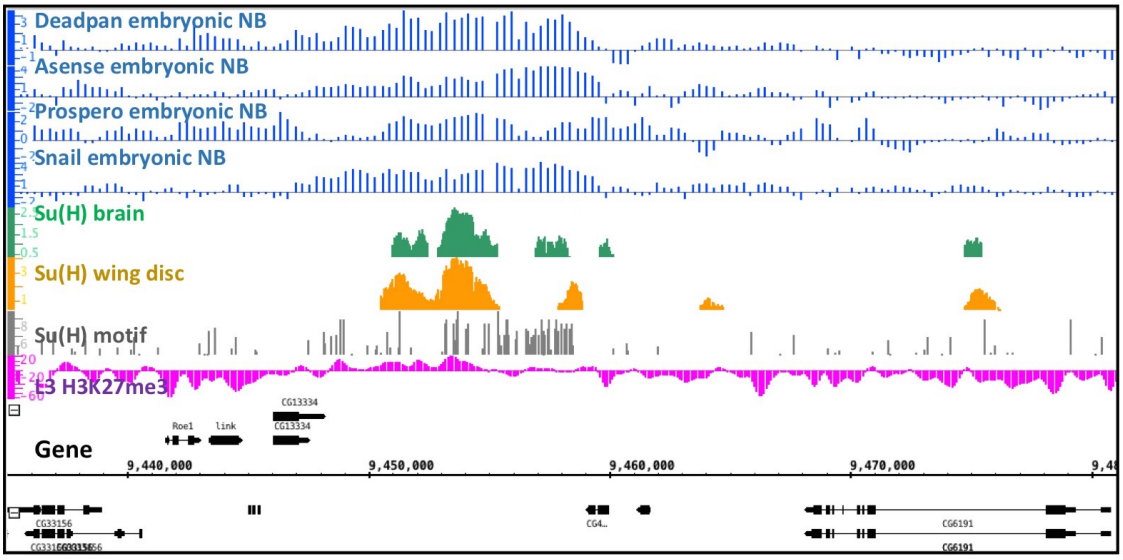

Fig 5.13. Regulatory possibility of *CG6191Big* enhancer. (A) Binding profiles for indicated transcription factors at *CG6191Big* loci in neural stem cells. Blue bars indicate binding of different transcription factors (Dpn, Ase, Pros and Snail); Bar heights are proportional to the average of normalised log2 ratio of intensities from DamID *in vivo* binding site experiments (Southall & Brand 2009). Su(H) binding profile in brain (green) and wing discs (orange) and L3 larval H3K27me3 profiling (magenta, Schertel et al. 2015) are shown as well (enrichment relative to input AvgM, log scale is as indicated).

Cables encodes a protein with a cyclin-related domain but relatively little is known about its normal function (Fig 5.3B). To investigate, and to determine the relevance of the *CG6191Big* enhancer, two deletion strains were generated. Both had similar phenotypes, with subtle effects on NB proliferation. When deleted, NBs had a lower division rate (from EdU incorporation) but a longer mitotic phase. As E2F was unchanged, it suggests there is no effect on S phase, while the Dap results were inconclusive. To investigate further, markers of other cell cycle phases, like Cyclin E and components of the APC/C complex could be examined. One explanation could be that there is a problem with the mitotic check point, which ensures the chromosomes are aligned correctly. It will be helpful therefore to also examine the ploidy of the mutant NBs to see if there is any aneuploidy, a condition which causes delays in cell cycle progression and premature differentiation of NSCs (Gogendeau et al. 2015). However, these results point to a role

of Cables in promoting proliferation, which is not consistent with its tumour suppressor role in mammals. Nevertheless, it may fit with recent results suggesting that Cables promotes neurite growth (Zukerberg, Patrick, Nikolic, Humbert, C. L. Wu, et al. 2000). Further experiments are needed to determine how *cables* promotes normal mitosis and proliferation.

One common phenotype for Δ*CG6191Big* and Δ*cables* was that crosses between homozygous males and homozygous females were infertile. This implies that there is normally maternally supplied Cables function, which is sufficient for the viability of the homozygous mutant animals. Eggs produced from mutant female flies lack this maternally supplied protein, but can be rescued by expression from the paternal chromosome in the zygote. So only when both parents are homozygous mutant are the embryos totally devoid of protein and unable to survive. Given my result showing that Cables is required for cell cycle progression, it would be important to examine the cell divisions in these maternal and zygotic null embryos to see whether they are affected. It is also possible that some protein normally persists until larval stages in the zygotic nulls, so that the effects seen on EdU and pH3 may only be partial phenotypes and not the phenotypes that would be seen with complete *cables* depletion.

My results suggest that there is a long-range enhancer that confers Notch regulation on Cables. It would therefore be relevant to also test whether the deletion of *cables* can modify the tumour phenotype produced by constitutive Notch activity. Likewise, it would be interesting to establish whether similar remote regulation of cables is conserved in mammals. The Hi-C data indicates that CABLES1 is found in a topological domain. Analysis of these interacting sites merits further investigation.

Chapter VI

General Conclusion and Discussion

Notch signalling is constitutively active in NSCs where it plays important roles in regulating their behaviours through its downstream target effectors. A number of Notch target genes in neural stem cells have been characterized, such as *E(spl)mγ, dpn, grh* and *myc,* and their functions defined (Almeida & Bray 2005; San-Juán & Baonza 2011; Zacharioudaki et al. 2012; Babaoğlan et al. 2013; Zacharioudaki et al. 2016). However, previous genome-wide study from our lab suggested that there is a larger group of potential Notch target genes in *Drosophila* NSCs (Zacharioudaki et al. 2016). In this thesis, I confirmed that several of these, *path*, *cables* and *Asph* are Notch target genes in *Drosophila* NSCs. Furthermore, the expression pattern and function of *path* were further examined in *Drosophila* brains. Path is expressed in NSCs, loss of which causes an increase in NSC size and a reduction in the number of NSC progeny. In contrast, upon Notch over-activation, Path switches from promoting to restricting NSC proliferation by suppressing p4EBP. In addition, I found that *pathNRE* is a nutrition-dependent enhancer, whose expression is reduced in nutrition restriction. Path is also expressed in glial cells and is required for protecting brain growth under NR by regulating Jeb. In addition, the Notch response element and function of *cables* was also defined in *Drosophila* NSCs. I

identified that a remote NRE is required for *cables* expression in NSCs. Both the remote NRE and *cables* are important for normal NSCs proliferation.

6.1 Notch target genes in NSCs

DNA-binding proteins Su(H)/CSL are the essential effectors of Notch pathway. In the widely accepted model for Notch-regulated target genes, target loci are bound by Su(H)-co-repressors complex to keep genes silenced in the absence of Notch activity. Upon activation, the intracellular domain of Notch receptor, NICD is released and interacts with Su(H) to promote the expression of target genes (Kopan & Ilagan 2009; Bray 2016). The method used to identify putative Notch targets was to identify genomic regions bound by Su(H) in NΔECD over-expressing brains and correlate those with genes whose expression was up-regulated in comparison to wild-type. From the 185 genes identified in this way, a subset was selected for investigation.

Results indicated that a proportion of the 6 genes analysed exhibited characteristics that fit with them being direct Notch targets. Thus, *path*, *cables* and *Asph* all fulfilled the criteria for containing Notch-regulated enhancers. Firstly, the NRE-GFP reporters containing the identified enhancers from these genes were expressed in NBs, and were sensitive to Notch modulation. Mutations in the Su(H) binding motifs also compromised their expression. Thus these 3 genes appear to be Notch-regulated genes in the NSCs and may therefore give further insights into Notch functions in these cells.

On the other hand, two of the other genes with Su(H) binding in their enhancers, did not clearly exhibit characteristics that supported direct Notch regulation. These fell into two

categories. First, *syp*, whose enhancer was expressed in NBs, did not show further evidence of Notch regulation. Thus there was no change in expression when Notch activity was modulated nor were the Su(H) sites essential for expression. This might be explained if convergent signalling pathways directed *syp* expression, so that modulation of Notch alone was not sufficient. Another explanation could be that *syp* has multiple enhancers, like *grh*, for which two NSC-specific enhancers have been identified (Prokop et al. 1998; Brody et al. 2012). Further studies including finding new transcription factors binding to the *syp* enhancer and identifying new enhancers of *syp* might be helpful for defining the function of Su(H) for *syp*. The second example was *lola*, whose Su(H) bound enhancer was not expressed in NBs. One possible explanation is that Su(H) binding is associated with another factor, as observed in Pancreatic lineages, and is not sensitive to Notch(Nakhai et al. 2008) (Nakhai et al., 2008). Another is that the enhancer is Notch-responsive in other cell types, but prevented from expression in NBs due to the presence of a repressor similar to the effects seen with IKaros in T-cell lineages (Kleinmann et al. 2008). Finally, it may be a "false positive" in that enrichment was detected in the ChIP but this was due to background rather than specific binding.

In conclusion, the genomic profiling approach has successfully identified several Notch regulated genes. However, caution is needed and further experiments are required on a gene-by-gene basis to determine those that are relevant targets for Notch function in NSCs. One caveat of the methods used to identify the putative Notch target genes, was that it was largely based on expression microarrays data from the whole brains with Notch over-activated NSCs, in which NSCs only account for 3% (Kang & Reichert 2015). Due to the small amount of NSCs in the whole population, the change of some Notch

target genes might be masked. FACS could be an approach to purify large numbers of NSCs. Based on different cell size and GFP intensity (driven by *ase-Gal4*), a relatively purified population of NSCs was able to be isolated and the transcriptome of purified NSCs was analysed by the bulk mRNA sequencing (Berger et al. 2012). However, NBs are very adhesive to their progeny and the GFP protein is still in the progeny cells, which could significantly affect the purity of NBs. Recent single cell mRNA sequencing techniques, for example, drop-seq based on droplet barcoding, might provide us a new way to study NSCs (Klein et al. 2015; Macosko et al. 2015). Since drop-seq is able to read about 5,000 cells at once, the transcriptome of the whole *Drosophila* brain after dissociating can be analysed at a single cell level with this method. Then the cells could be grouped into several clusters based on their specific mRNA expression profiles, including the cluster of NSCs. By comparing the transcriptome of NSCs (Notch on) and that of their progeny (Notch off) in the same data set and that of Notch over-activated NSCs from another data set, the function of Notch on determining NSCs cell identity could be better understood and more Notch targets might be identified. In addition, this might also provide specific surface makers for NSCs, which could be used for FACS.

6.2 Notch target genes and stem cell identity

Many key signalling pathways, such as Wnt, Hedgehog and Notch, are not only involved in various developmental processes, but also continue to persist in adulthood to maintain normal homeostatic organ function. The functions of the same pathway are very context-dependent, and could be either similar or opposite; for example, Notch

was reported to initiate and maintain cancer stem cells in lung adenocarcinoma and colorectal cancer, and its over-activation induced stem cell hyperplasia (Hassan et al. 2013; Winton 2013; Takebe et al. 2015). Similarly, Notch is normally active in NSCs, but quickly turns to be inactive in their progeny. Sustained over-activation of Notch could cause over-proliferation of NSCs, resulting in brain tumour (Wang et al. 2006; Weng et al. 2010). In contrast, Notch activation induced growth arrest in acute myelogenous leukaemia and B-cell malignancy (Kannan et al. 2013; Zweidler-McKay et al. 2005). Thus the context-dependent roles of Notch are associated with different functional outputs (Bray 2016). For example, Notch-regulated genes in NSC hyperplasia were quite different from those in an epithelial hyperplasia induced by excessive Notch activity in wing imaginal discs. The 246 putative Notch target genes in NSCs hyperplasia were mainly associated with cell fate determining and transcription, while those (278 genes) in the epithelial hyperplasia were enriched in signalling pathways and proliferation control (Alexandre Djiane et al. 2013; Zacharioudaki et al. 2016); they only shared nine overlapping genes. These differences highlight the importance of identifying the Notch-regulated targets in different contexts.

Accumulating evidence suggests that the general outcome for Notch-induced NSC-expressed genes might be to keep the self-renewal identities of NSCs (Berger et al. 2012; Tony D Southall & Brand 2009a; Zacharioudaki et al. 2012; Zacharioudaki et al. 2016). One of the important Notch downstream targets in NSCs is *E(spl)mγ*, and its over-expression could partially mimic Notch-induced over-proliferation in NSCs (Zacharioudaki et al. 2012). In addition, deletion of the zinc-finger protein Klu, led to premature differentiation of NSCs and excessive Klu caused brain tumours, similar to

over-activation of Notch (Berger et al. 2012). These results indicate that Notch determines NSC identity and behaviour through delicate regulation of several downstream transcription factors.

Although deletion/over-expression of some Notch-specific target genes alone could affect the characteristics of the Notch-induced NSCs hyperplasia, manipulation of most single targets may not change NSC phenotypes dramatically. This could in part be explained by the redundant or overlapping functions of multiple target genes, resulting in high robustness in Notch regulatory network maintaining stem cell identity and behaviour. For example, only simultaneously deleting both of Notch target genes *grh* and *wor* could decrease the number of intermediate neural progenitors and ganglion mother cells compared with either single mutant alone (Zacharioudaki et al. 2016). This indicates that manipulation of the expression of a single target gene might have no effect on Notch-determined NSC identity, which does not necessarily mean each gene has no function in NSC maintenance.

So far the majority of targets analysed have been transcription factors. It is likely that Notch activity also impinges more directly on NB maintenance and both Path and Cables have potential roles in regulating NBs. *cables* was one of the nine shared overlapping genes between epithelial and NB hyperplasia (Alexandre Djiane et al. 2013; Zacharioudaki et al. 2016). Ablation of *cables* in the former caused a reduction in wing size, suggesting that it might contribute to tissue growth in normal development (Alexandre Djiane et al. 2013). Consistent with these previous findings, in this study *cables* was also found required for normal NSC proliferation. In this thesis, when *cables* was deleted, NSCs had a lower division rate but a longer mitotic phase with unchanged

E2F, suggesting that Cables might affect other cell cycle phases, rather than S phase. Similarly, Path encodes an amino acid transporter, depletion of which causes an increase in NSC cell size and a reduction in the number of NB progeny under normal conditions. Interestingly, Path switches from promoting to restricting proliferation when Notch is over-activated, which might act through suppressing 4EBP phosphorylation. Interestingly, Path is also expressed in glia. The glia-expressed Path, but not the NB-expressed, is important for brain sparing under NR, which involved the regulation of Jeb.

Neither *path* nor *cables* knock down gave very strong changes in NBs. To better understand the biological functions of Notch target genes, combinatorial knock down of different targets with potential similar functions would be a consideration. For example, depletion of Path caused an increase in cell size of NSCs and a reduction in the number of their progeny. Similarly, c*ables* was found to be required for normal NSC proliferation. The NSC phenotypes from combined depletion of both genes might give synergistic/additive effects and could be informative about cell size regulation.

6.3 Concluding remarks

In the past few decades, *Drosophila* has been used as an essential developmental and genetic model organism for addressing various fundamental biological questions. Studies on *Drosophila* have also facilitated a dramatic progress in our understanding of fundamental stem cell biology. It is possible that the genes identified here could play more widespread roles in stem cell identity and behaviour.

Reference

Almeida, M.S. & Bray, S.J., 2005. Regulation of post-embryonic neuroblasts by Drosophila Grainyhead. *Mechanisms of Development*, 122(12), pp.1282–1293.

Anon, 1998. Notch signalling inDrosophila: three ways to use a pathway. *Seminars in Cell & Developmental Biology*, 9(6), pp.591–597.

Arnason, T. et al., 2013. Cables1 is a tumor suppressor gene that regulates intestinal tumor progression in ApcMin mice. *Cancer Biology and Therapy*, 14(7), pp.672–678.

Arnett, K.L. et al., 2010. Structural and mechanistic insights into cooperative assembly of dimeric Notch transcription complexes. *Nature Structural and Molecular Biology*, 17(11), pp.1312–1317.

Artavanis-Tsakonas, S., Matsuno, K. & Fortini, M., 1995. Notch signaling. *Science*, 268(5208), pp.225–232.

Artavanis-Tsakonas, S., Rand, M.D. & Lake, R.J., 1999. Notch signaling: cell fate control and signal integration in development. *Science (New York, N.Y.)*, 284(5415), pp.770–6.

Ashraf, S.I. et al., 2004. Worniu, a snail family zinc-finger protein, is required for brain development in Drosophila. *Developmental Dynamics*, 231(2), pp.379–386.

Babaoğlan, A.B. et al., 2013. Deadpan Contributes to the Robustness of the Notch Response B. Jennings, ed. *PLoS ONE*, 8(9), p.e75632.

Bailey, A.M. & Posakony, J.W., 1995. Suppressor of hairless directly activates transcription of enhancer of split complex genes in response to Notch receptor activity. *Genes and Development*, 9(21), pp.2609–2622.

Barbarulo, A. et al., 2011. Notch3 and Canonical NF- B Signaling Pathways Cooperatively Regulate Foxp3 Transcription. *The Journal of Immunology*, 186(11), pp.6199–6206.

Basak, O. et al., 2012. Neurogenic Subventricular Zone Stem/Progenitor Cells Are Notch1-Dependent in Their Active But Not Quiescent State. *Journal of Neuroscience*, 32(16), pp.5654–5666.

Bellen, H.J. & Yamamoto, S., 2015. Morgan's Legacy: Fruit Flies and the Functional Annotation of Conserved Genes. *Cell*, 163(1), pp.12–14.

Bello, B.C. et al., 2008. Amplification of neural stem cell proliferation by intermediate progenitor cells in Drosophila brain development. *Neural Development*, 3(1), p.5.

Beres, T.M. et al., 2006. PTF1 is an organ-specific and notch-independent basic helix-loop-helix complex containing the mammalian suppressor of hairless (RBP-J) or its paralogue, RBP-L. *Molecular and Cellular Biology*, 26(1), pp.117–130.

Berger, C. et al., 2012. FACS purification and transcriptome analysis of Drosophila neural stem cells reveals a role for Klumpfuss in self-renewal. *Cell Reports*, 2(2), pp.407–418.

Boone, J.Q. & Doe, C.Q., 2008. Identification of Drosophila type II neuroblast lineages containing transit amplifying ganglion mother cells. *Developmental neurobiology*, 68(9), pp.1185–95.

Borgas, D.L. et al., 2015. Potential Role of Phosphorylation as a Regulator of Aspartyl-(asparaginyl)-beta-hydroxylase: Relevance to Infiltrative Spread of Human Hepatocellular Carcinoma. *Liver Cancer*, 4(3), pp.139–153.

Bou Dib, P. et al., 2014. A Conserved Role for p48 Homologs in Protecting Dopaminergic

Neurons from Oxidative Stress B. Lu, ed. *PLoS Genetics*, 10(10), p.e1004718.
Bowman, S.K. et al., 2008. The tumor suppressors Brat and Numb regulate transit-amplifying neuroblast lineages in Drosophila. *Developmental cell*, 14(4), pp.535–46.
Brand, A.H. & Perrimon, N., 1993. Targeted gene expression as a means of altering cell fates and generating dominant phenotypes. *Development (Cambridge, England)*, 118(2), pp.401–15.
Bray, S.J., 1997. Expression and function of Enhancer of split bHLH proteins during Drosophila neurogenesis. *Perspectives on developmental neurobiology*, 4(4), pp.313–23.
Bray, S.J., 2006. Notch signalling: A simple pathway becomes complex. *Nature Reviews Molecular Cell Biology*, 7(9), pp.678–689.
Bray, S.J., 2016. Notch signalling in context. *Nature Reviews Molecular Cell Biology*, 9(17), pp.722–735.
Brody, T. et al., 2012. Use of a Drosophila genome-wide conserved sequence database to identify functionally related cis-regulatory enhancers. *Developmental dynamics : an official publication of the American Association of Anatomists*, 241(1), pp.169–89.
Cantarini, M.C. et al., 2006. Aspartyl-asparagyl beta hydroxylase over-expression in human hepatoma is linked to activation of insulin-like growth factor and notch signaling mechanisms. *Hepatology*, 44(2), pp.446–457.
Castel, D. et al., 2013. Dynamic binding of RBPJ is determined by notch signaling status. *Genes and Development*, 27(9), pp.1059–1071.
Chell, J.M. & Brand, A.H., 2010. Nutrition-responsive glia control exit of neural stem cells from quiescence. *Cell*, 143(7), pp.1161–1173.
Cheng, L.Y. et al., 2011. Anaplastic Lymphoma Kinase spares organ growth during nutrient restriction in Drosophila. *Cell*, 146(3), pp.435–447.
Chi, Z. et al., 2012. Botch Promotes Neurogenesis by Antagonizing Notch. *Developmental Cell*, 22(4), pp.707–720.
Chia, W., Somers, W.G. & Wang, H.Y., 2008. Drosophila neuroblast asymmetric divisions: cell cycle regulators, asymmetric protein localization, and tumorigenesis. *Journal of Cell Biology*, 180(2), pp.267–272.
Chintapalli, V.R., Wang, J. & Dow, J.A.T., 2007. Using FlyAtlas to identify better *Drosophila melanogaster* models of human disease. *Nature Genetics*, 39(6), pp.715–720.
Chitnis, A. et al., 1995. Primary neurogenesis in Xenopus embryos regulated by a homologue of the Drosophila neurogenic gene Delta. *Nature*, 375(6534), pp.761–766.
Cohen, E., Baerts, W. & Van Bel, F., 2015. Brain-Sparing in Intrauterine Growth Restriction: Considerations for the Neonatologist. *Neonatology*, 108(4), pp.269–276.
Collins, K.J., Yuan, Z. & Kovall, R.A., 2014. Structure and function of the CSL-KyoT2 corepressor complex: A negative regulator of Notch signaling. *Structure*, 22(1), pp.70–81.
D'Souza, B., Meloty-Kapella, L. & Weinmaster, G., 2010. Canonical and non-canonical notch ligands. *Current Topics in Developmental Biology*, 92(C), pp.73–129.
Dinchuk, J.E. et al., 2002. Absence of post-translational aspartyl beta-hydroxylation of epidermal growth factor domains in mice leads to developmental defects and an

increased incidence of intestinal neoplasia. *Journal of Biological Chemistry*, 277(15), pp.12970–12977.

Dinchuk, J.E. et al., 2000. Aspartyl beta-hydroxylase (Asph) and an evolutionarily conserved isoform of Asph missing the catalytic domain share exons with junctin. *Journal of Biological Chemistry*, 275(50), pp.39543–39554.

Djiane, A. et al., 2013. Dissecting the mechanisms of Notch induced hyperplasia. *The EMBO journal*, 32(1), pp.60–71.

Djiane, A. et al., 2013. Dissecting the mechanisms of Notch induced hyperplasia. *Embo Journal*, 32(1), pp.60–71.

Doe, C.Q., 2008. Neural stem cells: balancing self-renewal with differentiation. *Development*, 135(9), pp.1575–1587.

Dong, Q. et al., 2003. Loss of cables, a novel gene on chromosome 18q, in ovarian cancer. *Modern Pathology*, 16(9), pp.863–868.

Dunwoodie, S.L. et al., 1997. Mouse Dll3: a novel divergent Delta gene which may complement the function of other Delta homologues during early pattern formation in the mouse embryo. *Development*, 124(16), pp.3065–76.

Ehm, O. et al., 2010. RBPJkappa-dependent signaling is essential for long-term maintenance of neural stem cells in the adult hippocampus. *The Journal of neuroscience : the official journal of the Society for Neuroscience*, 30(41), pp.13794–807.

Elkabetz, Y. & Studer, L., 2008. Human ESC-derived neural rosettes and neural stem cell progression. In *Cold Spring Harbor Symposia on Quantitative Biology*. pp. 377–387.

Endo, K. et al., 2012. Chromatin modification of Notch targets in olfactory receptor neuron diversification. *Nature Neuroscience*, 15(2), pp.224–233.

Fan, S.-J. et al., 2016. PAT4 levels control amino-acid sensitivity of rapamycin-resistant mTORC1 from the Golgi and affect clinical outcome in colorectal cancer. *Oncogene*, 35(23), pp.3004–3015.

Fehon, R.G. et al., 1990. Molecular interactions between the protein products of the neurogenic loci Notch and Delta, two EGF-homologous genes in Drosophila. *Cell*, 61(3), pp.523–534.

Fischer, A. & Gessler, M., 2007. Delta Notch and then? Protein interactions and proposed modes of repression by Hes and Hey bHLH factors. *Nucleic Acids Research*, 35(14), pp.4583–4596.

Fischer, J.A. et al., 1988. GAL4 activates transcription in Drosophila. *Nature*, 332(6167), pp.853–856.

Fleming, R.J., Gu, Y. & Hukriede, N. a, 1997. Serrate-mediated activation of Notch is specifically blocked by the product of the gene fringe in the dorsal compartment of the Drosophila wing imaginal disc. *Development*, 124(15), pp.2973–2981.

Flood, K. et al., 2014. The role of brain sparing in the prediction of adverse outcomes in intrauterine growth restriction: results of the multicenter PORTO Study. *American journal of obstetrics and gynecology*, 211(3), p.288.e1-5.

Fortini, M.E., 2009. Notch Signaling: The Core Pathway and Its Posttranslational Regulation. *Developmental Cell*, 16(5), pp.633–647.

Fortini, M.E. & Bilder, D., 2009. Endocytic regulation of Notch signaling. *Current Opinion in Genetics and Development*, 19(4), pp.323–328.

Furukawa, T. et al., 2000. rax, Hes1, and notch1 promote the formation of Muller glia by postnatal retinal progenitor cells. *Neuron*, 26(2), pp.383–394.

Gaiano, N. & Fishell, G., 2002. The role of Notch in promoting glial and neural stem cell fates. *Annual Review of Neuroscience*, 25, pp.471–490.

Gaiano, N., Nye, J.S. & Fishell, G., 2000. Radial glial identity is promoted by Notch1 signaling in the murine forebrain. *Neuron*, 26(2), pp.395–404.

Goberdhan, D.C.I. et al., 2005. PAT-related amino acid transporters regulate growth via a novel mechanism that does not require bulk transport of amino acids. *Development (Cambridge, England)*, 132(10), pp.2365–2375.

Goberdhan, D.C.I., Wilson, C. & Harris, A.L., 2016. Amino Acid Sensing by mTORC1: Intracellular Transporters Mark the Spot. *Cell Metabolism*, 23(4), pp.580–589.

Goberdhan, D.C.I., Wilson, C. & Harris, A.L., 2016. Amino Acid Sensing by mTORC1: Intracellular Transporters Mark the Spot. *Cell Metabolism*, 23(4), pp.580–589.

Goeke, S. et al., 2003. Alternative splicing of lola generates 19 transcription factors controlling axon guidance in Drosophila. *Nature neuroscience*, 6(9), pp.917–24.

Gogendeau, D. et al., 2015. Aneuploidy causes premature differentiation of neural and intestinal stem cells. *Nature Communications*, 6, p.8894.

Gonçalves, J.T., Schafer, S.T. & Gage, F.H., 2016. Adult Neurogenesis in the Hippocampus: From Stem Cells to Behavior. *Cell*, 167(4), pp.897–914.

Gordon, W.R. et al., 2007. Structural basis for autoinhibition of Notch. *Nature Structural and Molecular Biology*, 14(4), pp.295–300.

Groeneweg, J.W. et al., 2011. cables1 Is Required for Embryonic Neural Development: Molecular, Cellular, and Behavioral Evidence From the Zebrafish. *Molecular Reproduction and Development*, 78(1), pp.22–32.

Gu, Y., Hukriede, N.A. & Fleming, R.J., 1995. Serrate expression can functionally replace Delta activity during neuroblast segregation in the Drosophila embryo. *Development (Cambridge, England)*, 121(3), pp.855–65.

Gurudatta, B. V, Ramos, E. & Corces, V.G., 2012. The BEAF insulator regulates genes involved in cell polarity and neoplastic growth. *Developmental biology*, 369(1), pp.124–32.

Haines, N. & Irvine, K.D., 2003. Glycosylation regulates notch signalling. *Nature Reviews Molecular Cell Biology*, 4(10), pp.786–797.

Haines, N. & Irvine, K.D., 2003. Glycosylation regulates Notch signalling. *Nature Reviews Molecular Cell Biology*, 4(10), pp.786–797.

Hassan, K.A. et al., 2013. Notch pathway activity identifies cells with cancer stem cell-like properties and correlates with worse survival in lung adenocarcinoma. *Clinical Cancer Research*, 19(8), pp.1972–1980.

Heublein, S. et al., 2010. Proton-assisted amino-acid transporters are conserved regulators of proliferation and amino-acid-dependent mTORC1 activation. *Oncogene*, 29(28), pp.4068–4079.

Hietakangas, V. & Cohen, S.M., 2009. Regulation of tissue growth through nutrient sensing. *Annual review of genetics*, 43(1), pp.389–410.

Homem, C.C.F. et al., 2014. Ecdysone and mediator change energy metabolism to terminate proliferation in Drosophila neural stem cells. *Cell*, 158(4), pp.874–88.

Homem, C.C.F. & Knoblich, J. a, 2012. Drosophila neuroblasts: a model for stem cell biology. *Development (Cambridge, England)*, 139(23), pp.4297–310.

Homem, C.C.F., Repic, M. & Knoblich, J.A., 2015. Proliferation control in neural stem and progenitor cells. *Nature Reviews Neuroscience*, 16(11), pp.647–659.

Housden, B.E. et al., 2013. Transcriptional dynamics elicited by a short pulse of notch

activation involves feed-forward regulation by E(spl)/Hes genes J. Lewis, ed. *PLoS Genetics*, 9(1), p.e1003162.

Housden, B.E., Millen, K. & Bray, S.J., 2012. Drosophila Reporter Vectors Compatible with ΦC31 Integrase Transgenesis Techniques and Their Use to Generate New Notch Reporter Fly Lines. *G3 (Bethesda, Md.)*, 2(1), pp.79–82.

Huang, J.-R. et al., 2017. The emerging role of Cables1 in cancer and other diseases. *Molecular Pharmacology*, p.mol.116.107730.

Imayoshi, I. et al., 2010. Essential Roles of Notch Signaling in Maintenance of Neural Stem Cells in Developing and Adult Brains. *The Journal of Neuroscience*, 30(9), pp.3489–3498.

Iso, T., Kedes, L. & Hamamori, Y., 2003. HES and HERP families: multiple effectors of the Notch signaling pathway. *Journal of cellular physiology*, 194(3), pp.237–55.

Jen, W.C. et al., 1997. The Notch ligand, X-Delta-2, mediates segmentation of the paraxial mesoderm in Xenopus embryos. *Development*, 124(6), pp.1169–1178.

Jennings, B. et al., 1994. The Notch signalling pathway is required for Enhancer of split bHLH protein expression during neurogenesis in the Drosophila embryo. *Development (Cambridge, England)*, 120(12), pp.3537–48.

Kageyama, R. & Ohtsuka, T., 1999. The Notch-Hes pathway in mammalian neural development. *Cell Research*, 9(3), pp.179–188.

Kageyama, R., Shimojo, H. & Imayoshi, I., 2015. Dynamic expression and roles of Hes factors in neural development. *Cell and Tissue Research*, 359(1), pp.125–133.

Kang, K.H. & Reichert, H., 2015. Control of neural stem cell self-renewal and differentiation in Drosophila. *Cell and Tissue Research*, 359(1), pp.33–45.

Kannan, S. et al., 2013. Notch activation inhibits AML growth and survival: a potential therapeutic approach. *The Journal of Experimental Medicine*, 210(2), pp.321–337.

Kao, H.Y. et al., 1998. A histone deacetylase corepressor complex regulates the Notch signal transduction pathway. *Genes and Development*, 12(15), pp.2269–2277.

Kim, M.Y. et al., 2011. The intracellular domain of Jagged-1 interacts with Notch1 intracellular domain and promotes its degradation through Fbw7 E3 ligase. *Experimental Cell Research*, 317(17), pp.2438–2446.

Klein, A.M. et al., 2015. Droplet barcoding for single-cell transcriptomics applied to embryonic stem cells. *Cell*, 161(5), pp.1187–1201.

Kleinmann, E. et al., 2008. Ikaros represses the transcriptional response to Notch signaling in T-cell development. *Molecular and cellular biology*, 28(24), pp.7465–75.

Kopan, R. & Ilagan, M.X.G., 2009. The canonical Notch signaling pathway: Unfolding the activation mechanism. *Cell*, 137(2), pp.216–233.

Krejcí, A. et al., 2009. Direct response to Notch activation: signaling crosstalk and incoherent logic. *Science signaling*, 2(55), p.ra1.

Krejčí, A. & Bray, S., 2007. Notch activation stimulates transient and selective binding of Su(H)/CSL to target enhancers. *Genes and Development*, 21(11), pp.1322–1327.

Lai, S.L. et al., 2012. The snail family member worniu is continuously required in neuroblasts to prevent Elav-Induced premature differentiation. *Developmental Cell*, 23(4), pp.849–857.

Lanet, E., Gould, A.P. & Maurange, C., 2013. Protection of neuronal diversity at the expense of neuronal numbers during nutrient restriction in the Drosophila visual system. *Cell Reports*, 3(3), pp.587–94.

Lanet, E. & Maurange, C., 2014. Building a brain under nutritional restriction: Insights on sparing and plasticity from Drosophila studies. *Frontiers in Physiology*, 5 MAR, p.117.

Lecourtois, M. & Schweisguth, F., 1995. The neurogenic suppressor of hairless DNA-binding protein mediates the transcriptional activation of the enhancer of split complex genes triggered by Notch signaling. *Genes & development*, 9(21), pp.2598–608.

Lee, K.-S. et al., 2013. Roles of PINK1, mTORC2, and mitochondria in preserving brain tumor-forming stem cells in a noncanonical Notch signaling pathway. *Genes & development*, 27(24), pp.2642–7.

Li, P. et al., 1997. Inscuteable and staufen mediate asymmetric localization and segregation of prospero RNA during Drosophila neuroblast cell divisions. *Cell*, 90(3), pp.437–447.

Lin, H.F. & Schagat, T., 1997. Neuroblasts: A model for the asymmetric division of stem cells. *Trends in Genetics*, 13(1), pp.33–39.

Lin, W.-Y. et al., 2015. The SLC36 transporter Pathetic is required for extreme dendrite growth in Drosophila sensory neurons. *Genes & Development* , 29(11), pp.1120–1135.

Liu, Z. et al., 2015. Opposing intrinsic temporal gradients guide neural stem cell production of varied neuronal fates. *Science (New York, N.Y.)*, 350(6258), pp.317–20.

Louvi, A. & Artavanis-Tsakonas, S., 2006. Notch signalling in vertebrate neural development. *Nature Reviews Neuroscience*, 7(2), pp.93–102.

Luca, V.C. et al., 2015. Structural basis for Notch1 engagement of Delta-like 4. *Science*, 347(6224), pp.847–853.

Lugert, S. et al., 2010. Quiescent and active hippocampal neural stem cells with distinct morphologies respond selectively to physiological and pathological stimuli and aging. *Cell Stem Cell*, 6(5), pp.445–456.

Macosko, E.Z. et al., 2015. Highly parallel genome-wide expression profiling of individual cells using nanoliter droplets. *Cell*, 161(5), pp.1202–1214.

Malamitsi-Puchner, A., Nikolaou, K.E. & Puchner, K.P., 2006. Intrauterine growth restriction, brain-sparing effect, and neurotrophins. In *Annals of the New York Academy of Sciences*. Blackwell Publishing Inc, pp. 293–296.

Matsuoka, M. et al., 2003. ik3-2, a relative to ik3-1/Cables, is involved in both p53-mediated and p53-independent apoptotic pathways. *Biochemical and Biophysical Research Communications*, 312(2), pp.520–529.

Maurange, C., Cheng, L. & Gould, A.P., 2008. Temporal transcription factors and their targets schedule the end of neural proliferation in Drosophila. *Cell*, 133(5), pp.891–902.

McDermott, S.M. et al., 2012. Drosophila Syncrip binds the gurken mRNA localisation signal and regulates localised transcripts during axis specification. *Biology Open*, 1(5), pp.488–97.

Melzer, J. et al., 2013. The p21-activated kinase Mbt is a component of the apical protein complex in central brain neuroblasts and controls cell proliferation. *Development*, 140(9), pp.1871–1881.

Mirth, C.K. & Shingleton, A.W., 2012. Integrating body and organ size in Drosophila: Recent advances and outstanding problems. *Frontiers in Endocrinology*, 3(APR),

p.49.
Mohr, O., 1919. Character changes caused by mutation of an entire region of a chromosome in Drosophila. *Genetics*, 275(4), pp.275–282.
Moloney, D.J. et al., 2000. Fringe is a glycosyltransferase that modifies Notch. *Nature*, 406(6794), pp.369–375.
Muralidharan Pillai, S. & Meredith, D., 2011. SLC36A4 (hPAT4) is a high affinity amino acid transporter when expressed in Xenopus laevis oocytes. *Journal of Biological Chemistry*, 286(4), pp.2455–2460.
Nakao, K. & Campos-Ortega, J.A., 1996. Persistent expression of genes of the enhancer of split complex suppresses neural development in Drosophila. *Neuron*, 16(2), pp.275–286.
Nakhai, H. et al., 2008. Conditional ablation of Notch signaling in pancreatic development. *Development*, 135(16), pp.2757–2765.
Neumuller, R.A. et al., 2008. Mei-P26 regulates microRNAs and cell growth in the Drosophila ovarian stem cell lineage. *Nature*, 454(7201), pp.241-U72.
Neumüller, R.A. et al., 2011. Genome-wide analysis of self-renewal in Drosophila neural stem cells by transgenic RNAi. *Cell Stem Cell*, 8(5), pp.580–593.
Nyfeler, Y. et al., 2005. Jagged1 signals in the postnatal subventricular zone are required for neural stem cell self-renewal. *EMBO Journal*, 24(19), pp.3504–3515.
O'Neil, J. et al., 2007. FBW7 mutations in leukemic cells mediate NOTCH pathway activation and resistance to gamma-secretase inhibitors. *J Exp Med*, 204(8), pp.1813–1824.
Ohsako, T. et al., 2003. Drosophila lola encodes a family of BTB-transcription regulators with highly variable C-terminal domains containing zinc finger motifs. *Gene*, 311, pp.59–69.
Ohtsuka, T. et al., 2001. Roles of the Basic Helix-Loop-Helix Genes Hes1 and Hes5 in Expansion of Neural Stem Cells of the Developing Brain. *Journal of Biological Chemistry*, 276(32), pp.30467–30474.
Okajima, T., 2005. Chaperone Activity of Protein O-Fucosyltransferase 1 Promotes Notch Receptor Folding. *Science*, 307(5715), pp.1599–1603.
Osterfield, M., Berg, C.A. & Shvartsman, S.Y., 2017. Epithelial Patterning, Morphogenesis, and Evolution: Drosophila Eggshell as a Model. *Developmental Cell*, 41(4), pp.337–348.
Panin, V.M. et al., 1997. Fringe modulates Notch-ligand interactions. *Nature*, 387(6636), pp.908–912.
Park, D.Y. et al., 2007. The cables gene on chromosome 18q is silenced by promoter hype rmethyl ati on and allelic loss in human colorectal cancer. *American Journal of Pathology*, 171(5), pp.1509–1519.
Pierfelice, T., Alberi, L. & Gaiano, N., 2011. Notch in the Vertebrate Nervous System: An Old Dog with New Tricks. *Neuron*, 69(5), pp.840–855.
Port, F. et al., 2014. Optimized CRISPR/Cas tools for efficient germline and somatic genome engineering in Drosophila. *Proceedings of the National Academy of Sciences of the United States of America*, 111(29), pp.E2967-76.
Prado, E.L. & Dewey, K.G., 2014. Nutrition and brain development in early life. *Nutrition Reviews*, 72(4), pp.267–284.
Prokop, A. et al., 1998. Homeotic regulation of segment-specific differences in neuroblast numbers and proliferation in the Drosophila central nervous system.

Mechanisms of development, 74(1–2), pp.99–110.
Pu, Z. et al., 2017. Cables1 Inhibits Proliferation and Induces Senescence by Angiotensin II via a p21-Dependent Pathway in Human Umbilical Vein Endothelial Cells. *Journal of Vascular Research*, 54(1), pp.13–21.
Read, R.D. et al., 2009. A Drosophila model for EGFR-Ras and PI3K-dependent human glioma E. Rulifson, ed. *PLoS Genetics*, 5(2), p.e1000374.
Rebeiz, M., Reeves, N.L. & Posakony, J.W., 2002. SCORE: a computational approach to the identification of cis-regulatory modules and target genes in whole-genome sequence data. *Proc Natl Acad Sci U S A*, 99(15), pp.9888–9893.
Rebsamen, M. et al., 2015. SLC38A9 is a component of the lysosomal amino acid sensing machinery that controls mTORC1. *Nature*, 519(7544), pp.477–481.
Rhee, J. et al., 2007. Cables links Robo-bound Abl kinase to N-cadherin-bound beta-catenin to mediate Slit-induced modulation of adhesion and transcription. *Nature Cell Biology*, 9(8), pp.883-U30.
Robinson, D.R. et al., 2011. Functionally recurrent rearrangements of the MAST kinase and Notch gene families in breast cancer. *Nature Medicine*, 17(12), pp.1646–1651.
Roussel-Gervais, A. et al., 2016. The Cables1 Gene in Glucocorticoid Regulation of Pituitary Corticotrope Growth and Cushing Disease. *The Journal of Clinical Endocrinology & Metabolism*, 101(2), pp.513–522.
Sakamoto, H. et al., 2008. Mechanisms of Cables 1 gene inactivation in human ovarian cancer development. *Cancer Biology & Therapy*, 7(2), pp.180–188.
Salic, A. & Mitchison, T.J., 2008. A chemical method for fast and sensitive detection of DNA synthesis in vivo. *Proceedings of the National Academy of Sciences of the United States of America*, 105(7), pp.2415–2420.
San-Juán, B.P. & Baonza, A., 2011. The bHLH factor deadpan is a direct target of Notch signaling and regulates neuroblast self-renewal in Drosophila. *Developmental biology*, 352(1), pp.70–82.
Sato, H., Nishimoto, I. & Matsuoka, M., 2002. ik3-2, a relative to ik3-1/Cables, is associated with cdk3, cdk5, and c-abl. *Biochimica Et Biophysica Acta-Gene Structure and Expression*, 1574(2), pp.157–163.
Schertel, C. et al., 2015. A large-scale, in vivo transcription factor screen defines bivalent chromatin as a key property of regulatory factors mediating Drosophila wing development. *Genome Research*, 25(4), pp.514–523.
Schweisguth, F. & Posakony, J.W., 1992. Suppressor of Hairless, the Drosophila homolog of the mouse recombination signal-binding protein gene, controls sensory organ cell fates. *Cell*, 69(7), pp.1199–1212.
Severson, E. et al., 2017. Genome-wide identification and characterization of Notch transcription complex-binding sequence-paired sites in leukemia cells. *Science Signaling*, 10(477).
Shang, P. et al., 2017. The amino acid transporter SLC36A4 regulates the amino acid pool in retinal pigmented epithelial cells and mediates the mechanistic target of rapamycin, complex 1 signaling. *Aging Cell*, 16(2), pp.349–359.
Shi, Z. et al., 2015. Cables1 controls p21/Cip1 protein stability by antagonizing proteasome subunit alpha type 3. *Oncogene*, 34(19), pp.2538–2545.
Shimojo, H., Ohtsuka, T. & Kageyama, R., 2008. Oscillations in Notch Signaling Regulate Maintenance of Neural Progenitors. *Neuron*, 58(1), pp.52–64.
Siebel, C. & Lendahl, U., 2017. Notch Signaling in Development, Tissue Homeostasis, and

Disease. *Physiological Reviews*, 97(4), pp.1235–1294.
Skalska, L. et al., 2015. Chromatin signatures at Notch-regulated enhancers reveal large-scale changes in H3K56ac upon activation. *The EMBO journal*, 34(14), pp.1889–1904.
Slaninova, V. et al., 2016. Notch stimulates growth by direct regulation of genes involved in the control of glycolysis and the tricarboxylic acid cycle. *Open biology*, 6(2), p.150155-.
Song, Y. & Lu, B., 2011. Regulation of cell growth by Notch signaling and its differential requirement in normal vs. tumor-forming stem cells in Drosophila. *Genes & development*, 25(24), pp.2644–58.
Sousa-Nunes, R., Yee, L.L. & Gould, A.P., 2011. Fat cells reactivate quiescent neuroblasts via TOR and glial insulin relays in Drosophila. *Nature*, 471(7339), pp.508–12.
Southall, T.D. & Brand, A.H., 2009a. Neural stem cell transcriptional networks highlight genes essential for nervous system development. *The EMBO journal*, 28(24), pp.3799–807.
Southall, T.D. & Brand, A.H., 2009b. Neural stem cell transcriptional networks highlight genes essential for nervous system development. *The EMBO journal*, 28(24), pp.3799–807.
Southall, T.D. & Brand, A.H., 2009. Neural stem cell transcriptional networks highlight genes essential for nervous system development. *Embo Journal*, 28(24), pp.3799–3807.
Spana, E.P. & Doe, C.Q., 1995. THE PROSPERO TRANSCRIPTION FACTOR IS ASYMMETRICALLY LOCALIZED TO THE CELL CORTEX DURING NEUROBLAST MITOSIS IN DROSOPHILA. *Development*, 121(10), pp.3187–3195.
Spokony, R.F. & Restifo, L.L., 2009. Broad Complex isoforms have unique distributions during central nervous system metamorphosis in Drosophila melanogaster. *The Journal of comparative neurology*, 517(1), pp.15–36.
Stanley, P., 2007. Regulation of Notch signaling by glycosylation. *Current Opinion in Structural Biology*, 17(5), pp.530–535.
Stump, G. et al., 2002. Notch1 and its ligands Delta-like and Jagged are expressed and active in distinct cell populations in the postnatal mouse brain. *Mechanisms of Development*, 114(1–2), pp.153–159.
Sun, Y. et al., 2001. Neurogenin promotes neurogenesis and inhibits glial differentiation by independent mechanisms. *Cell*, 104(3), pp.365–376.
Takebe, N. et al., 2015. Targeting Notch, Hedgehog, and Wnt pathways in cancer stem cells: Clinical update. *Nature Reviews Clinical Oncology*, 12(8), pp.445–464.
Torella, R. et al., 2014. A combination of computational and experimental approaches identifies DNA sequence constraints associated with target site binding specificity of the transcription factor CSL. *Nucleic Acids Research*, 42(16), pp.10550–10563.
Trujillo-Paredes, N. et al., 2016. Regulation of differentiation flux by Notch signalling influences the number of dopaminergic neurons in the adult brain. *Biology Open*, 5(3), pp.336–347.
Tsuji, K. et al., 2002. Differential effect of ik3-1/Cables on p53-and p73-induced cell death. *Journal of Biological Chemistry*, 277(4), pp.2951–2957.
Vaccari, T. et al., 2008. Endosomal entry regulates Notch receptor activation in Drosophila melanogaster. *The Journal of cell biology*, 180(4), pp.755–62.
Vanderwielen, B.D. et al., 2011. Transcriptional repression in the Notch pathway:

Thermodynamic characterization of CSL-MINT (Msx2-interacting nuclear target protein) complexes. *Journal of Biological Chemistry*, 286(17), pp.14892–14902.
Wang, H. et al., 2006. Aurora-A acts as a tumor suppressor and regulates self-renewal of Drosophila neuroblasts. *Genes & Development*, 20(24), pp.3453–3463.
Wang, H. et al., 2011. Genome-wide analysis reveals conserved and divergent features of Notch1/RBPJ binding in human and murine T-lymphoblastic leukemia cells. *Proceedings of the National Academy of Sciences*, 108(36), pp.14908–14913.
Wang, H. et al., 2014. NOTCH1-RBPJ complexes drive target gene expression through dynamic interactions with superenhancers. *Proceedings of the National Academy of Sciences of the United States of America*, 111(2), pp.705–710.
Wang, H. et al., 2015. The role of notch receptors in transcriptional regulation. *Journal of Cellular Physiology*, 230(5), pp.982–988.
Wang, H.Y. et al., 2007. Polo inhibits progenitor self-renewal and regulates Numb asymmetry by phosphorylating Pon. *Nature*, 449(7158), pp.96-U70.
Wang, N. et al., 2010. Cables1 protects p63 from proteasomal degradation to ensure deletion of cells after genotoxic stress. *EMBO reports*, 11(8), pp.633–9.
Wang, S. et al., 2015. Lysosomal amino acid transporter SLC38A9 signals arginine sufficiency to mTORC1. *Science (New York, N.Y.)*, 347(6218), pp.188–94.
Weng, M., Golden, K.L. & Lee, C.-Y., 2010. dFezf/Earmuff maintains the restricted developmental potential of intermediate neural progenitors in Drosophila. *Developmental cell*, 18(1), pp.126–35.
Winton, D.J., 2013. MiR-34a sets the 'sweet spot' for notch in colorectal cancer stem cells. *Cell Stem Cell*, 12(5), pp.499–501.
Witkowski, M.T. et al., 2015. Activated Notch counteracts Ikaros tumor suppression in mouse and human T-cell acute lymphoblastic leukemia. *Leukemia*, 29(6), pp.1301–1311.
Wodarz, A. & Huttner, W.B., 2003. Asymmetric cell division during neurogenesis in Drosophila and vertebrates. *Mechanisms of Development*, 120(11), pp.1297–1309.
Wu, J.S. & Luo, L., 2007. A protocol for mosaic analysis with a repressible cell marker (MARCM) in Drosophila. *Nature Protocols*, 1(6), pp.2583–2589.
Xiao, Q., Komori, H. & Lee, C.Y., 2012. klumpfuss distinguishes stem cells from progenitor cells during asymmetric neuroblast division. *Development*, 139(15), pp.2670–2680.
Yoon, K. & Gaiano, N., 2005. Notch signaling in the mammalian central nervous system: insights from mouse mutants. *Nature Neuroscience*, 8(6), pp.709–715.
Yoon, K.J. et al., 2008. Mind Bomb 1-Expressing Intermediate Progenitors Generate Notch Signaling to Maintain Radial Glial Cells. *Neuron*, 58(4), pp.519–531.
Zacharioudaki, E. et al., 2016. Genes implicated in stem cell identity and temporal programme are directly targeted by Notch in neuroblast tumours. *Development*, 143(2), pp.219–231.
Zacharioudaki, E., Magadi, S.S. & Delidakis, C., 2012. bHLH-O proteins are crucial for Drosophila neuroblast self-renewal and mediate Notch-induced overproliferation. *Development*, 139(7), pp.1258–1269.
Zhang, H. et al., 2005. Aberrant splicing of Cables gene, a CDK regulator, in human cancers. *Cancer Biology & Therapy*, 4(11), pp.1211–1215.
Zhang, Y. et al., 2008. Epigenetic Blocking of an Enhancer Region Controls Irradiation-Induced Proapoptotic Gene Expression in Drosophila Embryos. *Developmental Cell*, 14(4), pp.481–493.

Zheng, L. & Carthew, R.W., 2008. Lola regulates cell fate by antagonizing Notch induction in the Drosophila eye. *Mechanisms of development*, 125(1–2), pp.18–29.

Zhu, S. et al., 2006. Gradients of the Drosophila Chinmo BTB-zinc finger protein govern neuronal temporal identity. *Cell*, 127(2), pp.409–422.

Zielke, N. et al., 2014. Fly-FUCCI: A versatile tool for studying cell proliferation in complex tissues. *Cell Reports*, 7(2), pp.588–98.

Zukerberg, L.R., Patrick, G.N., Nikolic, M., Humbert, S., Wu, C.L., et al., 2000. Cables links Cdk5 and c-Abl and facilitates Cdk5 tyrosine phosphorylation, kinase upregulation, and neurite outgrowth. *Neuron*, 26(3), pp.633–646.

Zukerberg, L.R., Patrick, G.N., Nikolic, M., Humbert, S., Wu, C., et al., 2000. Cables Links Cdk5 and c-Abl and Facilitates Upregulation , and Neurite Outgrowth. *Neuron*, 26, pp.633–646.

Zukerberg, L.R. et al., 2004. Loss of cables, a cyclin-dependent kinase regulatory protein, is associated with the development of endometrial hyperplasia and endometrial cancer. *Cancer Research*, 64(1), pp.202–208.

Zweidler-McKay, P.A. et al., 2005. Notch signaling is a potent inducer of growth arrest and apoptosis in a wide range of B-cell malignancies. *Blood*, 106(12), pp.3898–3906.